

**METASTABLE STATES  
IN MEDIUM- AND  
HEAVY- WEIGHT NUCLEI**

**BY  
AUGUST ALEXANDER EBEL**

Thesis  
E15

THESIS  
E15

Library  
U. S. Naval Postgraduate School  
Annapolis, Md.











METASTABLE STATES IN INDIUM-

AND HEAVY-WEIGHT NUCLEI.

by

August Alexander Ebel

B.A. Iowa State Teachers College  
(1942)

Submitted in Partial Fulfillment of the  
Requirements for the Degree of

DOCTOR OF PHILOSOPHY

at the

MASSACHUSETTS INSTITUTE OF TECHNOLOGY

(1950)



# TABLE OF CONTENTS

	Page Number
ABSTRACT	1
I. INTRODUCTION	3
ORIGIN OF THE PROBLEM	3
HISTORY OF ISOMERISM	4
EXCITATION OF METASTABLE STATES	8
II. THEORETICAL CONSIDERATIONS	11
WIEZACKER HYPOTHESIS	11
ANGULAR MOMENTUM SELECTION RULE	14
PARITY SELECTION RULE	15
INTERNAL CONVERSION	15
NEUTRON EXCITATION OF METASTABLE LEVELS	17
COMPARISON OF NEUTRON AND PHOTON EXCITATION	22
III. EXPERIMENTAL EQUIPMENT	24
NEUTRON SOURCE	24
ROCKEFELLER GENERATOR	25
LONG COUNTER	26
SCINTILLATION COUNTER	28
IV. INVESTIGATION OF GOLD	34
HISTORY OF Au <sup>197</sup> * EXCITATION	34
DESCRIPTION OF THE ENERGY LEVELS IN Au <sup>197</sup>	37

1000  
1000

1

CHAPTER I

2

I. INTRODUCTION

3

DEFINITION OF THE SUBJECT

4

HISTORY OF THE SUBJECT

5

EXPLANATION OF THE SUBJECT

11

II. THE SUBJECT MATTER

12

DEFINITION OF THE SUBJECT

13

DEFINITION OF THE SUBJECT

14

DEFINITION OF THE SUBJECT

15

DEFINITION OF THE SUBJECT

16

DEFINITION OF THE SUBJECT

17

DEFINITION OF THE SUBJECT

21

III. THE SUBJECT MATTER

22

DEFINITION OF THE SUBJECT

23

DEFINITION OF THE SUBJECT

24

DEFINITION OF THE SUBJECT

25

DEFINITION OF THE SUBJECT

31

IV. THE SUBJECT MATTER

32

DEFINITION OF THE SUBJECT

33

DEFINITION OF THE SUBJECT

DESCRIPTION OF EXPERIMENTAL SETUP	15
TREATMENT OF THE DATA	49
COMPARISON OF THE THEORETICAL AND EXPERIMENTAL CROSS SECTIONS	56
 V. INVESTIGATION OF INDIUM	 65
HISTORY OF $\text{In}^{115*}$ EXCITATION	65
DESCRIPTION OF ENERGY LEVELS IN $\text{In}^{115}$	66
EXPERIMENTAL SETUP	72
TREATMENT OF THE DATA	76
DISCUSSION OF THE RESULTS	78
 VI. CONCLUSIONS AND SUGGESTIONS FOR FURTHER INVESTIGATION	 82
SUMMARY OF RESULTS	82
FURTHER INVESTIGATION OF $\text{Au}^{197*}$	82
FURTHER INVESTIGATION OF $\text{In}^{115*}$	83
INVESTIGATION OF OTHER ISOTOPES	84
 VII. ACKNOWLEDGMENTS	 87
 REFERENCES	 89
BIOGRAPHICAL SKETCH	92

10

11

12

13

14

15

16

17

18

19

20

21

22

23

24

25

THE UNITED STATES OF AMERICA  
DEPARTMENT OF JUSTICE

INVESTIGATION OF THE

ACTIVITIES OF THE

COMMUNIST PARTY, U.S.A.

INVESTIGATION OF THE

ACTIVITIES OF THE

COMMUNIST PARTY, U.S.A.

INVESTIGATION OF THE

ACTIVITIES OF THE

COMMUNIST PARTY, U.S.A.

INVESTIGATION OF THE

ACTIVITIES OF THE

INVESTIGATION OF THE

ACTIVITIES OF THE

COMMUNIST PARTY, U.S.A.



## A B S T R A C T

This thesis describes an experimental investigation of the excitation of the metastable states in  $\text{Ir}^{115}$  and  $\text{Au}^{197}$  by inelastic scattering of neutrons. The results are compared with those for quantum excitation of these states.

The neutron excitation curve for gold shows two pronounced discontinuities in slope at  $1.14 \pm 0.03$  Mev and  $1.44 \pm 0.03$  Mev, corresponding to energy levels that decay to the metastable state. The threshold for production of the isomer with neutrons is found to coincide with the energy of the metastable level.

It is shown that the spin of the metastable state must be at least  $11/2$ . A comparison of the cross section for the direct production of this state with the cross section for formation of the compound nucleus indicates that the state is excited by an  $\ell = 3$  neutron. This fixes the spin at  $11/2$  with parity opposite to that of the ground state.

An analysis of quantum-excitation data shows the 1.14-Mev level to have a spin of  $5/2$  or  $7/2$  also with parity opposite that of the ground state. From the properties of the isomeric transition, the spin of the known level between the metastable level and ground is shown to have a spin of  $5/2$  with parity opposite that of the ground state.

The curve obtained by neutron excitation of indium reveals a threshold at  $600 \pm 40$  kev and other excited levels at  $960 \pm 40$  kev and  $1.37 \pm 0.04$  Mev. The last two have been reported from quantum excitation at 1.04 and 1.42 Mev.

The first of these is the fact that the energy levels of the system are not equally spaced. This is due to the fact that the potential energy of the system is not a simple harmonic oscillator. The energy levels are given by the following equation:

$$E_n = \hbar \omega \left( n + \frac{1}{2} \right) + \frac{\hbar^2 \omega^2}{24} \left( n + \frac{1}{2} \right)^3 + \dots$$

where  $\omega$  is the angular frequency of the oscillator. The first term represents the harmonic oscillator energy, and the subsequent terms represent the anharmonic corrections. The energy levels are shown in the following figure:

It is seen that the energy levels are not equally spaced. The spacing between the levels decreases as the quantum number  $n$  increases. This is due to the fact that the potential energy of the system is not a simple harmonic oscillator. The energy levels are given by the following equation:

$$E_n = \hbar \omega \left( n + \frac{1}{2} \right) + \frac{\hbar^2 \omega^2}{24} \left( n + \frac{1}{2} \right)^3 + \dots$$

where  $\omega$  is the angular frequency of the oscillator. The first term represents the harmonic oscillator energy, and the subsequent terms represent the anharmonic corrections. The energy levels are shown in the following figure:

The curve obtained by numerical solution of the Schrödinger equation is shown in the following figure. The energy levels are given by the following equation:

Spin assignments of  $1/2$  for the metastable state and  $3/2$  or  $5/2$  for the 600-kev level have been made. The parity of both levels is opposite to that of the ground state.

Confirmation is given to the existence of a beta-decay of the metastable state of  $\text{In}^{115}$ .

[illegible]

at least about 10 years ago. When some more recent (1970's) year class

- Grain Harvest all the best of winter

add to your record in the continuing field of history of paleontology

211 to state education

...the ... ..

... ..

1. The first group of people who are interested in the study of the history of the United States are the people who are interested in the history of the United States.

1990-1991

*(Faint, illegible handwritten notes)*

THE FOLLOWING INFORMATION IS FOR THE USE OF THE OFFICE OF THE ATTORNEY GENERAL

1. The first group of people who are interested in the study of the history of the United States are the people who are interested in the history of the United States. This group of people is interested in the history of the United States because they want to know more about the United States. They want to know more about the United States because they want to know more about the United States.

## I. INTRODUCTION

## ORIGIN OF THE PROBLEM

Of special interest in nuclear physics is the determination of the energy, spin, and parity of excited levels in nuclei. With only a few exceptions, the lifetimes of these levels are too short to permit a direct measurement. Instead, their characteristics must be inferred from transitions to and from the ground state. Such studies involve nuclear reactions which leave the nucleus excited. The inelastic scattering of neutrons is one such reaction. In addition to its value in the theory of nuclear structure, inelastic scattering is of considerable practical importance in the problem of nuclear shielding.

Measurements of neutron inelastic scattering are difficult because of the small cross section and the inherently large background. In a few cases, however, the lifetime of the excited state is long enough to permit its measurement to be made after the beam of incident neutrons has been removed. Thus, neutron excitation of metastable states affords a very convenient method of investigating inelastic scattering in certain nuclei.

The purpose of this thesis is to investigate the inelastic scattering levels in  $\text{Au}^{197}$  and  $\text{In}^{115}$  which decay to the metastable states of these isotopes. From an analysis of the neutron excitation curves, the spin and relative parity of many of these levels will be determined.



## HISTORY OF ISOMERISM

An isomeric state is generally defined to be an excited state of a nucleus which exists for a measurable length of time. It differs from other excited states only in the probability of decay to a lower state. With the recent advances in techniques of measurement, many states have been reclassified isomeric, and many more are being found.

The first case of isomerism was the discovery by Mahn<sup>1</sup> in 1921 that  $\text{Pa}^{234}$  had two half-lives, one of 1.15 minutes and the other of 6.7 hours, associated with two beta-decay energies. He was able to show that both states grew out of the beta-decay of  $\text{Th}^{234}$ . In spite of the search for other examples, it was not until the year after the discovery of artificial radioactivity in 1934 that the next isomeric pair was found. Neutron, especially slow neutron, bombardment of bromine yielded three different radioactive decay constants, although bromine was known to have only two isotopes,  $\text{Br}^{79}$  and  $\text{Br}^{81}$ . It was shown that these three periods were due to capture of neutrons giving  $\text{Br}^{80}$ ,  $\text{Br}^{82}$ , and an isomer of the former.

Table I lists the lifetime and excitation energy of 23 known isomers of stable nuclei, together with the relative isotopic abundance of the stable state. Also included are the properties of the radiation arising from neutron capture which might interfere seriously with measurements of the neutron activation of the isomeric state.

With the existence of isomerism well established, the next step was a theoretical explanation by Weizsacker<sup>4</sup>. He established that the assumption of an excited level of a few hundred kev above the ground





TABLE I

## Isomers of Stable Nuclei

Isomeric Activity			Capture Activity		
Isotope	Half-Life	Excitation	Isotope	Half-Life	Rel. Abund.
		Energy MeV			
$^{72}_{32}\text{Ge}$	$5 \times 10^{-7}$ s	0.70			
$^{77}_{31}\text{Se}$	17.5 s	0.15	$^{83}_{31}\text{Se}$	67 s	3.4
$^{83}_{36}\text{Kr}$	113 h	(0.029) (0.016)	$^{84}_{36}\text{Kr}$	4.5 h	1.0
			$^{86}_{36}\text{Kr}$	74 h	4.
$^{87}_{38}\text{Sr}$	2.7 h	0.306	$^{84}_{38}\text{Sr}$	70 h	0.170
$^{93}_{41}\text{Nb}$	42 d				
$^{103}_{45}\text{Rh}$	15-48 h	0.06			
$^{107}_{47}\text{Ag}$	40 s	0.093	$^{107}_{47}\text{Ag}$	2.3 h	2.8
					52.5

THE

FOR THE YEAR 1932

Figure 1

1954

1000

卷之六

[illegible]

OFFICIAL

1000

1915

112

0745

275-2082

5

23

214

卷之四

13

1997

3

200

48

010

105

沈氏

3

0.35

57

33

153

103

22

5

FOR THE

25-12

230

22

14

$^{109}_{47}\text{Ag}$	39 h	0.038	43.7	$^{109}_{47}\text{Ag}$	24 s	2.6	47.5
$^{111}_{48}\text{Cd}$	43.7 h	0.119	12.75				
$^{113}_{48}\text{Cd}$	2.3 h		12.3				
$^{113}_{49}\text{In}$	105 h	0.393	4.2				
$^{115}_{49}\text{In}$	4.5 h	0.338	95.8	$^{115}_{49}\text{In}$	54 h	0.85	95.8
$^{119}_{50}\text{Sn}$	13 d	0.250	8.6	$^{122}_{50}\text{Sn}$	10 d	2.6	6.11
$^{125}_{52}\text{Te}$	60 d	0.125	7.0	$^{125}_{52}\text{Te}$	90 d	0.76	7.0
$^{135}_{56}\text{Ba}$	28.7 y	0.29	6.59	$^{128}_{52}\text{Te}$	32 d	1.80	31.7
$^{137}_{56}\text{Ba}$	158 s	0.663	11.32				
$^{169}_{69}\text{Tm}$	$1 \times 10^{-6}$ s	0.19	100				

Year	Month	Day	Time	Location	Remarks
1900	Jan	1	10:00	San Francisco	Arrived from New York
1900	Jan	2	11:00	San Francisco	Left for Los Angeles
1900	Jan	3	12:00	San Francisco	Arrived from Los Angeles
1900	Jan	4	13:00	San Francisco	Left for San Diego
1900	Jan	5	14:00	San Francisco	Arrived from San Diego
1900	Jan	6	15:00	San Francisco	Left for Portland
1900	Jan	7	16:00	San Francisco	Arrived from Portland
1900	Jan	8	17:00	San Francisco	Left for Seattle
1900	Jan	9	18:00	San Francisco	Arrived from Seattle
1900	Jan	10	19:00	San Francisco	Left for Tacoma
1900	Jan	11	20:00	San Francisco	Arrived from Tacoma
1900	Jan	12	21:00	San Francisco	Left for Everett
1900	Jan	13	22:00	San Francisco	Arrived from Everett
1900	Jan	14	23:00	San Francisco	Left for Bellingham
1900	Jan	15	24:00	San Francisco	Arrived from Bellingham
1900	Jan	16	25:00	San Francisco	Left for Skagitway
1900	Jan	17	26:00	San Francisco	Arrived from Skagitway
1900	Jan	18	27:00	San Francisco	Left for Port Townsend
1900	Jan	19	28:00	San Francisco	Arrived from Port Townsend
1900	Jan	20	29:00	San Francisco	Left for Seattle
1900	Jan	21	30:00	San Francisco	Arrived from Seattle
1900	Jan	22	31:00	San Francisco	Left for Tacoma
1900	Jan	23	32:00	San Francisco	Arrived from Tacoma
1900	Jan	24	33:00	San Francisco	Left for Everett
1900	Jan	25	34:00	San Francisco	Arrived from Everett
1900	Jan	26	35:00	San Francisco	Left for Bellingham
1900	Jan	27	36:00	San Francisco	Arrived from Bellingham
1900	Jan	28	37:00	San Francisco	Left for Skagitway
1900	Jan	29	38:00	San Francisco	Arrived from Skagitway
1900	Jan	30	39:00	San Francisco	Left for Port Townsend
1900	Jan	31	40:00	San Francisco	Arrived from Port Townsend

<sup>177</sup> <sup>72</sup> Hf <sup>179</sup>	19 s	0.20	(177-18.5 179-13.8)
<sup>181</sup> <sup>73</sup> Ta	2 x 10 <sup>-5</sup> s	0.133-0.478	100
<sup>183</sup> <sup>74</sup> Hf	5.5 s	0.100	14.24
<sup>187</sup> <sup>75</sup> Re	0.65 x 10 <sup>-6</sup> s	0.135	62.9
<sup>197</sup> <sup>79</sup> Au	7.4 s	0.250	100
<sup>204</sup> <sup>82</sup> Pb	65-68 h	1.1	1.5
		3.32 h	0.70
		<sup>82</sup> Pb <sup>200</sup>	52.3

The data in this table are taken from tabulations by Segre and Nishihara<sup>2</sup> and by Seaborg and Perlman<sup>3</sup>. The capture activity, which might confuse measurements on the isomer, is listed according to the stable isotope which captures the neutron.

(S-67) (J-10)

252

紅

Figure 6

10

3

12

65



22

26

100



卷之三

THE UNIVERSITY OF CHICAGO

state with a spin difference several units was sufficient to predict such lifetimes.

It had long been suspected that an isomer is merely a metastable level, but the influence of atomic spectra in which large spin changes do not appear was carried over into nuclear considerations. Flugge<sup>5</sup> showed this difference very clearly when he compared the atomic case having a Coulomb potential with a nuclear case assuming a potential well in a Fermi gas model. According to the build-up principle for electrons, the principal quantum numbers,  $n$ , and the azimuthal quantum numbers,  $\ell$ , are such that, although  $n$  gets very large, nowhere does  $\Delta\ell$  exceed three. In Flugge's hypothetical nuclear model, on the other hand, it is found that  $\Delta\ell$  may be four or five for protons and as high as six or seven for neutrons. This scheme also shows that isomerism is unlikely in light nuclei.

More recently Mayer<sup>6</sup> has proposed a model based on strong spin-orbit coupling which predicts the existence of large spin differences in low-lying levels. This explains in a rough way the "islands" of isomerism that have been observed in tabulations of isotopes. In many cases, however, the predicted spins and parity of the excited state do not agree with the experimentally determined values<sup>7</sup>.

#### EXCITATION OF METASTABLE STATES

The excitation of metastable states may be accomplished in general by two methods:

1. Electromagnetic excitations by high-energy x-rays or the electric field of charged particles; and,





## 2. Nuclear reactions.

With the exception of a few measurements to indicate the threshold for neutron excitation, all determinations of the levels decaying to the metastable state have been made by the first method.

Excitation curves giving the energies of levels decaying to the isomer have been determined by x-rays for  $\text{In}^{115}$ ,  $\text{Au}^{197}$ ,  $\text{Rh}^{103}$ ,  $\text{Cd}^{111}$ , and Ag. Indium is described in Chapter V and gold in Chapter IV.

The other three isomers have been studied by Wiedenbeck<sup>8,9</sup>. Unfortunately, he found it necessary to use a thick target to produce x-rays, so that the decision on the existence and location of the levels is subject to large error. Figure 1 shows the level diagrams that have been reported for these nuclei.

The two stable isotopes of silver,  $\text{Ag}^{107}$  and  $\text{Ag}^{109}$ , have metastable states with very similar properties, the first having a half-life of 40 seconds and an energy of 93 kev compared to 39 seconds and 88 kev for the second. It was therefore impossible to separate the levels belonging to one isotope from the other.

Neutron excitation by the  $(n,n)$  reaction to obtain an excitation curve has been reported for  $\text{In}^{115}$  by Cohen<sup>10</sup> in the region above 2 Mev and at four points between 600 and 1500 kev by Taschek<sup>11</sup>. Neither of these investigations shows the presence of levels other than the threshold level. Wiedenbeck<sup>12</sup> has studied  $\text{Au}^{197}$  in the vicinity of the photon threshold. However, no careful examination has been made of the neutron excitation function of any metastable state in the region from its threshold to 2 Mev with an attempt to locate the various different levels which decay to such a state.



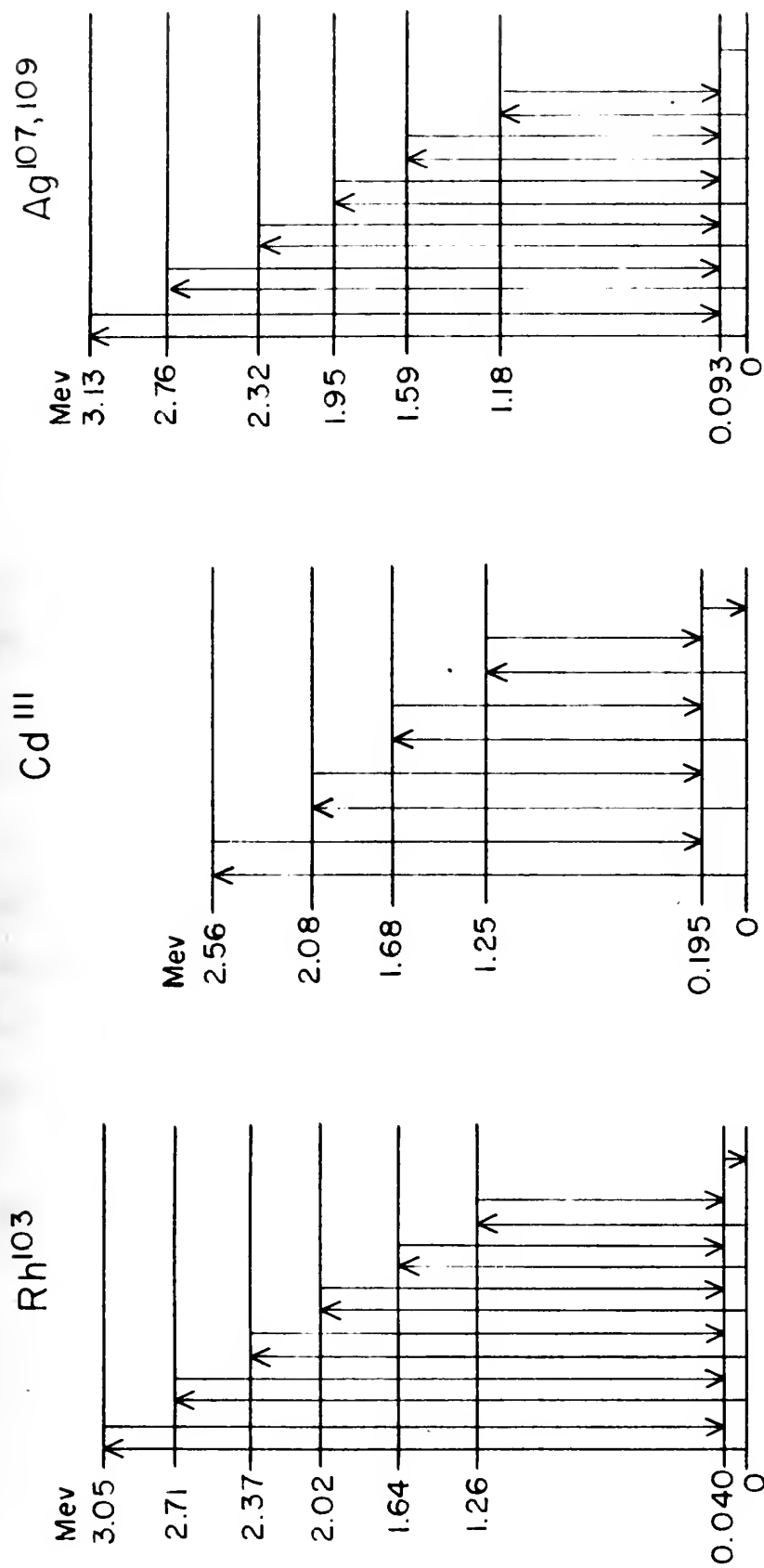


Figure 1

ENERGY LEVEL DIAGRAMS for Rh<sup>103</sup>, Cd<sup>113</sup> and Ag<sup>107,109</sup> PROPOSED by  
 WIEDENBECK from QUANTUM EXCITATION CURVES.  
 (From Phys. Rev. 67, 267 (1945) and Phys. Rev. 67, 92 (1945)).



## II. THEORETICAL CONSIDERATIONS

## SINGAGION HYPOTHESIS

A quantitative explanation of the lifetime of metastable states is complicated by the lack of detailed knowledge of the nucleus. As a result, there are many expressions for the calculation of the half-life of an isomeric state, depending on the assumption of the motion of charges in the nucleus.

From classical electrodynamics, considering an oscillating system of charges, the electric field at a point  $R, \Omega$  may be expressed as<sup>13</sup>

$$\underline{E} = -\frac{1}{c^2} \frac{e^{i\omega(t - R/c)}}{R} \int \underline{j}_\perp e^{i\mathbf{k} \cdot \underline{n} \cdot \underline{r}} d\tau$$

where  $\underline{j}_\perp$  is the projection of the current vector on the plane perpendicular to the unit vector,  $\underline{n}$ , in the direction of the point  $R, \Omega$ , and  $r, \theta$  are the coordinates of the charge producing the current. The integration is to be carried over the distribution of charges.

According to a well-known expansion, the exponential may be expressed as

$$e^{i\mathbf{k} \cdot \underline{n} \cdot \underline{r}} = \sum_{\ell=0}^{\infty} \frac{i^\ell (k r)^\ell}{1 \cdot 3 \cdot 5 \dots (2\ell - 1)} P_\ell(\cos \theta)$$



in the case in which the wave length of the radiation is long compared with the size of the charge distribution.

This leads to an expression for  $\underline{E}$  as the sum of integrals of various powers of  $kr = r/\lambda$  corresponding to the electric field of different  $2^\ell$  multipole orders. The first few terms are given below:

$$\underline{E} = -\frac{1}{c^2 R} \omega e^{i\omega(t - R/c)} \left\{ \int \underline{j}_\perp P_0(\theta) d\tau \right. \\ \left. + \int \underline{j}_\perp kr P_1(\theta) d\tau + \int \underline{j}_\perp \frac{(kr)^2}{3} P_2(\theta) d\tau + \dots \right\}$$

Consideration of the magnetic field leads to a similar result.

The transition probability may be computed by forming the Poynting vector and dividing by the energy of the radiation. Collecting the terms of like powers of  $kr$  gives an expansion for  $W_\gamma$  of the form:

$$W_\gamma = W_{E_1} + (W_{M_1} + W_{E_2}) + (W_{M_2} + W_{E_3}) + \dots$$

in which

$$W_{M_{\ell-1}} = W_{E_\ell} = (1/\lambda)^{2\ell+1} \frac{e^2}{\hbar} \eta^2 \frac{(r/\lambda)^{2\ell}}{[1.3.5 \dots (2\ell-1)]^2}$$

Let us consider the case of a single particle.

The wave function of a single particle is given by the Schrödinger equation. The wave function of a system of particles is given by the many-body wave function.

$$\left[ \frac{1}{2} \left( \frac{\partial}{\partial x} \right)^2 + V(x) \right] \psi(x) = E \psi(x)$$

$$\left\{ \dots + \left[ \frac{1}{2} \left( \frac{\partial}{\partial x} \right)^2 + V(x) \right] \psi(x) + \dots \right\}$$

The wave function of a system of particles is given by the many-body wave function. The wave function of a system of particles is given by the many-body wave function. The wave function of a system of particles is given by the many-body wave function.

$$\dots + \left[ \frac{1}{2} \left( \frac{\partial}{\partial x} \right)^2 + V(x) \right] \psi(x) + \dots$$

in which

$$\left[ \frac{1}{2} \left( \frac{\partial}{\partial x} \right)^2 + V(x) \right] \psi(x) = E \psi(x)$$



The approximation to the probability for gamma-decay of the isomeric state given above was based on Bethe's<sup>14</sup> assumption of a uniform-charge distribution throughout the nucleus. Various other models have been assumed for this derivation. Hebb and Uhlenbeck<sup>15</sup> have assumed the radiation to be due to the electromagnetic field of a single alpha-particle moving in a potential well formed by the nucleus. Their result shows approximately the same dependence on the multipole order but includes a dependence on the charge of the nucleus. They give for the transition probability of the  $2^\ell$  electric or  $2^{\ell-1}$  magnetic radiation:

$$\lambda = 8 \left( \frac{1}{\kappa} \right) \left( \frac{\ell+1}{\ell} \right) \frac{e^2}{\hbar} \left( \frac{(r/\kappa)^{2\ell}}{2(1.3.5 \dots (2\ell+1)^2)} \right)$$

Flügge<sup>16</sup> does not consider the charge distribution performing a linear oscillation, but instead he pictures the radiation arising from a rotational excitation of a charged drop. This leads to another expression similar to others but differing in the constants arising from the nuclear properties and is of the form:

$$\lambda = Z^2 \frac{e^2}{\hbar c} \frac{\hbar}{\Theta} \frac{E}{M c^2} (r/\kappa)^{2\ell}$$

where  $\Theta$  is the moment of inertia and  $M$  the rest mass of the nucleus.

The accuracy of any of these formulae is sufficient to determine the  $\ell$  value of the transition in most cases because of the vast dif-



ference in lifetimes for different multipole-order transitions. However, an error of as much as  $10^\ell$  to  $10^{2\ell}$  may be expected due to the inaccuracy of the particular model. None of these models appear at present to have much advantage over the others.

#### ANGULAR MOMENTUM SELECTION RULE

By a consideration of the fields of the region in which they do not decay as  $R^{-1}$  close to the source, Heitler<sup>17</sup> has shown that quantization of these fields results in the radiation of a  $2^\ell$  electric or magnetic pole having an angular momentum of  $\ell \hbar$  with respect to the multipole origin.

Since vector angular momentum of the nucleus must be conserved, the emission of radiation changes the angular momentum in accordance with the multipole order of the radiation. If the initial and final states of the nucleus differ by more than one unit of momentum in absolute magnitude, this places a lower limit on the order of the multipole. Conversely, if the lifetime of the excited state indicates that the lowest multipole order present is  $2^\ell$ , it can be stated that  $|I| - |I'| = \ell$ .

Although  $2^\ell$  may be the lowest-order multipole radiation possible, higher-order radiation is of course also possible up to the limit determined by  $|I| + |I'|$ . However, barring a coincidence of charge distribution that reduces the strength of the  $2^\ell$  pole far below that which would be predicted from the size of the nucleus, only the lowest-order radiation would be observed because of its much greater probability.

The first part of the paper is devoted to a review of the literature on the subject of the structure of the nucleus. It is found that the most common view is that the nucleus is a collection of nucleons, which are themselves made up of quarks and gluons. This view is based on the fact that the nucleon has a spin of  $\frac{1}{2}$ , which can be explained if it is made up of three quarks, each with a spin of  $\frac{1}{6}$ . The quarks are held together by gluons, which are the carriers of the strong interaction.

The second part of the paper is devoted to a discussion of the experimental evidence for the existence of quarks and gluons. It is found that there is a wealth of evidence from a variety of experiments, including deep inelastic scattering, which strongly supports the existence of quarks and gluons.

The third part of the paper is devoted to a discussion of the theoretical models for the structure of the nucleus. It is found that there are a number of different models, each of which has its own strengths and weaknesses. The most commonly used model is the quark model, which is based on the fact that the nucleon is made up of three quarks. Other models include the bag model, the soliton model, and the Skyrme model.

The fourth part of the paper is devoted to a discussion of the future of research on the structure of the nucleus. It is found that there are a number of interesting problems that remain to be solved, and that there is a need for further experimental and theoretical work.

## PARITY SELECTION RULE

Another selection rule that must always be obeyed is the conservation of parity in a transition. It can be shown by a consideration of the symmetry properties of the eigenfunction of the nucleus that emission of a  $2^{\ell-1}$  magnetic or  $2^{\ell}$  electric radiation always involves a parity change for the nucleus if  $\ell$  is odd and never if  $\ell$  is even. Thus, although these transitions involve the same probability in the rough derivation above, it is impossible for both to occur between the same two states.

## INTERNAL CONVERSION

Any comparison of these results with theory involves a correction for the competing reaction, internal conversion. Taylor and Mott<sup>18</sup> have shown that internal conversion, being a one-step process and not a photoelectric effect of the outgoing gamma-ray on the atomic electrons, is in fact a competing reaction reducing the lifetime of the excited nucleus. Therefore, it is correct to define the internal-conversion coefficient as the ratio of the conversion electrons to the number of gamma-ray quanta and not as the ratio to their sum.

The calculation of these coefficients involves an evaluation of the probability of transmitting to the atomic electrons the excitation energy of the nucleus by a perturbation of their wave functions, this perturbation being caused by a multipole in the nucleus of such strength that it radiates one quantum per second. Since the fields due to the higher multipole orders decrease much more rapidly with distance than do

the first of these is the fact that the probability of a collision between two particles is proportional to the square of the relative velocity. This is because the relative velocity is a vector, and the probability of a collision is proportional to the square of the magnitude of the vector. The second of these is the fact that the probability of a collision is proportional to the cross-section of the particles. This is because the cross-section is a measure of the area of the particles, and the probability of a collision is proportional to the area of the particles. The third of these is the fact that the probability of a collision is proportional to the number of particles. This is because the probability of a collision is proportional to the number of particles, and the probability of a collision is proportional to the number of particles.

# INTERNAL COLLISIONS

Any collision of two particles with their centers a certain distance apart is a collision. This is because the probability of a collision is proportional to the square of the relative velocity. This is because the relative velocity is a vector, and the probability of a collision is proportional to the square of the magnitude of the vector. The second of these is the fact that the probability of a collision is proportional to the cross-section of the particles. This is because the cross-section is a measure of the area of the particles, and the probability of a collision is proportional to the area of the particles. The third of these is the fact that the probability of a collision is proportional to the number of particles. This is because the probability of a collision is proportional to the number of particles, and the probability of a collision is proportional to the number of particles.

those of the lower orders, this factor provides another check on the order of an observed transition.

Such a calculation in the general case is so complicated that the formulae derived are very restricted in their application. Gancoff and Morrison<sup>19</sup> have obtained expressions for the case in which the emitted electrons can be treated nonrelativistically and in the relativistic case in which the binding energy of the electrons in the shell can be neglected. However, numerical integration of the wave functions by Rose<sup>20</sup> shows that, even in this limited region, the predicted values may be in error by a factor of three or more especially for the higher-order multipoles and magnetic conversion. There are several other approximate formulae available, but these are no better when checked with Rose's data. Therefore, at the present time, all calculations of internal conversion coefficients must involve numerical integration of the Schrodinger equation.

The accurate experimental determination of the internal conversion coefficient is difficult because of the uncertainty of the relative efficiencies of the detectors for electrons and gamma-rays. The ratio of the coefficients for the K and L shells is much more accurately determined and is a more sensitive function of the transition, particularly in separating electric and magnetic transitions of similar probabilities. For example, gold has a measured K to L ratio of 3.4. Assuming electric  $2^4$  transition gives 0.51 for this factor, and a magnetic  $2^3$  pole has 4.8. The transition is therefore considered to be magnetic.

The present work is a study of the properties of the  $\beta$ -transition in the  $^{14}\text{C}$  nucleus. The  $\beta$ -transition is a transition in which the nucleus changes from one state to another by the emission of a  $\beta$ -particle. The  $\beta$ -transition is a transition in which the nucleus changes from one state to another by the emission of a  $\beta$ -particle. The  $\beta$ -transition is a transition in which the nucleus changes from one state to another by the emission of a  $\beta$ -particle.



Axel and Dancoff<sup>21</sup> have compared the lifetimes of 53 known isomers with the theoretical lifetimes predicted by the Weissacker hypothesis corrected for internal conversion and find that these isomers do in fact fall into groups characteristic of  $\ell = 4$  and  $\ell = 5$  spin change, with one case, that of  $\text{Pb}^{204}$ , corresponding to  $\ell = 6$ . This agreement indicates that the hypothesis is valid.

### NEUTRON EXCITATION OF METASTABLE LEVELS

The neutron excitation of a metastable state is a special case of inelastic scattering of neutrons. The process is shown diagrammatically in Figure 2. On the left is shown the bombarded nucleus with mass number  $A$ , and on the right is the compound nucleus with mass number  $A + 1$  more tightly bound by the binding energy of the additional particle (on the order of 8 Mev). Nucleus  $A$  has a ground state  $G$  and a first excited level  $E$ .

Bombardment by a neutron with energy less than the energy of level  $E$  is shown by the dotted line. In this case, the compound state can emit a neutron leaving the nucleus  $A$  only in the ground state. However, if the bombarding neutron has a higher energy than does the excited level, the compound nucleus can decay to level  $E$  or to the ground state, as shown by the solid lines. The lowest neutron energy that excites level  $E$  is the energy of that level, provided the neutron is able to carry the difference in angular momentum between states  $G$  and  $E$ . If this is not the case, it may be necessary to excite a higher state  $E'$ , whose angular momentum lies between that of  $E$  and  $G$ . Level  $E$  may then be excited by the emission of a gamma-ray by level  $E'$ .



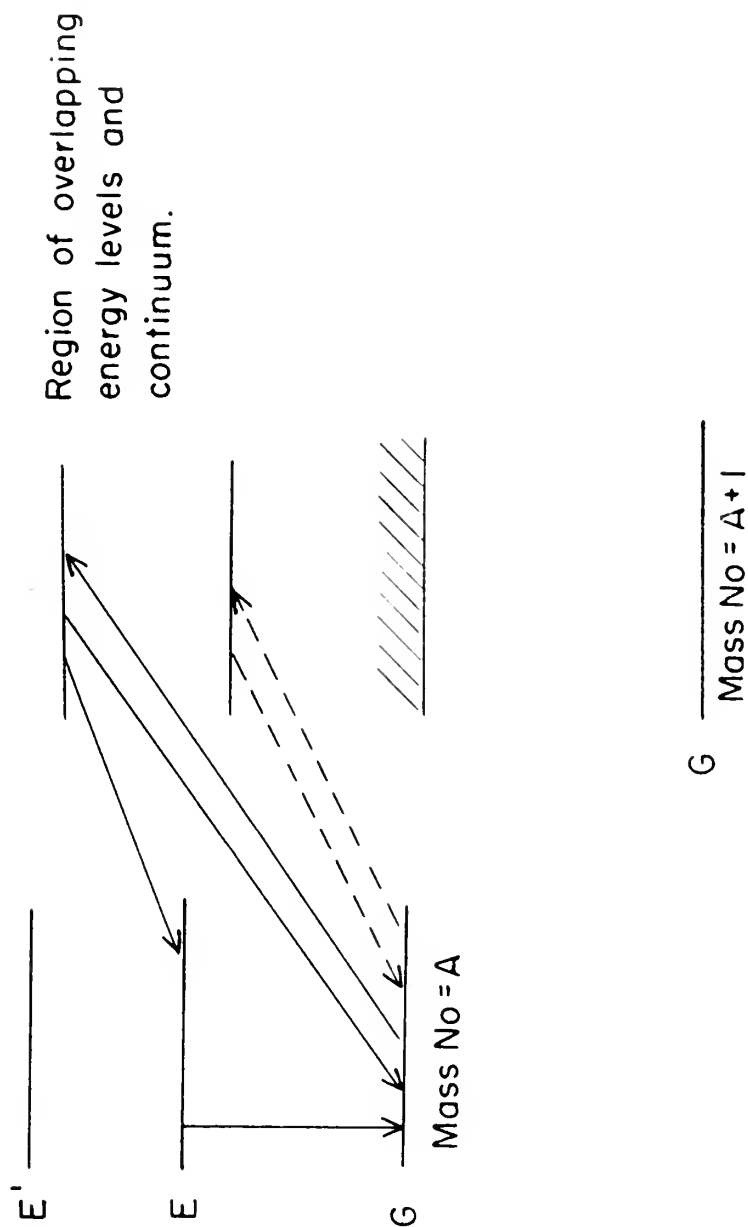


Figure 2  
SCHEMATIC DIAGRAM of NEUTRON SCATTERING with NEUTRON  
ENERGY LESS (broken lines) and GREATER (solid lines) THAN  
FIRST EXCITED LEVEL  $E$ .



The cross section for exciting level  $\ell$  is the product of the cross section of exciting the compound nucleus,  $\sigma_c$ , and the probability,  $W_\ell$ , of that nucleus decaying to level  $\ell$ .

Blatt and Weisskopf<sup>22</sup> have derived an expression for the cross section for formation of the compound nucleus as a function of the energy and orbital momentum of the neutron with respect to the target nucleus. This is given to be:

$$\sigma_c(\ell) = (2\ell + 1) \pi \lambda^2 T_\ell$$

where  $\lambda$  is the wave length of the incident neutron and  $T_\ell$  is the transmission coefficient for the neutron through the "centrifugal" potential and also includes the reflection due to the energy discontinuity at the nuclear surface.

Assuming a square potential well for the nucleus, the transmission coefficient is shown to be:

$$T_\ell \approx 4 \frac{x}{X} v_\ell$$

for the case in which the wave number  $K$  of the neutron in the nucleus is large compared with the wave number  $k$  outside the nucleus. In this expression  $x = kR$  and  $X = KR$ , where  $R$  is the nuclear radius and  $v_\ell$  is a factor determined by the wave function of the neutron beam at the surface of the nucleus.

The values of  $v_\ell$  may be calculated from a tabulation of Blatt and Weisskopf giving:

1. The first step is to identify the problem or question that needs to be answered. This involves understanding the context and the specific requirements of the task.

...this is given as follows:

$$S_T S_{T+n} (I + \lambda S) = (I)_{T+n}$$

where  $\lambda$  is the wavelength of the incident neutron and  $\ell$  is the transmission coefficient for the neutron through the "central" potential and also includes the reflection due to the energy discontinuity at the nuclear surface.

Assuming a square potential well for the nucleus, the transmission coefficient is shown to be:

$$e^V \frac{x}{t} d \approx e^T$$

and therefore giving:

The value of  $\gamma$  may be calculated from a tabulation of Blatt

of the neutron beam at the surface of the neutron.

nuclear radius and  $\gamma$  is a factor determined by the wave function

nuclear. In this expression  $r = R_0$  and  $k = k_0$ , where  $k$  is the

nuclear in large compared with the wave number  $k$  outside the

for the case in which the wave number  $k$  of the neutron in the

$$v_0 = 1$$

$$v_1 = x^2/(1 + x^2)$$

$$v_2 = x^4/(9 + 3x^2 + x^4)$$

$$v_3 = x^6/(225 + 45x^2 + x^4 + x^6)$$

$$v_\ell \rightarrow x^{2\ell} / [1.3.5 \dots (2\ell - 1)]^2$$

The last expression gives the value of  $v_\ell$  in the limit  $x \ll \ell$ .

It should be noted that the angular momentum a neutron can carry into the compound nucleus for a given energy is much greater than would be predicted from a simple quantization of the impact parameter. An 800-kev neutron incident on  $\text{Au}^{197}$  can react only when it has orbital angular momentum  $\ell = 0$  or  $\ell = 1$ , according to the naive approach. Actually, the cross section for  $\ell = 2$  is greater than for  $\ell = 0$  and over half that for  $\ell = 1$ .  $\ell = 3$  is more than one-tenth and even  $\ell = 4$  is more than one-hundredth of the  $\ell = 1$  value.

The probability for decay to a given state from the compound nucleus follows from a consideration of the reciprocity theorem which states that

$$\sigma(A \rightarrow B)/\lambda_A^2 = \sigma(B \rightarrow A)/\lambda_B^2$$

connects the cross section for a transition from state A to state B with the reverse transition. Neglecting all methods of decay of the compound nucleus other than neutron emission, the fraction of the compound nuclei which decays to state 1 with energy  $E_1$  above the ground state in competition with  $n$  other states 1 of energy  $E_1$  is given by:

$$\begin{aligned} & \psi(x) = \sum_{l=0}^{\infty} \frac{(-1)^l}{l!} \left( \frac{d}{dx} \right)^l \psi(0) \\ & \psi(x) = \sum_{l=0}^{\infty} \frac{(-1)^l}{l!} \left( \frac{d}{dx} \right)^l \psi(0) \end{aligned}$$

The last expression gives the value of  $\psi$  in the limit  $x \rightarrow 0$ .  
 It should be noted that the function  $\psi(x)$  is a function of  $x$  only.  
 into the compound nucleus for a given energy is much greater than would  
 be predicted from a simple distribution of the target parameter. An  
 800-mev neutron incident on  $^{235}\text{U}$  can react only when it has sufficient  
 angular momentum  $l = 0$  or  $l = 1$ , according to the above argument.  
 Actually, the cross section for  $l = 2$  is greater than for  $l = 0$   
 and over half that for  $l = 1$ .  $l = 3$  is more than one-tenth that  
 even  $l = 1$  is more than one-tenth that of the  $l = 1$  value.  
 The probability for decay to a given state from the compound  
 nucleus follows from a consideration of the reciprocity theorem which  
 states that

$$\sigma_{A \rightarrow B}(E) = \sigma_{B \rightarrow A}(E)$$

connects the cross section for a transition from state A to state B  
 with the reverse transition. Neglecting all effects of decay of the  
 compound nucleus other than neutron emission, the transition of the com-  
 pound nucleus which decays to state A with a rate  $\Gamma_A$  above the ground  
 state is comparable with a other states  $\Gamma_B$  of energy  $E_B$  is given



$$P_1 = \frac{(E - E_1) \sigma_c(1)}{\sum_{i=1}^n (E - E_i) \sigma_c(i)}$$

where  $\sigma_c(i)$  is the cross section for the formation of the compound nucleus from level  $i$  and  $E$  is the energy available for the transition from the compound nucleus to the ground state of the product nucleus.

In a small energy interval just above the threshold for level "1" the sum in the denominator will change only slightly, so that in this interval the probability is proportional to  $(E - E_1) \sigma_c(1)$ . As the energy of the compound nucleus is increased, the increase in the sum can no longer be neglected, and the probability will be less than predicted by the proportionality.

An inspection of the form of  $\sigma_c^{(\ell)}$  in the vicinity of the threshold shows that for the case  $\ell = 0$  the cross section  $\sigma_c^{(0)}$  decreases as  $(E - E_{th})^{-1/2}$ ; therefore, the probability of decay to that state increases as  $(E - E_{th})^{1/2}$ . For  $\ell = 1$ , for the neutron emitted in the decay, the probability increases as  $(E - E_{th})^{3/2}$  and in general as  $(E - E_{th})^{(\ell + 1/2)}$ . Thus, it is easily recognized if the decay to an excited state is accomplished by the emission of an  $\ell = 0$  neutron because the excitation curve will approach the threshold with a vertical tangent; whereas in cases of higher  $\ell$ , the tangent will be horizontal.

This type of calculation applies directly to the case in which the compound nucleus decays to the metastable state itself. In many

where  $\sigma_0^{(1)}$  is the cross section for the formation of the compound nucleus from level 1 and  $E$  is the energy available for the reaction from the compound nucleus in the ground state of the product nucleus.

In a small energy interval just above the threshold for level "1" the sum in the denominator will change only slightly, so that in this interval the probability is proportional to  $(E - E_1)^{1/2}$ . As the energy of the compound nucleus is increased, the increase in the sum can no longer be neglected, and the probability will be less than predicted by the proportionality.

An inspection of the form of  $\sigma_0^{(0)}$  in the vicinity of the threshold shows that for the case  $\ell = 0$  the cross section  $\sigma_0^{(0)}$  decreases as  $(E - E_{th})^{-1/2}$ ; conversely, the probability of decay to that state increases as  $(E - E_{th})^{1/2}$ . For  $\ell = 1$ , for the neutron emitted in the decay, the probability increases as  $(E - E_{th})^{3/2}$  and in general as  $(E - E_{th})^{(\ell + 1/2)}$ . Then, it is easily recognized if the decay to an excited state is accomplished by the emission of an  $\ell = 0$  neutron because the excitation curve will approach the threshold with a vertical tangent; whereas in cases of higher  $\ell$ , the tangent will be horizontal.

This type of calculation applies directly to the case in which the compound nucleus decays to the metastable state itself. In many

cases, however, this transition is so improbable because of spin changes involved that the compound nucleus decays to an excited state with an intermediate spin, and that excited state decays in turn to the metastable level. The cross section for production of the isomer must then be corrected considering the relative probability of decay from the excited state to the metastable state and the other available levels. For this, the calculations described earlier in this chapter according to the Weissacker hypothesis may be used.

#### COMPARISON OF NEUTRON AND PHOTON EXCITATION

Neutron and photon excitation of levels above the ground state differ in two fundamental respects. Since a neutron is re-emitted in neutron excitation, it is not necessary that the neutron have exactly the energy of the level, whereas, in the case of photons, the excitation is a line absorption. Hence, for photons, it is necessary to use a broad spectrum energy source, and increasing the photon energy gives an isochromat of the source. This makes the shape of the excitation curve dependent upon the photon source and not upon the excitation process.

The second difference is found in consideration of the angular momentum that can be carried in to change the nuclear spin from that in the ground state to that in the excited state. A dipole radiation can contribute only one unit and a quadrupole only two units. Excitation by higher-order multipole radiation is so unlikely that it is not detectable in the ordinary investigations. The same rules that make the transition from an excited state to the ground level by high

...the excited state ... the ground state ... the metastable level. The cross section for production of the ... must then be corrected considering the relative probability of decay from the excited state to the metastable state and the other available levels. For this, the calculations described earlier in this chapter according to the following assumptions may be used.

#### COMPARISON OF NEUTRON AND PHOTON EXCITATION

Neutron and photon excitation of levels above the ground state differ in two fundamental respects. Since a neutron is included in neutron excitation, it is not necessary that the neutron have exactly the energy of the level, whereas, in the case of photon, the excitation is a line absorption. Hence, for photons, it is necessary to use a broad spectrum energy source, and increasing the photon energy gives an improvement of the source. This makes the shape of the excitation curve dependent upon the photon source and not upon the excitation process.

The second difference is found in consideration of the angular momentum that can be carried in to change the nuclear spin from that in the ground state to that in the excited state. A dipole radiation can contribute only one unit and a quadrupole only two units. Higher order multipole radiation is so unlikely that it is not detectable in the ordinary investigation. The same rules that apply the transition from an excited state to the ground level by light

multipole radiation improbable hold for the case of exciting that state from the ground level by high-order multipole radiation. Therefore, it is impossible to excite a metastable state of moderate lifetime directly by photons.

However, neutrons may carry in several units of angular momentum depending upon their energy and the size of the target nucleus. In the case of  $\text{Au}^{197}$ , a 600-kev neutron can change the spin of the nucleus four units and is able to excite the metastable state directly. On the other hand, neutrons can also carry in small angular momentum changes with a high degree of probability, so that any state which can be excited by photons can also be excited by neutrons; and, in addition, neutrons can excite many states which cannot be excited by photons.

in the case of a single state, the probability of a transition from the ground state to an excited state is proportional to the square of the matrix element of the transition operator between the two states. This is the case for a single state, but for a continuous spectrum of states, the probability of a transition is proportional to the square of the matrix element of the transition operator between the ground state and the continuous spectrum of states.

However, the transition probability is not zero for a continuous spectrum of states. In the case of a continuous spectrum, the probability of a transition is proportional to the square of the matrix element of the transition operator between the ground state and the continuous spectrum of states. This is the case for a continuous spectrum, but for a discrete spectrum of states, the probability of a transition is proportional to the square of the matrix element of the transition operator between the ground state and the discrete spectrum of states. In the case of a discrete spectrum, the probability of a transition is proportional to the square of the matrix element of the transition operator between the ground state and the discrete spectrum of states. This is the case for a discrete spectrum, but for a continuous spectrum of states, the probability of a transition is proportional to the square of the matrix element of the transition operator between the ground state and the continuous spectrum of states.

photons. The probability of a transition from the ground state to a continuous spectrum of states is proportional to the square of the matrix element of the transition operator between the ground state and the continuous spectrum of states. This is the case for a continuous spectrum, but for a discrete spectrum of states, the probability of a transition is proportional to the square of the matrix element of the transition operator between the ground state and the discrete spectrum of states. In the case of a discrete spectrum, the probability of a transition is proportional to the square of the matrix element of the transition operator between the ground state and the discrete spectrum of states. This is the case for a discrete spectrum, but for a continuous spectrum of states, the probability of a transition is proportional to the square of the matrix element of the transition operator between the ground state and the continuous spectrum of states.

### III. EXPERIMENTAL EQUIPMENT

#### NEUTRON SOURCE

The neutrons used for activation of the metastable state were obtained from the  $\text{Li}^7(\text{p},\text{n})\text{Be}^7$  reaction, using protons from the M.I.T. Rockefeller generator. This reaction was chosen because it has a comparatively large cross section and provides nearly monoenergetic neutrons..

Since it was desired to study isomeric production near the threshold for this process, it was desirable that the reaction be endoergic so that neutrons with low energies could be obtained. With a  $Q$ -value of  $-1.63$  Mev, the  $\text{Li}^7(\text{p},\text{n})$  reaction satisfies this condition.

The presence of a lower-energy neutron group with relative intensity of about 10 percent has recently been reported<sup>23</sup> at 384 keV below the main group. Since the excitation curve for the metastable state rises quite rapidly, this lower-energy group causes no ambiguity in the results. It is of interest that the  $\text{Au}^{197}$  excitation curve (Figure 13) shows a slight rise within the statistical error at about 430 keV above threshold; this may be due to this effect, but the results are not conclusive.

The target was prepared by evaporating metallic lithium (92.6 percent  $\text{Li}^7$ ) on a 10-mil tantalum backing. To prevent the proton beam from boiling the lithium off, the target was rotated with the beam striking approximately one inch off center. An even coating was obtained by rotating the target while the lithium was being deposited.

THEORY OF THE REACTION

THEORY OF THE REACTION

The mechanism used for activation of the metastable state was obtained from the  $IL(p,n)$  reaction, which produces from the  $IL(p,n)$  reaction. This reaction was chosen because it has a comparatively large cross section and provides nearly monoenergetic neutrons.

Since it was desired to study fissionable production near the threshold for this process, it was desirable that the reaction be endothermic so that neutrons with low energies could be obtained. With a  $Q$ -value of  $-1.65$  mev, the  $IL(p,n)$  reaction satisfies this condition. The presence of a lower-energy neutron group with relative intensity of about 10 percent has recently been reported<sup>13</sup> at 130 kev below the main group. Since the excitation curve for the metastable state rises quite rapidly, this lower-energy group caused no difficulty in the results. It is of interest that the  $IL(p,n)$  excitation curve (Figure 13) shows a slight rise within the statistical error at about 130 kev above threshold; this may be due to this effect, but the results are not conclusive.

The target was prepared by evaporating metallic lithium (99.5 percent  $IL$ ) on a 10-mil tantalum backing. To prevent the lithium from boiling the lithium off, the target was rotated with the beam striking approximately one inch off center. An even coating was obtained by rotating the target while the lithium was being deposited.



Thus, the problem of installing the target without the lithium's being oxidized was eliminated.

The thickness of the targets used was of the order of 15 to 20  $\mu$ ev, as measured by the conventional method<sup>21</sup> of taking the thickness to be the energy between the neutron threshold and the first geometrical peak in the yield curve at 0 degrees.

#### ROCKEFELLER GENERATOR

The proton accelerator was an electrostatic generator originally used to accelerate electrons. During the past two years, this generator has been converted into a positive-ion accelerator by the Nuclear Shielding Group. Unfortunately, the beam emerged in a room located under ground so that the scattered neutron flux is quite high. The target was located 35 inches from the analyzing magnet and only 39 inches from the concrete floor. In other directions, the situation was considerably more favorable. For the measurements being reported, however, scattered neutrons offered no problem because the exposures were made in the region of high direct flux close to the target, and the scattered flux, being of lower energy, had a smaller cross section for interaction.

The beam was defined by crossed slits above the analyzing magnet and by horizontal slits beyond. Openings of 1 millimeter in the exit slits corresponded to an energy resolution of 0.1 percent in the proton beam. However, for the measurements on gold, it was necessary to open the slits wider to obtain sufficient neutron flux.

...the ... of the ...

...the ... of the ...

The ... of the ... was ...

...as measured by the ... method ...

...to be the ... between the ... and the ...

...peak in the yield curve at 0 ...

# ROCKWELL DEVELOPMENT

The ... was an ... originally

used to ... . During the ...

...has been converted into a ...

...the ... in a ...

...to that the ...

...is located ...

...from the ... floor. In other ...

...was considerably more ...

...however, ...

...in the ... of light ...

...the ... being of lower ...

for ...

The ... was defined by ...

...and by ...

...is ...

...however, for the ...

...the ...

The proton energies were determined by a generating voltmeter indicating on a 6 inch fan-type microammeter. This meter could be read to 0.1 of a division (about 5 kev in neutron energy), and measurements on the  $\text{Li}^7(\text{p},\text{n})$  threshold indicated that it was reproducible within this amount over the period of a run. Over a period of several weeks, however, the calibration on the generating voltmeter changed by as much as several percent; therefore, it was always checked against the  $\text{Li}^7(\text{p},\text{n})$  threshold (1.882 Mev) at the beginning and the end of each run.

In addition to this calibration point, the circuit has been checked for linearity using  $\text{Li}^7(\text{p}_2,\text{n})$ , in which the proton is accelerated in a singly charged  $\text{H}_2$  molecule, giving a threshold at 3.764 Mev, twice the  $\text{Li}^7(\text{p},\text{n})$  threshold, the  $\text{H}^3(\text{p},\text{n})$  with a threshold at 1.019 Mev, and the  $\text{C}^{13}(\text{p},\text{n})$  with a threshold at 3.236 Mev. It was found that the calibration of the meter against proton energy was linear in the region of interest, although the linear portion did not extrapolate to zero.

From the proton energy, the neutron energy can be calculated by application of conservation of momentum and energy. A tabulation of this calculation prepared by Willard<sup>25</sup> was used in this investigation.

#### LONG COUNTER

The neutron flux was measured, using a long counter of design similar to that of Hanson and McKibben<sup>26</sup>. This counter, shown with dimensions in Figure 3, consists of a cylinder of paraffin shielded by cadmium surrounding a  $\text{BF}_3$  counter. The  $\text{BF}_3$  counter was 1 inch in diameter with an active volume 12 inches long. The filling was of 96 percent enriched  $\text{BF}_3$  at 50 cm. of mercury pressure.



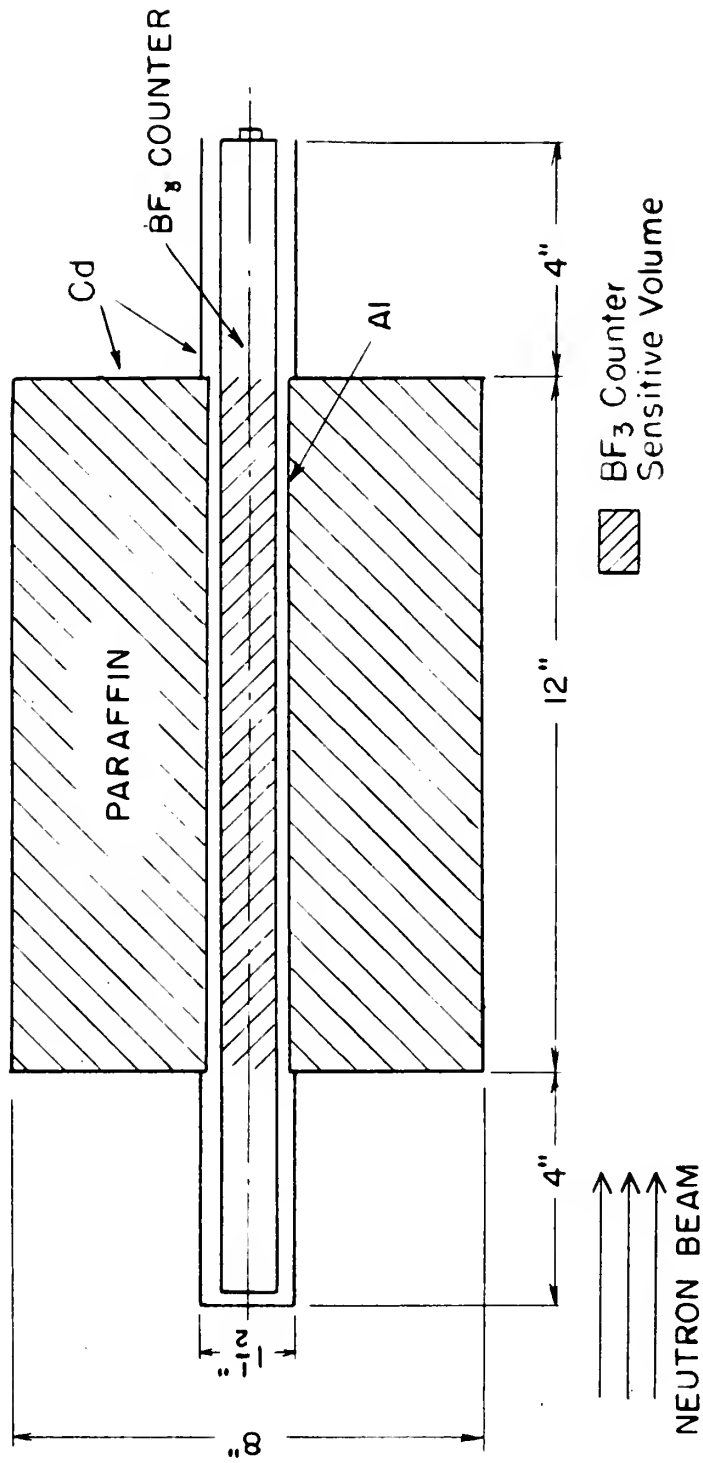


Figure 3. CROSS-SECTION of LONG COUNTER



Willard<sup>25</sup> compared the yield curve of the  $\text{Li}^7(\text{p},\text{n})$  reaction as determined by this long counter with the curve published for a 10-kev target by Hanson, Taschek, and Williams<sup>27</sup>. By assuming their yield curve to be correct, Willard was able to determine a calibration for the long counter. Figure 4 shows the relative response as a function of the energy of the incident neutrons. In addition, he found that, when located one meter from the target at 0 degrees, the counter gave 60 counts per microcoulomb of protons per kev target thickness in the flat portion of the  $\text{Li}^7(\text{p},\text{n})$  yield curve. The target thickness was measured by the initial rise in the yield curve. This gives an absolute calibration of the counter when compared to Hanson's curve.

The associated electronics were of conventional design, consisting of a high-voltage supply, a model 100 linear amplifier, and two scale-of-54 scalars operated in series.

#### SCINTILLATION COUNTER

Because it was hoped to take advantage of the difference in energy between the background and the radiation under investigation, a scintillation spectrometer was constructed. Although this discrimination did not prove feasible, the scintillation counter was used for the measurement of all induced isomeric transitions.

Figure 5 shows a block diagram of the counter setup.

The counter itself was an RCA type 5819 phototube with an optically clear anthracene crystal 0.5 by 2 by 4 centimeters cemented to the tube window with Canada balsam. For increased light reflection,

The associated electronics are of conventional design, consisting of a high-voltage supply, a model 100 linear amplifier, and two 6AL5-6 (2) tubes operated in series.

REINFORCED CONCRETE

Figure 2 shows a block diagram of the counter setup. The measurement of all induced currents was made with the use of a low level amplifier. The amplifier was used for the measurement of the induced currents. The amplifier was used for the measurement of the induced currents. The amplifier was used for the measurement of the induced currents.

The computer itself was an IBM type 7015 prototype with an optical tape as data storage. It was a 100,000 word machine, and it was the only one of its kind in the world. It was the first computer to use optical tape for data storage. It was the first computer to use optical tape for data storage. It was the first computer to use optical tape for data storage.



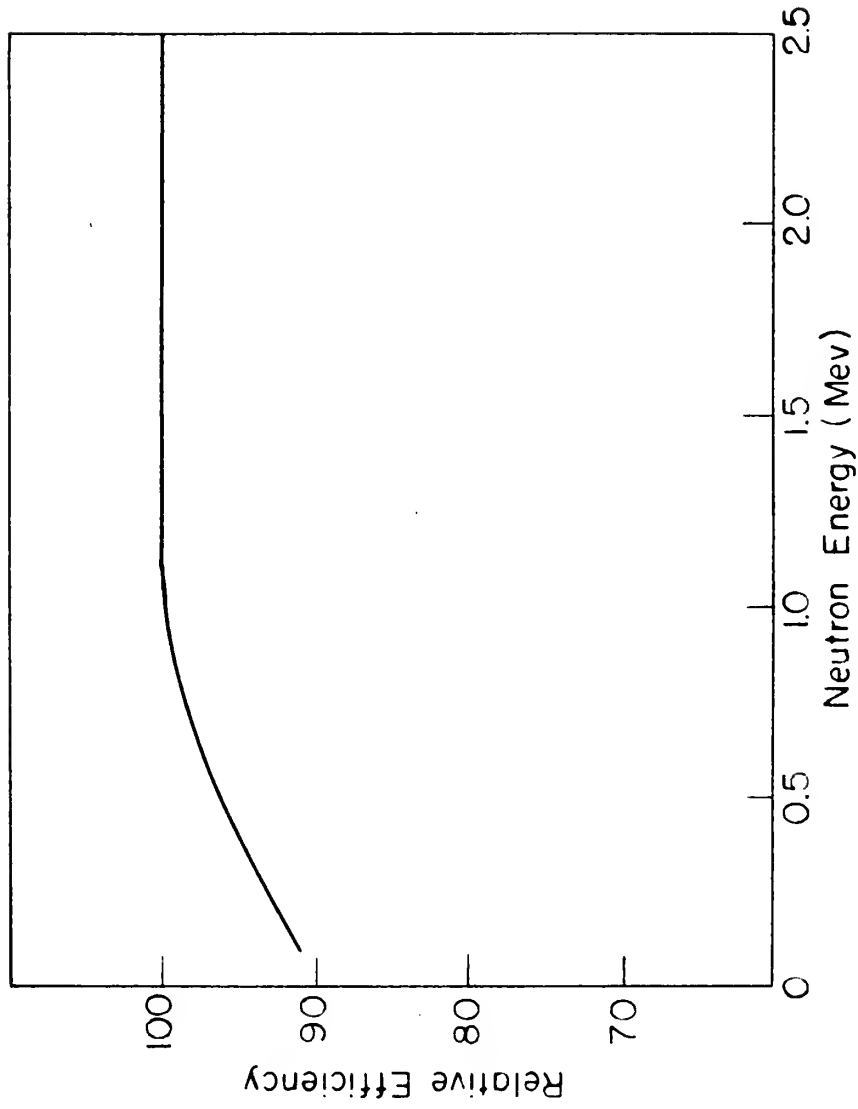


Figure 4  
LONG COUNTER EFFICIENCY for DIFFERENT ENERGY  
NEUTRONS



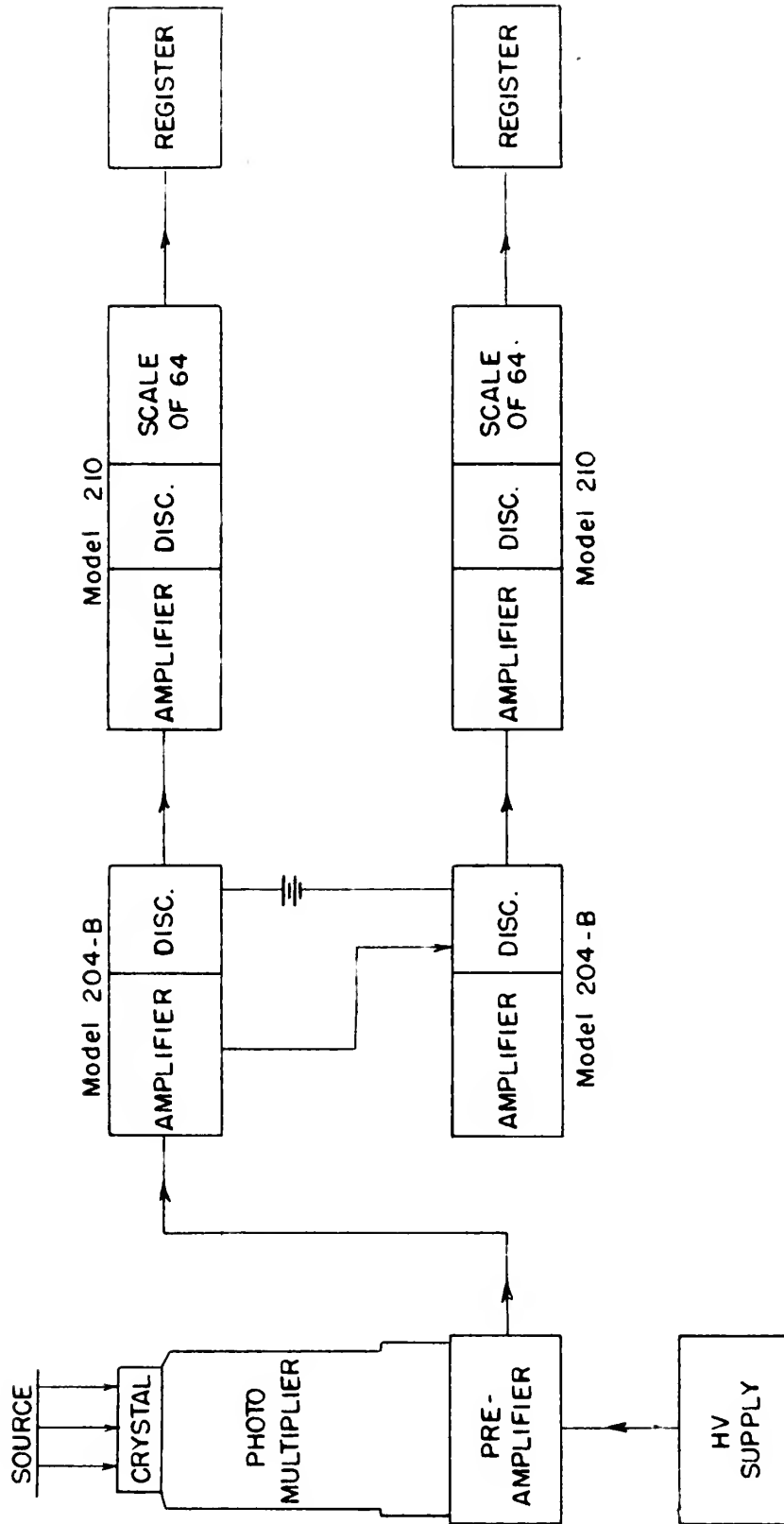


Figure 5  
SCINTILLATION BETA SPECTROMETER



the crystal was covered with thin aluminum foil (1 air cm. thick). The tube and crystal were surrounded on the sides by a 0.040 inch mu metal shield for reducing stray magnetic fields and by 3 inches of lead to reduce the radiation background.

To permit rapid changing of samples, a brass plate containing a slide was fitted on the crystal end of the lead shield. The sample, in the form of a 3-cm. diameter foil, could be placed in the slide and moved to a point opposite the crystal about 3 millimeters from it.

Because of the critical dependence of phototube pulse-height output on the dynode voltages, it is important that the high voltage be kept very constant. The high-voltage supply in the Atomic Instruments Model 105 Decade Scalar was used, and the voltage was monitored with an electrostatic voltmeter.

The phototube signal was fed through a one-tube cathode follower preamplifier into an Atomic Instrument Model 204B linear amplifier. This amplifier contains an integral pulse-height discriminator. Since the discriminator bias control furnished with the amplifier did not permit reproducible settings, it was replaced by a fifteen-turn Beckman helipot. To obtain a differential discriminator, the integral discriminator from another 204B amplifier was fed in parallel with the first discriminator. The voltage for the bias of the second discriminator was taken from the first with a mercury cell in series to provide the window. This system made the window error equal to the variation in the voltage of the series battery instead of the tracking error in two potentiometers. The two discriminators were fed into separate scalars, and the differential count obtained by subtraction.

The signal was then amplified by a 100 dB gain (1000). The  
 this and the signal was then amplified by a 100 dB gain (1000) and  
 shield for shielding against magnetic fields and by 3 inches of lead to  
 reduce the radiation background.

To permit rapid changing of samples, a brass plate containing a  
 slide was fitted on the crystal end of the lead shield. The sample,  
 in the form of a 3-cm. diameter foil, could be placed in the slide and  
 moved to a point opposite the crystal about 3 millimeters from it.

Because of the critical dependence of photoelectron pulse-height  
 output on the dynode voltages, it is important that the high voltage  
 be kept very constant. The high-voltage supply in the Atomic Instru-  
 ments Model 105 Beecle Sealer was used, and the voltage was monitored  
 with an electrostatic voltmeter.

The phototube signal was fed through a two-stage cathode follower  
 preamplifier into an Atomic Instrument Model 201B linear amplifier.  
 This amplifier contains an integral pulse-height discriminator. Since  
 the discriminator bias control furnished with the amplifier did not  
 permit reproducible settings, it was replaced by a fifteen-turn  
 potentiometer. To obtain a differential discriminator, the inte-  
 gral discriminator from another 201B amplifier was fed in parallel with  
 the first discriminator. The voltage for the bias of the second dis-  
 criminator was taken from the first with a movable coil in series to  
 provide the window. This system made the window error equal to the  
 variation in the voltage of the series battery instead of the track-  
 ing error in two potentiometers. The two discriminators were fed into  
 separate scalars, and the differential count obtained by subtraction.

Figure 6 shows the pulse-height distribution obtained from a  $\text{Cs}^{137}$  source. The cesium activity contains a strong 630-kev conversion electron line which provided an excellent energy calibration point for the counter.

Figure 1 shows the relative distribution obtained from a  
 Co<sup>60</sup> source. The central activity contains a strong 130-kev conversion  
 electron line which provides an excellent energy calibration point for  
 the counter.

The spectrum shown in Figure 2 was obtained from a  
 Co<sup>60</sup> source. The central activity contains a strong 130-kev conversion  
 electron line which provides an excellent energy calibration point for  
 the counter.

The spectrum shown in Figure 3 was obtained from a  
 Co<sup>60</sup> source. The central activity contains a strong 130-kev conversion  
 electron line which provides an excellent energy calibration point for  
 the counter.

The spectrum shown in Figure 4 was obtained from a  
 Co<sup>60</sup> source. The central activity contains a strong 130-kev conversion  
 electron line which provides an excellent energy calibration point for  
 the counter.

The spectrum shown in Figure 5 was obtained from a  
 Co<sup>60</sup> source. The central activity contains a strong 130-kev conversion  
 electron line which provides an excellent energy calibration point for  
 the counter.

The spectrum shown in Figure 6 was obtained from a  
 Co<sup>60</sup> source. The central activity contains a strong 130-kev conversion  
 electron line which provides an excellent energy calibration point for  
 the counter.

The spectrum shown in Figure 7 was obtained from a  
 Co<sup>60</sup> source. The central activity contains a strong 130-kev conversion  
 electron line which provides an excellent energy calibration point for  
 the counter.

The spectrum shown in Figure 8 was obtained from a  
 Co<sup>60</sup> source. The central activity contains a strong 130-kev conversion  
 electron line which provides an excellent energy calibration point for  
 the counter.

The spectrum shown in Figure 9 was obtained from a  
 Co<sup>60</sup> source. The central activity contains a strong 130-kev conversion  
 electron line which provides an excellent energy calibration point for  
 the counter.

The spectrum shown in Figure 10 was obtained from a  
 Co<sup>60</sup> source. The central activity contains a strong 130-kev conversion  
 electron line which provides an excellent energy calibration point for  
 the counter.



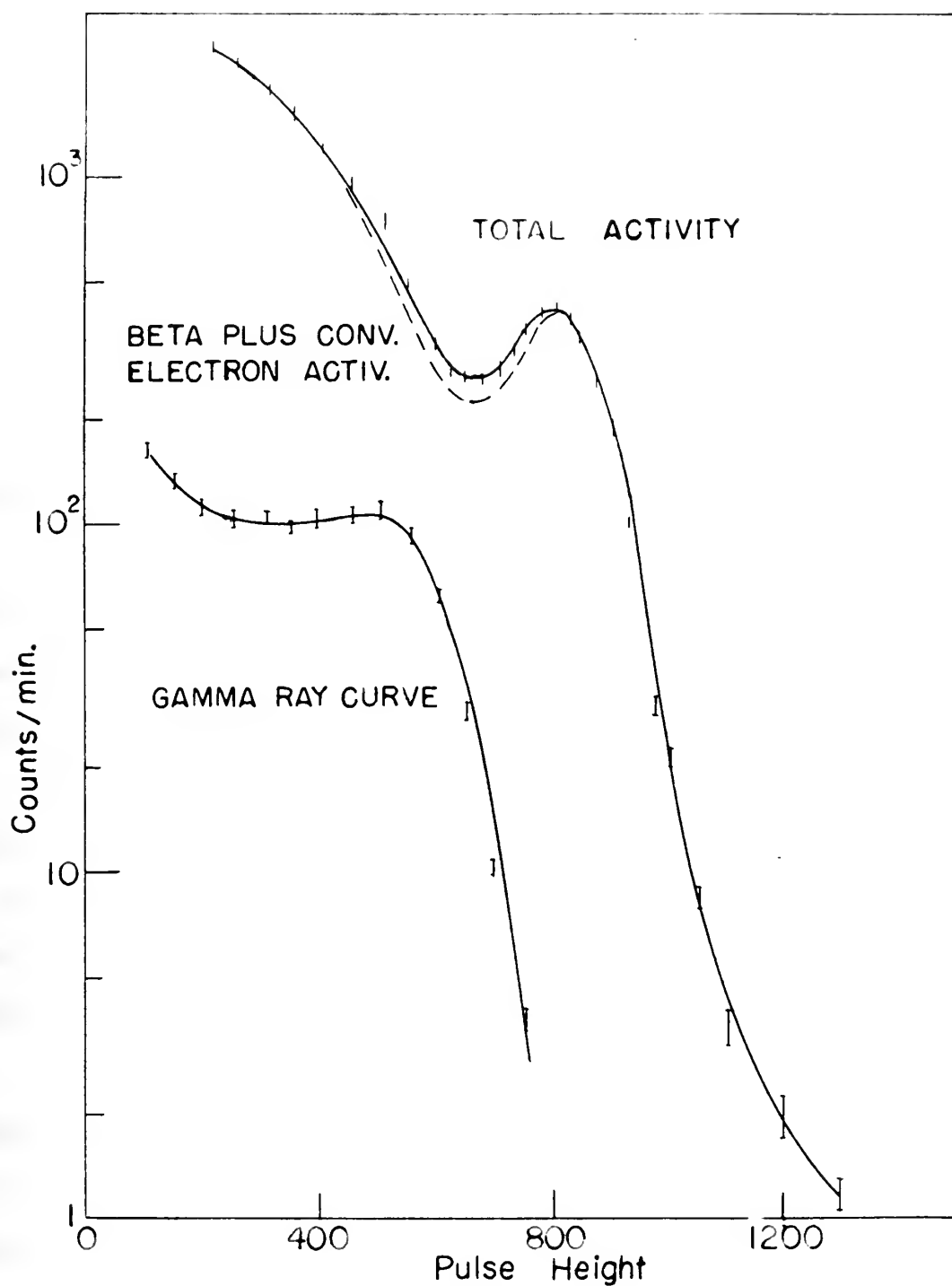


Figure 6

$\text{Cs}^{137}$  DIFFERENTIAL PULSE HEIGHT DISTRIBUTION SHOWING 630 Kev CONV. ELECTRON LINE USED FOR ENERGY CALIBRATION.



## IV. INVESTIGATION OF GOLD

HISTORY OF Au<sup>197</sup>\* EXCITATION

In an article surveying the field in 1941, Mattauch<sup>28</sup> observed that no cases of isomerism had been found for nuclei with a spin  $1/2 < I < 9/2$ . This observation became known as "Mattauch's second rule." The first exception to be found was Au<sup>197</sup> with a spin in the ground state of  $3/2$ . Later results indicate that the metastable state does not decay directly to the ground state, so that technically even this activity does not violate this empirical "rule."

Wiedenbeck<sup>29</sup> in 1945 reported a 7-second metastable state in gold excited by bombarding a gold cathode counter with x-rays. By using a thick gold target and aluminum absorbers, he was able to determine that the approximate energy of this level was 250 kev.

Subsequently, Wiedenbeck<sup>30</sup> investigated the quantum excitation curve for gold using the x-rays produced by monoenergetic electrons incident on a thick target. His results showed a series of levels starting with a threshold at 1.22 Mev and spaced about 0.4 Mev apart. The curve obtained and the levels assigned are shown in Figure 7.

In addition, he reported having excited this level by means of fast neutrons. Using a source of continuous x-rays, he obtained a broad distribution of neutron energies from the Be<sup>9</sup>( $\gamma$ ,n) reaction. The experimental arrangement is shown in Figure 8. In the region of maximum neutron energy from 1.22 to 1.3 Mev, the counting rate in his gold counter was considerably above background and increased linearly with energy in much the same way as with x-rays. He concluded that the

In an article appearing in the field in 1911, Wiedemann<sup>28</sup> observed  
 that in cases of ionization had been found for metal with a spin  
 $1/2 < 1/2$ . This observation became known as "Wiedemann's second  
 rule". The first exception to be found was in 1917 with a spin in the  
 ground state of  $3/2$ . Later results indicate that the metastable state  
 does not decay directly to the ground state, so that technically even  
 this activity does not violate this empirical "rule".  
 Wiedemann<sup>29</sup> in 1915 reported a 7-second metastable state in  
 gold excited by bombarding a gold cathode counter with x-rays. By  
 using a thick gold target and aluminum absorbers, he was able to deter-  
 mine that the approximate energy of this level was 250 kev.  
 Subsequently, Wiedemann<sup>30</sup> investigated the quantum excitation  
 curve for gold using the x-rays produced by monochromatic electrons  
 incident on a thick target. His results showed a series of levels  
 starting with a threshold at 1.55 mev and spaced about 0.1 mev apart.  
 The curve obtained and the levels assigned are shown in Figure 7.  
 In addition, he reported having excited this level by means of  
 fast neutrons. Using a source of continuous x-rays, he obtained a  
 broad distribution of neutron energies from the  $2\alpha(\gamma,n)$  reaction.  
 The experimental arrangement is shown in Figure 8. In the region of  
 maximum neutron energy from 1.55 to 1.9 mev, the counting rate in his  
 gold counter was considerably above background and increased linearly  
 with energy in much the same way as with x-rays. He concluded that the

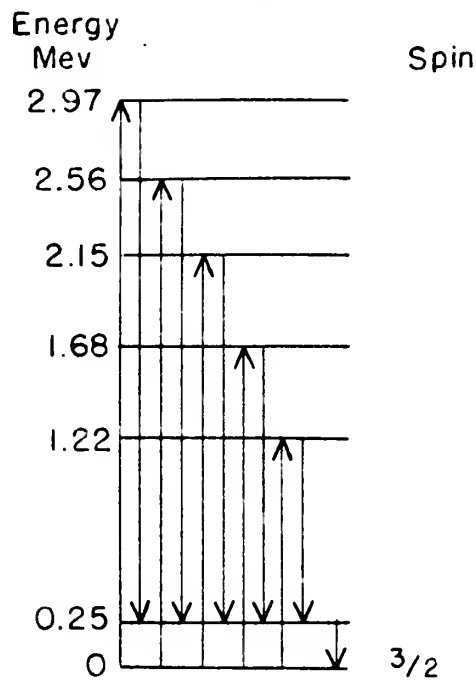
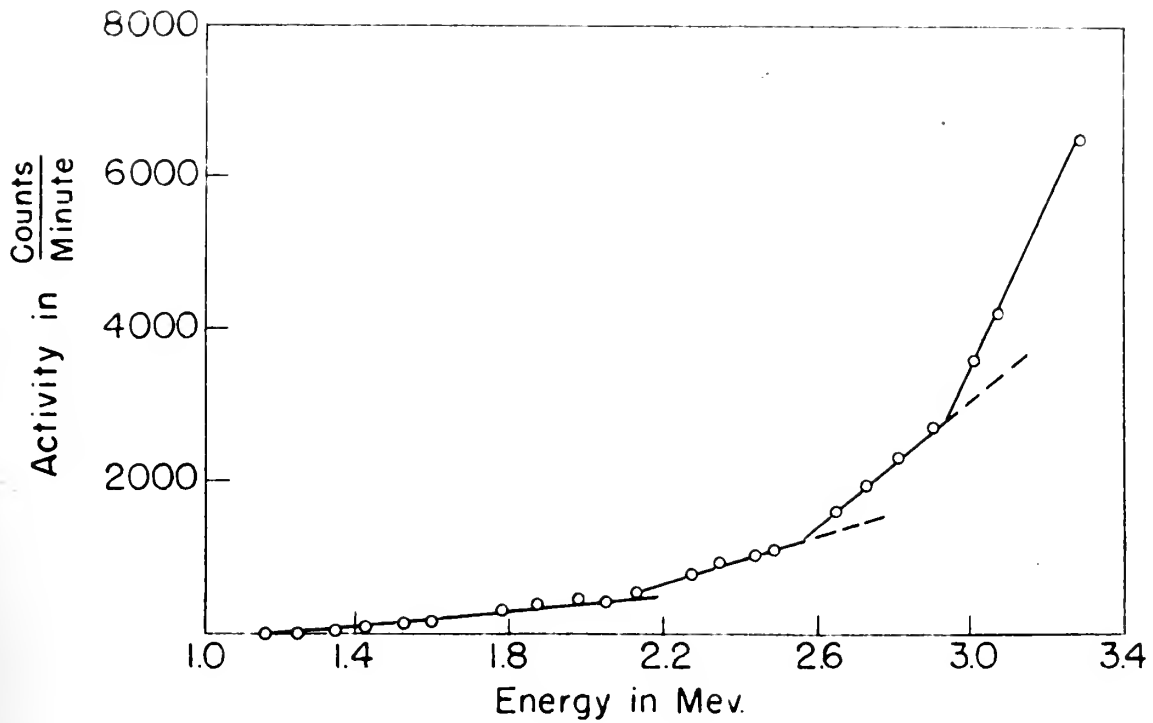


Figure 7  
 QUANTUM EXCITATION CURVE for  $\text{Au}^{197*}$  and LEVELS  
 OBTAINED by WIEDENBECK. (From Phys. Rev. 68, 1 (1945))



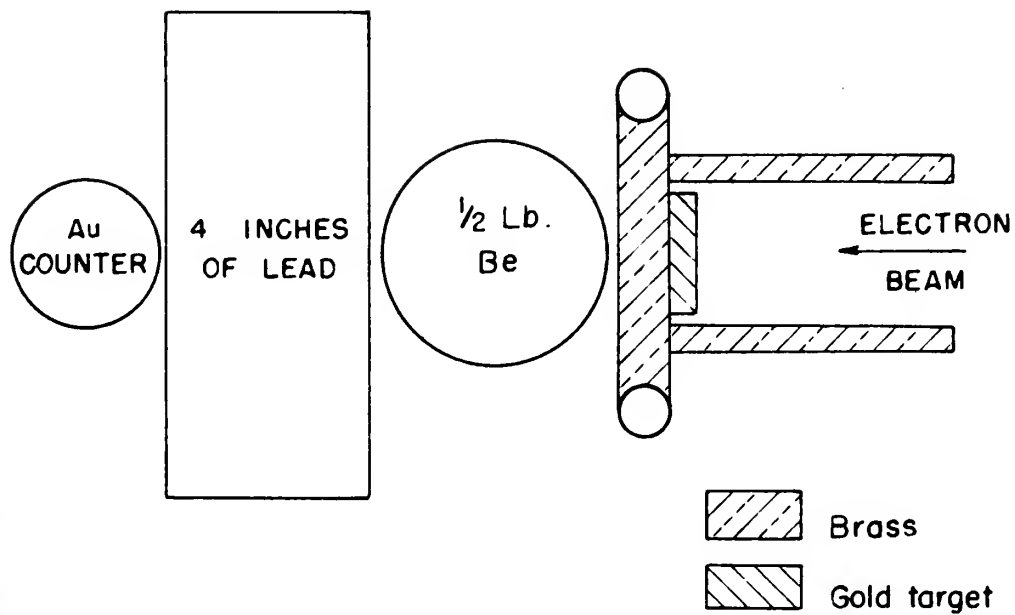


Figure 8

ARRANGEMENT USED by WIEDENBECK to INVESTIGATE NEUTRON EXCITATION of  $\text{Au}^{197}$ .

(From Phys. Rev. 68, 1 (1945))





threshold for neutron excitation was the same as for x-rays. His investigation, however, was limited to the energy interval close to the photon threshold by maximum neutron energy available.

In the determination of the excitation function, using either quanta or particles having a continuous energy distribution, the levels only appear as slight changes in the slope of a curve; hence, the energy assignment and often the existence of the level are uncertain and may even involve a subjective decision. If monoenergetic sources are used, the breaks in the curves are much sharper, and the results are considerably more certain.

#### DESCRIPTION OF THE ENERGY LEVELS IN Au<sup>197</sup>

Because of the complexity of its excited states, the various levels in gold have been the subject of a great deal of nuclear investigation. On the other hand, gold has the great simplification of being monoisotopic with a mass of 197. Another advantage in the present investigation is the absence of any short-lived neutron capture reaction; the only one known leads to Au<sup>198</sup> with a 2.7-day half-life.

The levels in Au<sup>197</sup> fall into three apparently independent groups,<sup>31</sup> with no evidence of transitions between any of the groups, as shown in Figure 9. The levels are shown in three groups to emphasize the improbability of transitions between the groups.

The first group consists of a level at 77 kev that is reached by K-capture from the lower 65-hour isomeric state of Hg<sup>197</sup>. It has been determined that this 77-kev level does not have an appreciable lifetime.

the photon is emitted by an excited electron energy level. The energy interval close to the photon is emitted by an excited electron energy level. In the determination of the excitation function, being either discrete or particles having a continuous energy distribution, the levels only appear as slight changes in the slope of a curve; hence, the energy assignment and often the existence of the level are uncertain and may even involve a subjective decision. If spectroscopic sources are used, the peaks in the curves are much sharper, and the results are considerably more certain.

# DESCRIPTION OF THE ENERGY LEVELS IN <sup>197</sup>Ir

Because of the complexity of the excited states, the various levels in gold have been the subject of a great deal of nuclear investigation. On the other hand, gold has the great simplification of being monoisotopic with a mass of 197. Another advantage in the present investigation is the absence of any short-lived members capable of being observed with a 2.7-day half-life.

The levels in <sup>197</sup>Ir fall into three apparently independent groups, with no evidence of transitions between any of the groups, as shown in Figure 2. The levels are shown in three groups to emphasize the independence of transitions between the groups. The first group consists of a level at 17 keV that is reached by  $\beta$ -capture from the lower  $\beta$ -decay isomeric state of <sup>197</sup>Ir. It has been determined that this 17-keV level does not have an appreciable lifetime.

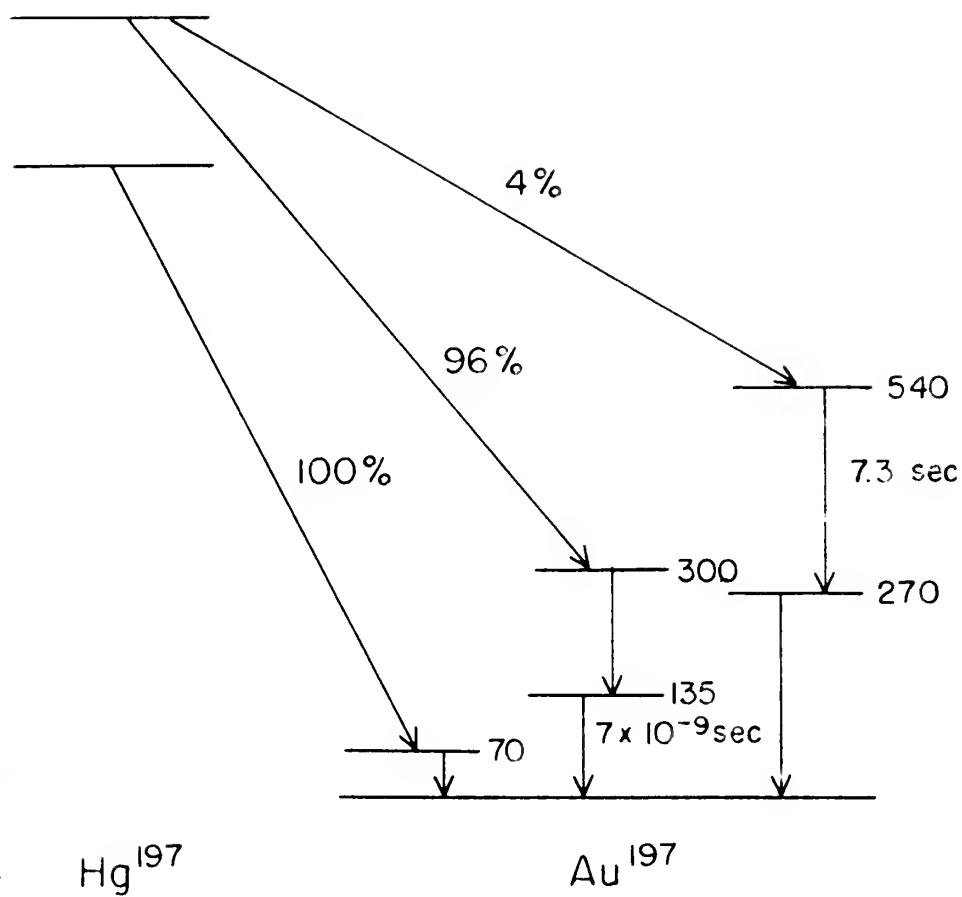


Figure 9

LEVELS in  $\text{Au}^{197}$  as DETERMINED by the  
 DECAY of  $\text{Hg}^{197}$  (Energy in Kev)



The upper isomeric state in mercury with a half-life of 25 hours also decays by K-capture. In 96 percent of the cases, the decay is followed by the emission of a 165-kev gamma-ray to a  $7 \times 10^{-9}$  second isomeric level which in turn decays by the emission of a 135-kev gamma-ray<sup>32,33</sup>. Assuming this transition to be electric quadrupole or magnetic dipole, the Weissacker hypothesis predicts a half-life for the gamma-transition of  $6.5 \times 10^{-9}$  seconds. This neglects the effect of internal conversion on the lifetime, but the calculations of Rose et al.<sup>34</sup> indicate that the conversion coefficient will be less than unity and, hence, not sufficient to reduce the predicted half-life for a higher-order transition below a few microseconds.

The remaining 4 percent of the nuclei in the 25-hour mercury decays to a 7.3-second level which in turn decays by the emission of two internally converted gammas both of about 270 kev<sup>35</sup>. Originally, the lower level was reported to be only of the order of 70 kev<sup>36</sup>, and this value is found in much of the literature. This determination was made by means of an absorption of the conversion electrons in aluminum by Frauenfelder, Huber et al. However, the reinvestigation by members of this group, using a magnetic spectrometer, revealed a coincidence rate in the K-conversion line for 270-kev gammas that was about twenty times the chance coincidence rate. The ratio of K- to L-conversion was also determined as 3.4.

Using the Weissacker calculation of the half-life with an energy of 270 kev, the following values are obtained for several different changes in nuclear angular momenta:

The remaining 1 percent of the nuclei in the 25-hour sample  
 decays to a 7.3-second level which in turn decays by the emission of  
 two internally converted gamma rays both of about 270 keV. Originally,  
 the lower level was reported to be only of the order of 10 keV, and  
 this value is found in much of the literature. This determination was  
 made by means of an absorption of the conversion electrons in aluminum  
 by Evans and al. However, the reinvestigation by  
 Evans and al. using a magnetic spectrometer, revealed a con-  
 siderable rate in the K-conversion line for 270-keV gamma rays that was about  
 twenty times the gamma coincidence rate. The ratio of K- to L-conver-  
 sion was also determined as 3.6.  
 Using the relationship of the half-life with an energy  
 of 270 keV, the following values are obtained for several different  
 changes in nuclear magnetic moments:

and, hence, not sufficient to reduce the predicted half-life for a  
 higher-order transition below a few microseconds.  
 This suggests the effect of  
 gamma-transition of  $0.5 \times 10^{-9}$  seconds. This suggests the effect of  
 nuclear dipole, the Weisskopf hypothesis predicts a half-life for the  
 transition to be about  $10^{-9}$  seconds. This suggests the effect of  
 internal conversion on the lifetime, but the calculations of Rose et  
 al. indicate that the conversion coefficient will be less than unity  
 and, hence, not sufficient to reduce the predicted half-life for a  
 higher-order transition below a few microseconds.

TABLE II

$\Delta$	Parity Change	Half-Life (Seconds)	Electric pole	Magnetic pole
2	no	$2.6 \times 10^{-10}$	$2^2$	$2^1$
3	yes	$5.4 \times 10^{-5}$	$2^3$	$2^2$
4	no	22.	$2^4$	$2^3$
5	yes	$1.6 \times 10^7$	$2^5$	$2^4$

The symbol  $\Delta$  is introduced to characterize an electric  $2^\Delta$  or magnetic  $2^{(\Delta-1)}$  transition, both having the same probability under the Weissacker hypothesis.

From this table, the transition from the 7-second state is evidently of the  $\Delta = 4$  type and, hence, accompanied by no change in parity. However, it is not possible to determine from the half-life whether the transition is an electric  $2^4$  pole which involves a spin change of 4 or is a magnetic  $2^3$  pole with a spin change of 3. The ambiguity is removed by the conversion coefficient data which show the transition to be of the magnetic type<sup>37</sup>.

Frauenfelder<sup>38</sup> reports that the state to which this isomeric level decays has no appreciable lifetime, and Segre and Helmholtz<sup>39</sup> set this lifetime at less than 1 microsecond. Later in this section, it will be shown that this transition cannot be of the  $\Delta = 2$  type, because of parity considerations. In view of the crudeness of the theoretical calculations of lifetimes, the possibility cannot be ruled out that this is a  $\Delta = 3$  transition with a predicted lifetime of 54 micro-

TABLE 1

$\Delta$	Transition Type	Half-life (seconds)	Excitation Energy
2	no	$2.0 \times 10^{-10}$	$2.5$
3	yes	$2.5 \times 10^{-10}$	$2.5$
4	no	25	$2.5$
5	yes	$1.0 \times 10^8$	$2.5$

The symbol  $\Delta$  is introduced to characterize an electric or magnetic  $2(\Delta - 1)$  transition, both having the same multiplicity under the Weisskopf hypothesis.

From this table, the transition from the  $1$ -second state is evidently of the  $\Delta = 1$  type and, hence, accompanied by no change in parity. However, it is not possible to determine from the half-life whether the transition is an electric  $2$  pole which involves a spin change of  $1$  or is a magnetic  $2$  pole with a spin change of  $2$ . The ambiguity is removed by the conversion coefficient data which show the transition to be of the magnetic type.

From this table, it is seen that the state to which this transition level decays has no appreciable lifetime, and hence and therefore not this lifetime at least than  $1$  microsecond. Later in this section it will be shown that this transition cannot be of the  $\Delta = 2$  type, because of parity considerations. In view of the existence of the rotational excitations of lifetimes, the possibility cannot be ruled out that this is a  $\Delta = 2$  transition with a predicted lifetime of  $10^{-10}$  seconds.



seconds. The other possibility corresponds to an electric dipole transition which in general does not occur because of the smallness of the electric dipole moment.

Figure 10 shows the energy levels involving the 7-second metastable level, together with the parity and spin assignments that may be made from neutron excitation of the isomer.

Because the decay of the 7-second level directly to the ground state is not observed, although the energy is twice that for decay in cascade, this transition must have a  $\Delta$  value greater than 4. However, this level may be excited directly by neutrons, as is shown later in this chapter.

A comparison with theory of the experimental cross section for the production of the isomeric state shows that the neutron cannot carry in more orbital angular momentum than  $\ell = 3$ . The shape of the excitation curve shows that the neutron is emitted with  $\ell = 0$ . To be added to this value of  $\ell = 3$  is the contribution of the neutron spin which may be -1, 0, or 1, depending upon the orientation of the spins of the incident and emitted neutrons relative to the orbital momentum. Thus, a  $\ell = 3$  neutron can excite a level with a spin differing from the ground state by 2, 3, or 4 units. This reaction gives a change in parity of the excited state due to the  $\ell$  value being odd for the incident neutron and even for the emitted neutron.

The spin changes of 2 or 3 between the ground and the excited state with a parity change both give a lifetime corresponding to  $\Delta = 3$  which is much too short. The only other possibility, the spin change 4

which is well known. The only other possibility, the spin change  $\Delta S = 1$  state with a parity change both give a likelihood corresponding to  $\Delta S = 1$ . The spin change of  $S$  or  $3$  between the ground and the excited the incident neutron and even for the excited neutron.

In parity of the excited state due to the  $\Delta$  value being odd for the ground state of  $S, 3$ , or  $1$  units. This transition gives a change from  $\Delta = 2$  neutron can excite a level with a spin differing from of the incident and excited neutron relative to the orbital momentum, which may be  $-1, 0$ , or  $1$ , depending upon the orientation of the spin added to this value of  $\Delta = 2$  is the contribution of the neutron spin excitation over shows that the neutron is excited with  $\Delta = 0$ . To be easy in more orbital angular momentum than  $\Delta = 2$ . The range of the the production of the isotopic state shows that the neutron excites  $\Delta$  compared with theory of the experimental cross section for later in this chapter.

over, this level may be excited directly by neutrons, as is shown elsewhere, this transition must have a  $\Delta$  value greater than  $1$ . However, states is not observed, although the energy is taken that for decay in because the decay of the  $\gamma$ -excited level directly to the ground to make from neutron excitation of the isomer.

stable level, together with the parity and spin assignments that may  $\Delta$  may be shown the energy levels involving the  $\gamma$ -excited state of the  $\gamma$ -excited level.

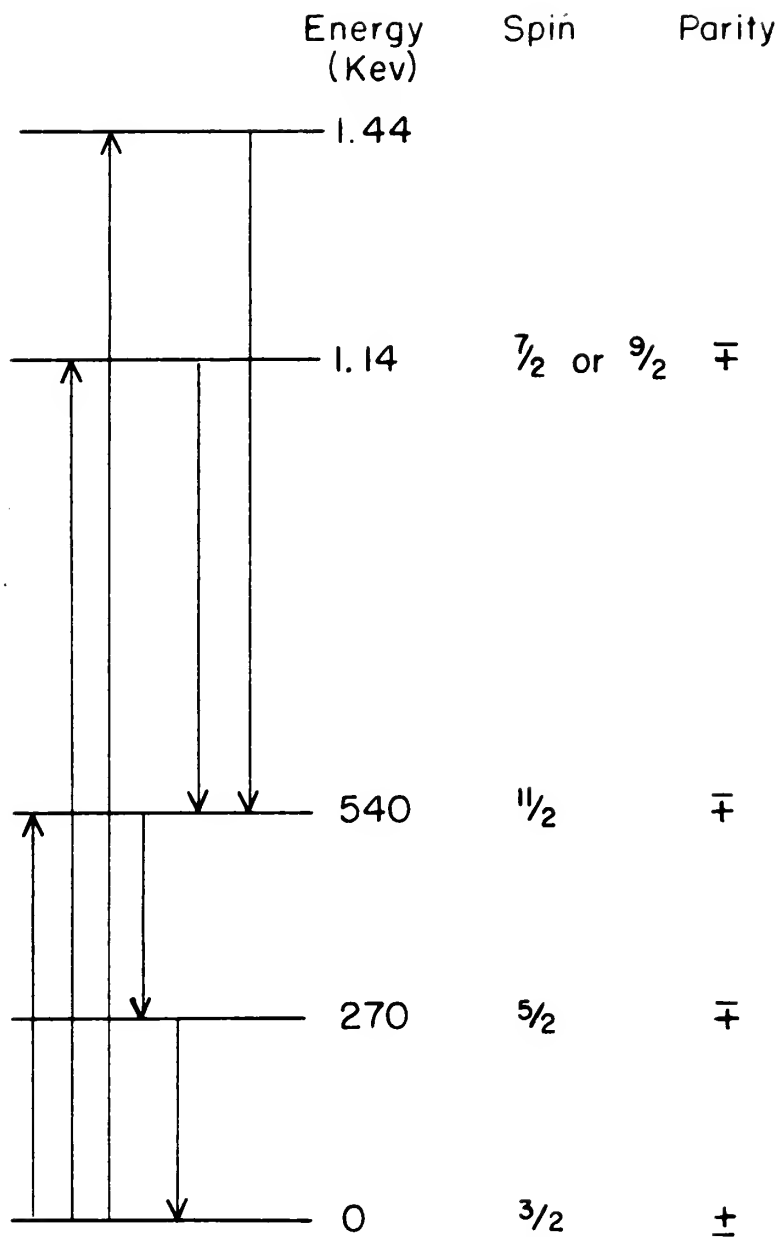


Figure 10

LEVELS EXCITED by NEUTRONS in  $\text{Au}^{197}$  which  
DECAY to the METASTABLE STATE at 540 Kev.



with a parity change, however, gives a magnetic  $2^{\frac{1}{2}}$ -pole transition with a lifetime approximated by letting  $\Delta = 5$ . Thus, the spin and parity relationship between the ground state and the 7-second metastable state are uniquely determined, and it is shown that the neutron enters the  $\text{Au}^{197}$  nucleus with orbital angular momentum of 3 and its spin parallel to the orbital axis, and it is emitted with angular momentum zero and its spin reversed.

Since the isomeric transition involves no parity change, the level to which it decays must also have a parity different from the ground state. This rules out the possibility of a transition from this state to the ground state having  $\Delta$  even, and in particular it excludes  $\Delta = 2$ .

Two other levels at 1.14 and 1.14 Mev are found that may be excited by fast neutrons of  $< 2$ -Mev energy. However, at these energies, the incident neutron may carry in even more angular momentum. At the same time, there is no lifetime requirement on the state, except that transitions to the metastable state are quite probable. Furthermore, the shape of the excitation curve for each level individually cannot be determined because of the uncertainty in the contribution of lower levels to the isomeric state. For these reasons, little can be deduced from the neutron excitation curve about these states other than their energy.

It is of interest to compare the energies determined by neutron excitation with those Wiedenbeck has reported for quantum excitation. In Chapter II it has been shown that any level excited by a quantum should be excited to an appreciable degree by neutrons. The level



excited by 1.11-Mev neutrons apparently corresponds to the threshold found for 1.22-Mev quanta. The agreement is considered satisfactory because of the difficulty of deducing this threshold accurately from the small slope between the quantum excitation curve and the axis. However, no evidence is found with neutrons of the level reported for quanta at 1.68 Mev.

The fact that the 1.11-Mev level can be excited by quanta enables a determination to be made of its spin relative to the ground state. The spin change of 1 from the ground state to the metastable state with a parity change must be accomplished by the absorption of a quantum plus the emission of another.

There are two possibilities with high enough probabilities for the process to occur. The excitation is either by an  $\ell = 2$  yes (magnetic quadrupole) radiation followed by decay to the isomeric state by  $\ell = 2$  no (electric quadrupole) radiation or excitation by  $\ell = 3$  yes (electric octupole) radiation followed by  $\ell = 1$  no (magnetic dipole) radiation. It is impossible to separate these since they both have the same probability according to the Weissacker hypothesis. However, the decision as to whether a transition corresponds to the excitation of the higher level or the decay to the metastable level is unambiguous because the decay to the metastable level must be able to compete successfully with the decay to the ground state in spite of the higher energy involved in the latter.

Unfortunately, the Wiedenbeck data do not permit even an inference regarding the probability of exciting the neutron level at 1.11 Mev with quanta.

...the small slope between the potential energy curve and the axis. However, no evidence is found with reference to the level reported for quanta at 1.60 eV.

The fact that the 1.11-eV level can be excited by quanta involving a determination to be made of the spin relative to the ground state. The spin change of 1 from the ground state to the metastable state with a parity change must be accompanied by the absorption of a quantum plus the emission of another.

There are two possibilities with high enough probability for the process to occur. The excitation is either by an  $L = 2$  photon (negative parity) or by an  $L = 1$  photon (positive parity) followed by an  $L = 2$  photon (negative parity) or an  $L = 1$  photon (positive parity) followed by an  $L = 1$  photon (negative parity). It is impossible to separate these since they both have the same probability according to the selection rules. However, the selection rule for the transition corresponds to the excitation of the higher level or the decay to the metastable level is forbidden because the decay to the metastable level must be able to compete successfully with the decay to the ground state in spite of the higher energy involved in the latter.

Unfortunately, the Winkler data do not permit even an inference regarding the probability of exciting the metastable level at 1.11 eV with quanta.



## DESCRIPTION OF EXPERIMENTAL SETUP

Measurement of the neutron excitation function of  $\text{Au}^{197*}$  was complicated by two factors:

1. The cross section for the excitation process is so small that it was necessary to sacrifice part of the energy resolution to obtain activities large compared to the background; and,
2. The half-life of the isomeric state is only 7 seconds.

Figure 11 shows the experimental setup used for the gold investigation.

The technique used involved irradiating the sample in the form of a foil with a known flux of monoenergetic neutrons for 15 seconds, cutting off the neutron beam, transferring the foil to a scintillation counter, and counting the activity for 15 seconds.

The gold foil was 3 cm. in diameter and 0.1 mm. thick with a mass of 1.420 grams. To permit rapid transfer of the foil from the irradiating position to the counting position, the foil was mounted in a depression at one end of a bakelite slide  $1/8$  inch thick by 1-1/2 inches wide by 3 feet in length. This slide was carried in a slot in the shield of the scintillation counter, which has been described previously. When the slide was against the stop at one end, the foil was accurately positioned next to the crystal of the counter. When it was against the stop at the other end, the slide was held by aluminum fingers in front of the beam to eliminate errors due to the flexibility of the slide. This arrangement was necessary to keep the counter out of the region of high neutron flux which would lead to high background counting rates for

to obtain activities large compared to the background; and

3. The half-life of the radioactive state is only 7 seconds.

The curve section for the radioactive process is so small that it was necessary to amplify the part of the energy resolution to obtain activities large compared to the background; and

3. The half-life of the radioactive state is only 7 seconds.

Figure 11 shows the experimental setup used for the gold inverse-

lighting.

The technique used involved irradiating the sample in the form

of a foil with a known flux of monoenergetic neutrons for 15 seconds,

extracting the foil to a detection

counter, and counting the activity for 15 seconds.

The gold foil was 3 cm in diameter and 0.1 mm thick with a mass

of 1.450 grams. To permit rapid transfer of the foil from the irradiat-

ing position to the counting position, the foil was mounted in a de-

pression at one end of a helical slide 1/8 inch thick by 1-1/2 inches

wide by 3 feet in length. This slide was carried in a slot in the

shaft of the scintillation counter, which has been described previously.

When the slide was against the stop at one end, the foil was accurately

positioned next to the crystal of the counter. When it was against the

stop at the other end, the slide was held by aluminum fingers in front

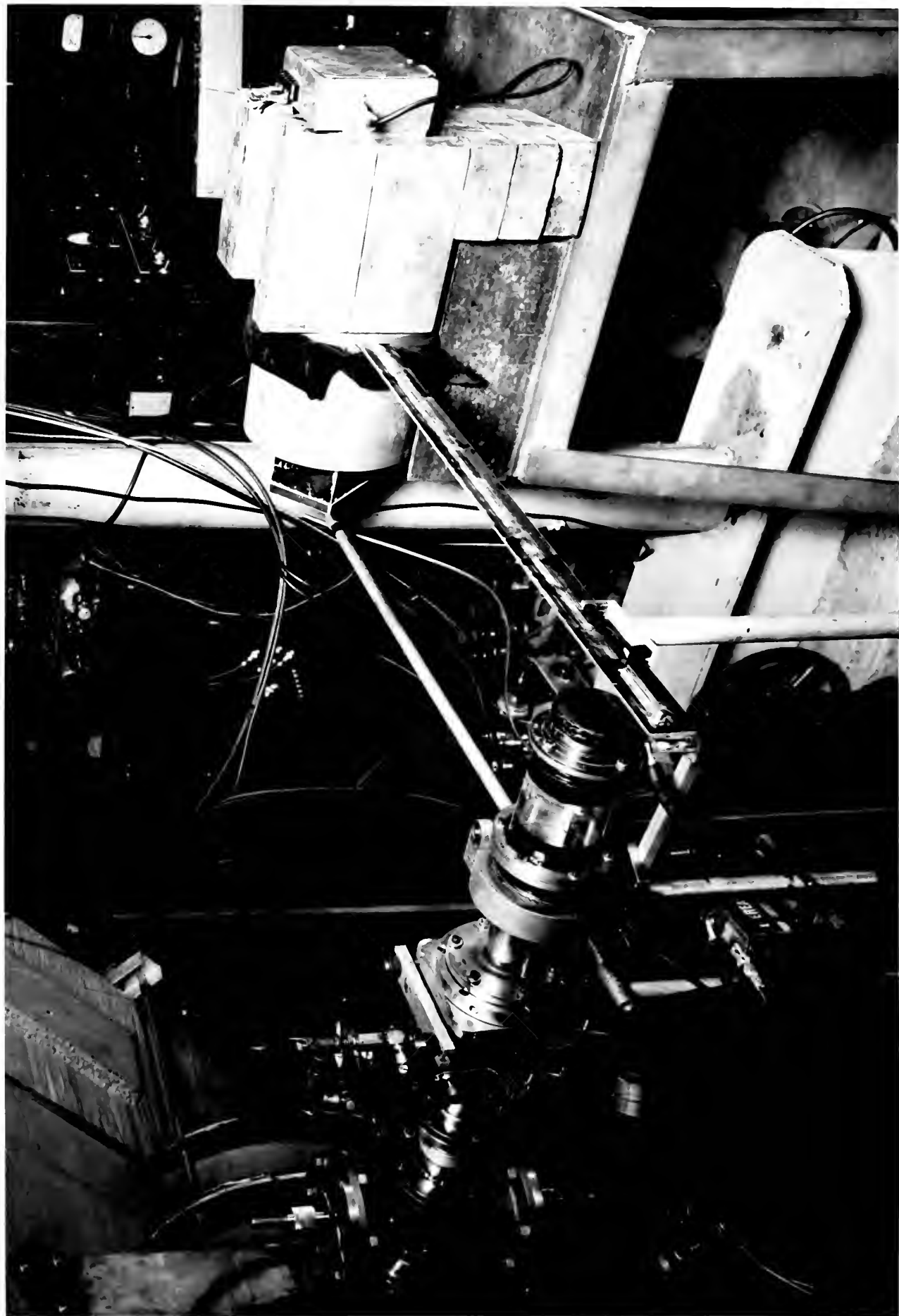
of the beam to eliminate errors due to the flexibility of the slide.

This arrangement was necessary to keep the counter out of the region of

high neutron flux which would lead to high background counting rates for

Figure 11. Arrangement for irradiating the gold foils, showing the bakelite slide and the two counters with their lead shields.







a short time after the beam was cut off. It also permitted shielding of the counter on all sides from the stray gamma-ray background that was present even when the beam was not striking the target.

During the counting periods, the neutron beam was cut off by closing a tantalum-backed flap valve in the proton beam. This valve, unfortunately, was located near the target instead of at the entrance slit of the deflection chamber. For this reason, slight wanderings resulted in the beam striking the chamber walls which caused large fluctuations in the background during the counting period.

To measure the background while the counting was taking place, another scintillation counter with characteristics as nearly as possible like the counter for the gold was set up. This new counter was placed beside the other with the same amount of shielding but also was shielded from the gold activity. The scalars for both counters were arranged so that they were controlled by the same switch. Test activation runs were then made which were identical to the true runs, except for the omission of the gold from the slide. These runs showed the backgrounds of the two counters under these conditions to be the same within a statistical uncertainty of about 5 percent. Since the background over most of the curve was of the order of 10 percent or less of the induced activity, the matching was considered satisfactory.

The neutron flux for these runs was determined by the long counter previously described. The counter was set up one meter from the target at zero degrees. The number of counts during each irradiation was recorded and corrected for the effect of neutron energy on the counter efficiency.

of the counter on all sides from the study background that was present even when the beam was not striking the target. During the counting periods, the neutron beam was cut off by closing a tantalum-backed flap valve in the proton beam. This valve, unfortunately, was located near the target instead of at the entrance slit of the deflection chamber. For this reason, slight wanderings resulted in the beam striking the chamber walls which caused large fluctuations in the background during the counting period.

To measure the background while the counting was taking place, another scintillation counter with characteristics as nearly as possible like the counter for the gold was set up. This new counter was placed beside the other with the same amount of shielding but also was shielded from the gold activity. The scalars for both counters were arranged so that they were controlled by the same switch. Some activation runs were then made which were identical to the true runs, except for the activation of the gold from the slide. These runs showed the backgrounds of the two counters under these conditions to be the same within a statistical uncertainty of about 2 percent. Since the background over most of the curve was of the order of 10 percent or less of the induced activity, the matching was considered satisfactory.

The neutron flux for these runs was determined by the long counter previously described. The counter was set up one meter from the target at zero degrees. The number of counts during each irradiation was recorded and corrected for the effect of neutron energy on the counter efficiency.



The exposure of the foil was initiated by the operator's pulling a cord with his left hand which opened the flap valve and allowed the proton beam to strike the target. After 15 seconds, the cord was released and the flap was closed by a counterweight. At the same time, the operator pulled a second cord with his right hand which moved the slide into position, and with his left hand, he started the counter. This arrangement prevented the accidental starting of the counter before the beam was off. With practice a rhythm was established that permitted starting the counting period one-half second after the end of the irradiation period with a variation of less than one-fourth of a second. This variation corresponds to a random error of less than 3 percent.

#### TREATMENT OF THE DATA

Each observation yielded on the order of 150 to 400 counts in the 15-second counting interval with a background of about 20 counts. At each energy, five or more identical runs were made and averaged to reduce the statistical and other random errors, such as variations in the length of time between the end of the irradiation and the beginning of the counting. An analysis of the individual readings taken at the same energy shows that they agree among themselves within the statistical error. The nonexistence of appreciable errors due to slow variations was shown by the reproducibility of the data over a period of several days.

Two tests were made to check that the 7-second isomeric state of gold was being counted. A decay curve of the radiation was taken by

the operator released a second cord with his right hand which moved the slide into position, and with his left hand, he started the counter. This arrangement prevented the accidental starting of the counter before the beam was off. With practice a rhythm was established that permitted starting the counting period one-half second after the end of the irradiation period with a variation of less than one-fourth of a second. This variation corresponds to a random error of less than 3 percent.

# TREATMENT OF THE DATA

Each observation yielded an average of 150 to 400 counts in the 15-second counting interval with a background of about 20 counts. At each energy, five or more identical runs were made and averaged to reduce the statistical and other random errors, such as variations in the length of time between the end of the irradiation and the beginning of the counting. An analysis of the individual readings taken at the same energy shows that they agree among themselves within the statistical error. The reproducibility of comparable errors due to slow variations was shown by the reproducibility of the data over a period of several days. Two tests were made to check that the 15-second counting interval of gold was being counted. A check error of the radiation was taken by

noting the number of counts at the end of each 5 seconds. This method was subject to large statistical and human errors, but the results were consistent with a half-life between 5 and 10 seconds. Since there are no other known activities which could be excited in gold with this half-life and since the activity was not found when the gold was removed from the slide, this was considered sufficient to identify the activity.

In addition, a pulse-height distribution curve was run to identify the energy. This curve also suffered from poor statistics but was consistent with the known characteristics of the isomeric state.

In the determination of the excitation curve, the energy resolution was affected by three major factors, the fluctuations in the energy of the proton beam, the thickness of the lithium target, and the dependence of the neutron energy on the angle of emission. A fourth factor, scattered neutrons, may be neglected because of their low intensity relative to the direct beam in the region in which the foil was exposed.

To increase the beam current striking the target, it was necessary to operate with the beam defining slits opened to 5 millimeters. This leads to a resolution of approximately 15 kev in the proton beam and, hence, in the neutron beam. Since the beam striking the slits was large compared to the opening, all energies in this region are approximately equally represented.

The effect of using a target of finite thickness is to give also a square number-energy distribution for the neutrons similar to that



caused by the slit opening. The effects are therefore additive and, according to measurements on the rise of the neutron yield curve at threshold, amount to a resolution of 30 kev in this investigation.

The third factor in the resolution, the angle at the target intercepted by the foil, must be considered because of the dependence of the neutron energy on angle. For those experiments in which the cross section for the reaction is quite small, it was found necessary to sacrifice angular and, hence, energy resolution in order to place the foils close enough to get sufficient activity. Accordingly, the foils were exposed 5 centimeters from the target. They intercepted a half angle of 17 degrees for the portion of the curve above 1.0 Mev. Below 1.4 Mev the exposure was made at 4 centimeters with a half angle of 21 degrees. This corresponds to an energy spread of 25 kev at 600 kev in the forward direction and to 35 kev at 2.0 Mev.

Figure 12 shows the correction that must be applied to the maximum neutron energy to obtain the mean energy of neutrons incident on the foil. This curve was obtained by the following considerations.

For the purpose of calculating the mean energy incident on the foil, the beam may be considered uniform in intensity over the angle involved since the energies involved are well above the  $\text{Li}(p,n)$  threshold.

Let the energy spread due to the slit width plus the target thickness be represented by  $\Delta E_p$  and that due to the finite solid angle intercepted be  $\Delta E_\theta$ .



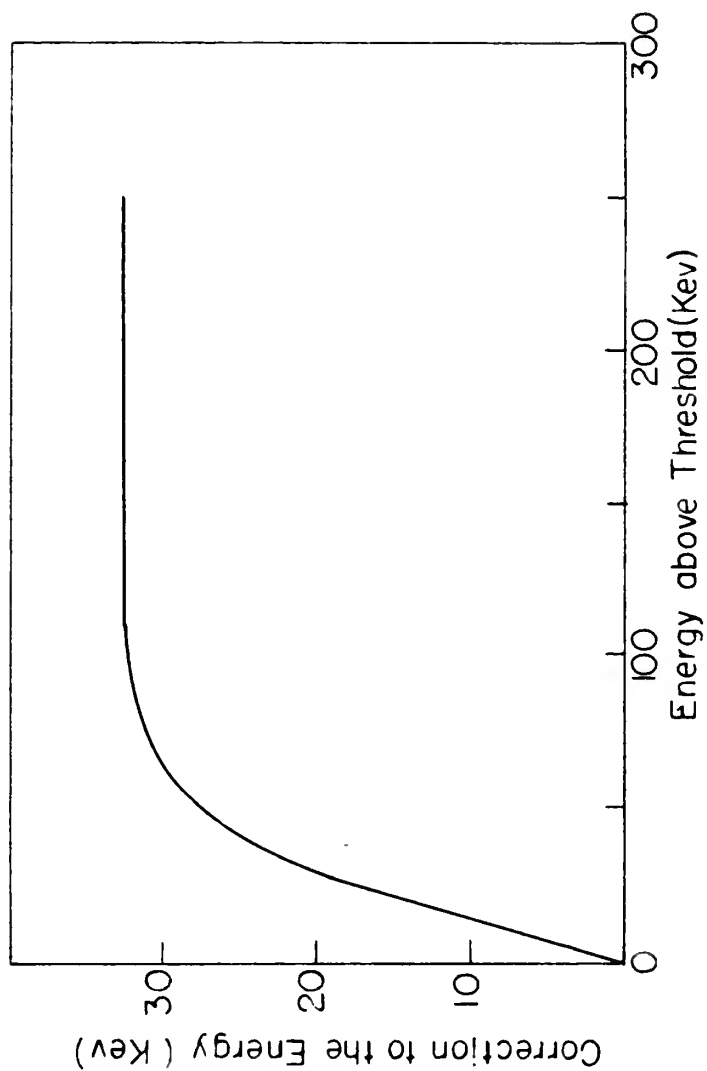


Figure 12

ENERGY CORRECTION to be SUBTRACTED from the  
MAXIMUM ENERGY INCIDENT on the FOIL in the  
VICINITY of the EXCITATION THRESHOLD.





The variation of the cross section for the production of the isomeric state may be considered constant over the energy spread  $\Delta E_0$  except at threshold. Assume for the moment that the neutron beam is monoenergetic at 0 degrees; that is, that  $\Delta E_p$  is zero. Then, the activity due to each increment of energy is proportional to the area of the target subtended by the corresponding increment of angle at the source. This obviously increases linearly with energy up to the angle intercepted by the whole target foil. The mean energy in terms of the activity it produces is then calculated to be 0.707 of the total spread,  $\Delta E_0$ , below the 0 degrees energy.

This result may now be integrated over the spread of neutron energies present at 0 degrees. Again assuming the cross section to be constant over the energies involved, the correction to be subtracted from the maximum energy is found to be:

$$0.5 \Delta E_p + 0.707 \Delta E_0$$

The calculation of course does not hold at threshold because of the assumptions on the effect of energy on cross section. When the maximum energy is just equal to the threshold for excitation, the correction must be zero because that is the only energy causing excitation.

Another point may be calculated by considering the case in which the lowest energy present is just the threshold energy. Again, with somewhat less justification, assume the cross section uniform over each  $\Delta E_0$ , but this time assume that the cross section over  $\Delta E_p$  increases

it is calculated for the reaction of the  
 is that the energy of the reaction is  
 except at the threshold. The energy of the reaction is  
 non-zero at 0 degrees; that is,  $\Delta E_p$  is zero. Then, the  
 activity due to each increment of energy is proportional to the area  
 of the target subtended by the corresponding increment of angle at the  
 source. This obviously increases linearly with energy up to the angle  
 intercepted by the whole target foil. The mean energy in terms of the  
 activity it produces is then calculated to be 0.707 of the total  
 spread,  $\Delta E_p$ , below the 0 degree energy.

This result may now be integrated over the spread of reaction  
 energies present at 0 degrees. Again assuming the cross section to be  
 constant over the energies involved, the correction to be subtracted  
 from the maximum energy is found to be:

$$0.2 \Delta E_p + 0.707 \Delta E_p$$

The calculation of course does not hold at threshold because of  
 the assumption on the effect of energy on cross section. When the  
 maximum energy is just equal to the threshold for excitation, the cor-  
 rection must be zero because that is the only energy causing excitation.  
 Another point may be calculated by considering the case in which  
 the lower energy present is just the threshold energy. Again, with  
 somewhat less justification, assume the cross section will not over each  
 $\Delta E_p$ , but this also assumes that the cross section over  $\Delta E_p$  increases

as  $(E - E_{th})^{1/2}$ . A calculation similar to that preceding gives a correction equal to:

$$0.37 \Delta E_p + 0.707 \Delta E_0$$

This correction is somewhat too large due to the assumption on  $\Delta E_0$  but gives a reasonable approximation of the true value.

The activity of the gold above background was divided by the neutron flux and is plotted in Figure 13 as a function of the mean energy of the neutron beam as corrected according to the preceding considerations. The upper portion of the curve taken with the foil 5 centimeters from the target was normalized to the activity expected at 4 centimeters to join with the lower portion of the curve. The two sections overlap in the energy interval from 1.0 to 1.4 Mev.

The neutron excitation curve shows the characteristic shape for three levels at  $530 \pm 20$  kev;  $1.14 \pm 0.03$  Mev; and  $1.44 \pm 0.03$  Mev with a possible fourth level at about 1.77 Mev. The errors assigned are estimates of the uncertainty in the determination of the energy of the neutrons and the location of the level on the curve.

The section of the curve in the vicinity of the 1.44-Mev level was checked with higher resolution to be sure that the level was actually present. It was found that the break in the curve was readily reproducible.

a very uniform and constant value of  $\Delta E$  was obtained.

correction was made:

$$\Delta E_{\text{corrected}} = \Delta E_{\text{observed}} + \Delta E_{\text{correction}}$$

This correction is somewhat too large due to the assumption of  $\Delta E$ .

but gives a reasonable approximation of the true value.

The activity of the gold sample was divided by the

neutron flux and is plotted in Figure 11 as a function of the mean

energy of the neutron beam as corrected according to the preceding

considerations. The upper portion of the curve taken with the foil 2

is consistent with the target was normalized to the activity observed at

1.0 e.v. with the lower portion of the curve. The two

sections overlap in the energy interval from 1.0 to 1.5 e.v.

The neutron excitation curve shows the characteristic shape for

three levels at  $2.30 \pm 0.03$  e.v.;  $1.11 \pm 0.03$  e.v.; and  $1.11 \pm 0.03$  e.v.

with a possible fourth level at about 1.1 e.v. The curves assigned

are as function of the uncertainty in the determination of the energy of

the neutrons and the location of the level on the curve.

The location of the curve in the vicinity of the 1.11-e.v. level

was checked with higher resolution to be sure that the level was not

split present. It was found that the level in the curve was really

unsplit.

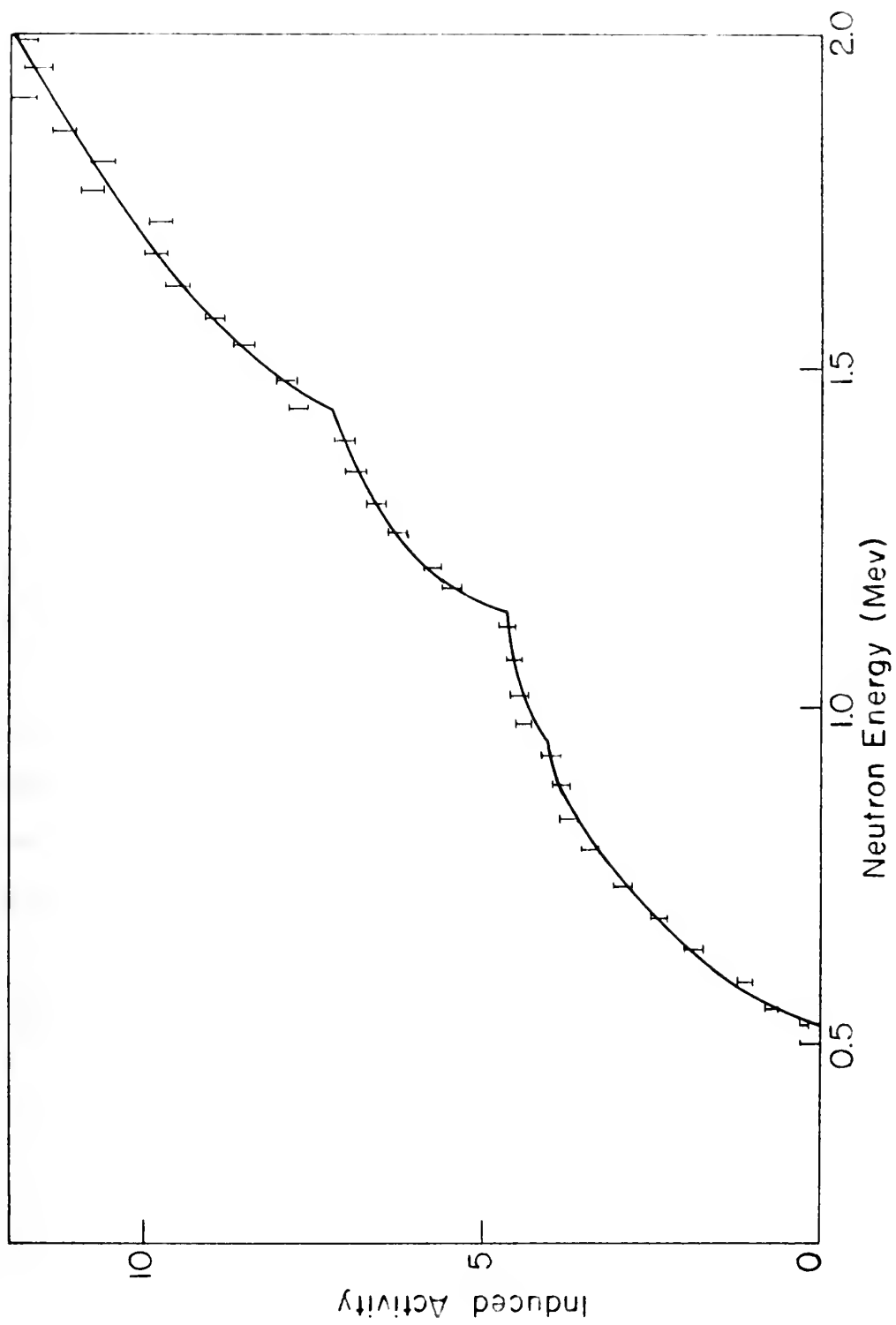


Figure 13  
NEUTRON EXCITATION CURVE for  $\text{Au}^{197}$ \*



The curve shows about a 10 percent rise 130 kev above threshold. Although this may be explained by statistical uncertainty, it seems more probable that this is due to the second energy group reported to be 384 kev below the main group with a relative intensity of 10 percent.

The threshold value is of special interest because it corresponds quite closely with Huber's measurement which shows the metastable level to be about 540 kev above the ground state. As a result, there appears to be little doubt that the neutrons are able to excite the metastable state directly.

#### COMPARISON OF THE THEORETICAL AND EXPERIMENTAL CROSS SECTIONS

A knowledge of the cross section for the formation of the metastable state is of great importance in assigning an  $\ell$  value to the incident neutron that excited that state. A comparison of this cross section with the  $\sigma_c^{(\ell)}$  cross section for the formation of the compound nucleus  $\text{Au}^{198}$  as a function of  $\ell$  for the incoming neutron is sufficient in this case to place a maximum on the angular momentum the neutron can carry in.

The calculation of  $\sigma_c^{(\ell)}$  following the method of Blatt and Weisskopf, as described in Chapter II, is carried out in the energy region of 600 to 1200 kev for  $0 \leq \ell \leq 4$ . The results are plotted in Figure 11.

Determination of the experimental cross section involves knowledge of the neutron flux on the gold foil and the efficiency of the

... of the ...  
... of the ...  
... of the ...  
... of the ...

... of the ...  
... of the ...  
... of the ...  
... of the ...

# ... OF THE ... ... OF THE ...

... of the ...  
... of the ...  
... of the ...  
... of the ...

... of the ...  
... of the ...  
... of the ...  
... of the ...

... of the ...  
... of the ...  
... of the ...  
... of the ...



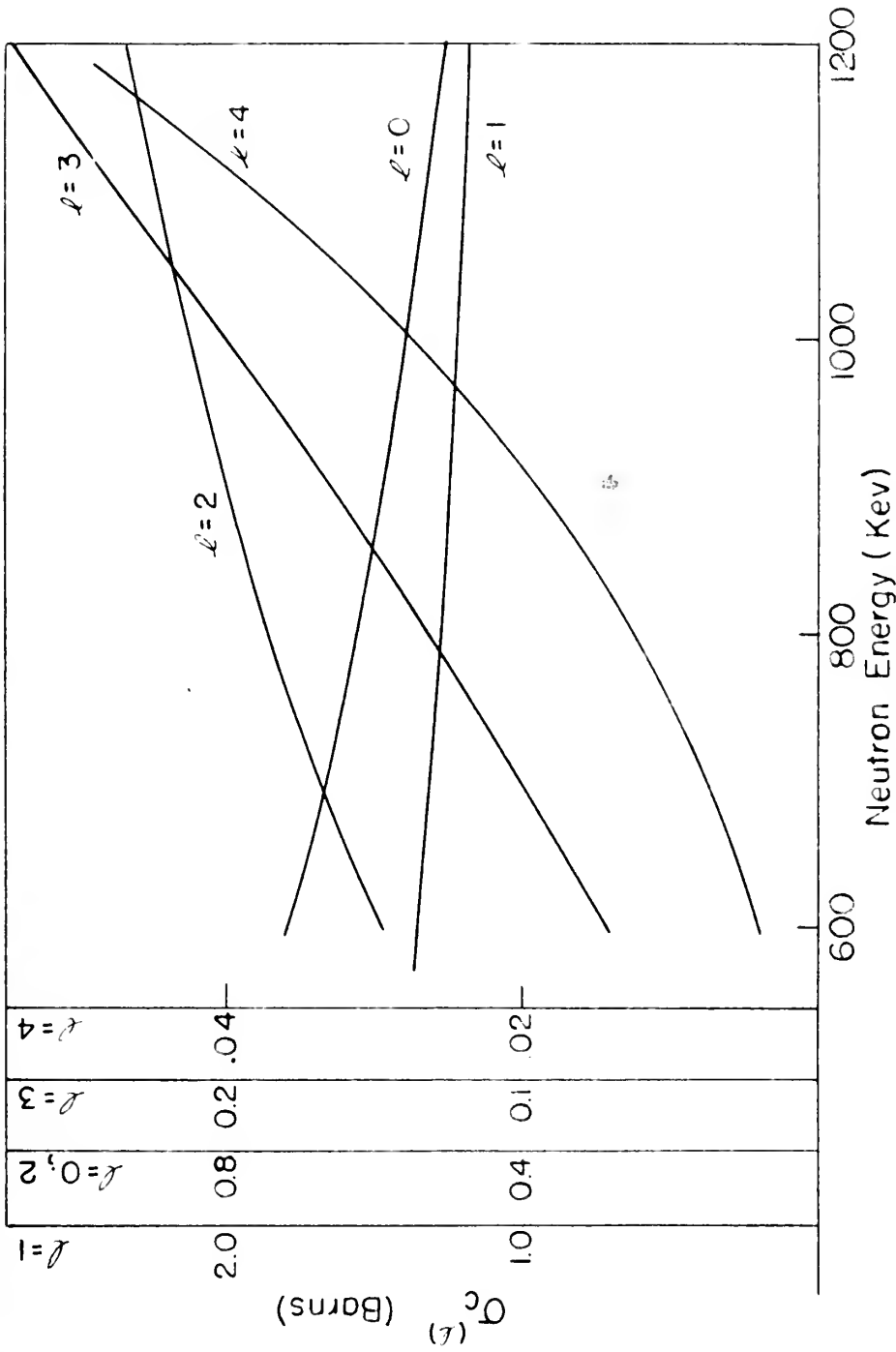


Figure 14

GROSS SECTION for FORMATION of the COMPOUND  
 NUCLEUS  $\text{Au}^{197} + n \rightarrow \text{Au}^{198}$   
 (Note the different scales for different  $l$ 's)



counter for counting the excited state. The largest error in this cross section will result from the difficulty in evaluating the second factor.

In the data plotted on Figure 13, the ordinate is the number of counts of the  $\text{Au}^{197*}$  activity divided by the number of register counts from the long counter when operating through a scale of 1024 scalar. Willard<sup>40</sup> has determined that the flat part of the neutron yield curve this counter at 0 degrees and one meter from the target gives 60 counts per microcoulomb of protons per kev of target thickness, the target thickness being measured by the initial rise of the neutron yield curve with good proton energy resolution. From the data of Hanson, Taschek, and Williams<sup>41</sup> on neutron yield, a 40-kev target in this energy region gives  $4.35 \times 10^6$  neutrons per microcoulomb per unit solid angle at 0 degrees. Therefore, each count on the long counter corresponds to 1610 neutrons per unit solid angle at 0 degrees.

When exposed at 4 centimeters, the 3-centimeter foil intercepts a solid angle of 0.128 steradians. Hence, each count on the long counter indicates that the foil has been traversed by 232 neutrons; or, taking into account the scaling factor, each register count stands for  $2.38 \times 10^5$  neutrons through the foil.

The area of the foil is 7.07 square centimeters, and the mass is 1.420 grams corresponding to  $4.34 \times 10^{21}$   $\text{Au}^{197}$  nuclei. Therefore, an ordinate of unity on the plot in Figure 13 is equivalent to a cross section of 0.0069 barns if it is assumed that the scintillation counter counts every gold nucleus excited. This, then, is the minimal value

and the largest error in this  
 error, which will result from the difference in evaluating the second  
 factor.  
 In the data plotted on Figure 13, the ordinate is the number of  
 counts of the  $^{197}\text{Au}$  activity divided by the number of register counts  
 from the long counter when operating through a scale of 1000 counts.  
 Willard<sup>10</sup> has determined that the endpoint of the neutron yield curve  
 this counter at 0 degrees and one meter from the target gives 60 counts  
 per microcoulomb of protons per cm of target thickness, the target  
 thickness being measured by the initial rise of the neutron yield curve  
 with good proton energy resolution. From the data of Hanson, Jacobson,  
 and Williams<sup>11</sup> on neutron yield, a 10-kev target in this energy region  
 gives  $1.35 \times 10^6$  neutrons per microcoulomb per unit solid angle at 0  
 degrees. Therefore, each count on the long counter corresponds to  
 1810 neutrons per unit solid angle at 0 degrees.  
 When exposed at 1 centimeter, the 3-centimeter foil intercepts  
 a solid angle of 0.128 steradians. Hence, each count on the long  
 counter indicates that the foil has been traversed by 232 neutrons; or,  
 taking into account the scaling factor, each register count stands for  
 $2.32 \times 10^7$  neutrons through the foil.  
 The area of the foil is 7.07 square centimeters, and the mass is  
 1.420 grams corresponding to  $1.34 \times 10^{21}$  nuclei. Therefore, an  
 ordinate of unity on the plot in Figure 13 is equivalent to a cross  
 section of 0.009 barns if it is assumed that the scattering cross-  
 section of every foil nucleus excited. This, then, is the minimal value

that the cross section can have. On Figure 15, the minimal cross section for the production of the metastable state in the vicinity of the threshold is plotted as a function of energy, together with the cross section for the formation of the  $\text{Au}^{198}$  compound nucleus by an  $\ell = 1$  neutron,  $\sigma_c^{(1)}$ . It is seen that  $\sigma_c^{(1)}$  is even less than this minimum over part of the region. This reaction can therefore be definitely ruled out as the method of exciting the 7-second state directly.

Of course, the minimal value computed is too low by a factor equal to the reciprocal of the overall efficiency of the counter for counting the metastable state. Since the foil thickness is over 10 times the range of the conversion electrons, their contribution to the efficiency may be neglected, and the counting rate may be considered to come entirely from the gold x-rays produced on their emission and from the unconverted gamma-rays. Due to the resolution of the scalar following the counter, the decay of the nonisomeric 270-kev state cannot be separated from the isomeric state.

Using the mass-absorption coefficient for the gold K-series x-rays of  $3.40 \text{ cm}^2/\text{gm}$ , it can be calculated that in the one-dimensional case of a source 0.1 millimeters thick, the self-absorption is 0.73. The attenuation of this radiation in the crystal may be calculated to be 0.76, corresponding to an absorption of 0.24.

For the 270-kev unconverted radiation, the self-absorption is small and the crystal absorption 0.20. This gives an efficiency for counting the x-rays from this source of about 0.18 and for the gamma-rays about the same figure. So far, it has been neglected that only



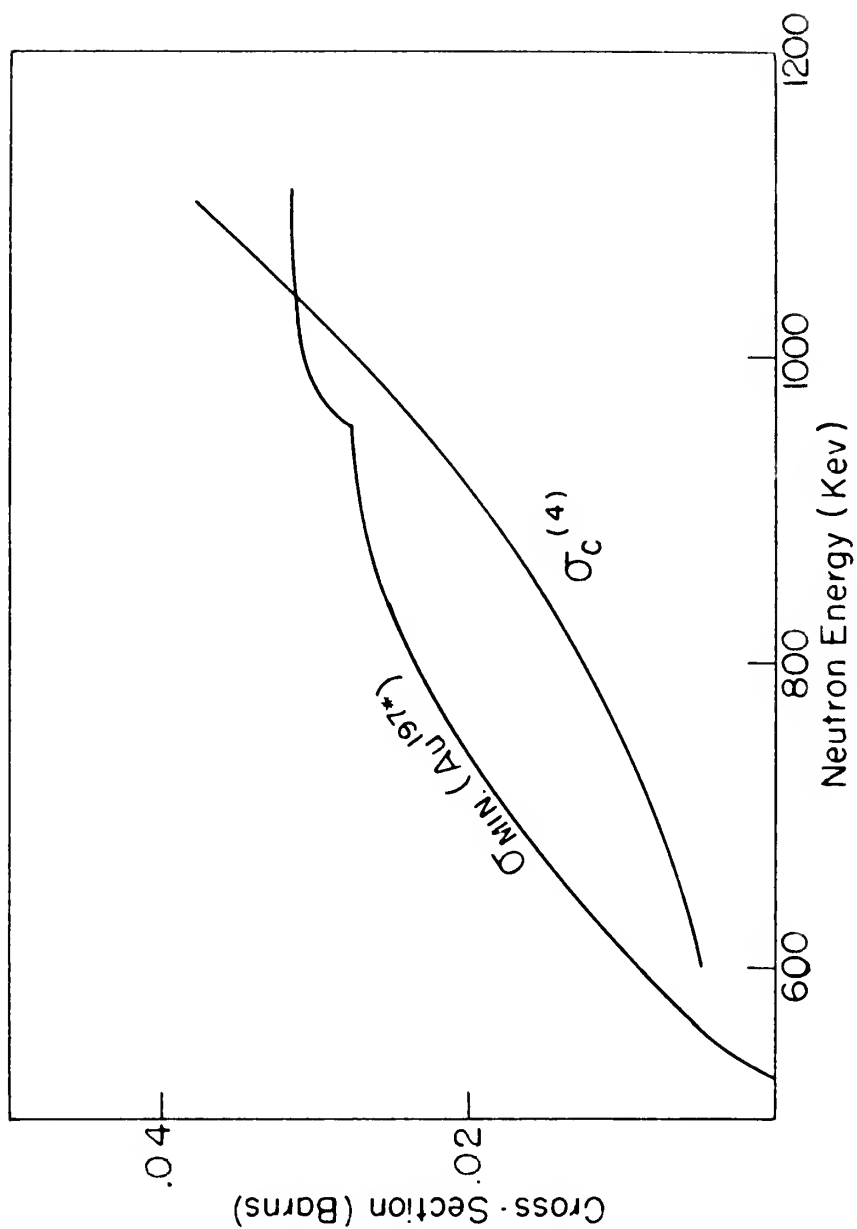


Figure 15

COMPARISON of MINIMAL CROSS-SECTION for PRODUCTION of  $\text{Au}^{197*}$  with  $\sigma_c^{(4)}$  SHOWING THAT  $\ell < 4$  for the INCIDENT NEUTRON.





half of the radiation is directed toward the counter and that two decays take place for each metastable nucleus. However, these factors will cancel each other to the extent of the uncertainty involved in this calculation. Softer x-rays, notably the L-series, have also been neglected in this approximation.

There is another factor to be considered, the efficiency of the photomultiplier for counting scintillations in the crystal. This has been checked by comparing the counting rate in this counter from a thin  $C^{14}$  source with that obtained in a 50 percent geometry windowless gas-flow counter. It is found that this factor, which also corrects for the scintillation counter geometry being slightly less than 50 percent, is 0.90.

From all these considerations, it is estimated that the scintillation counter counts about 16 percent of the  $Au^{197*}$  nuclei decaying during the counting interval. The bias on the discriminator, however, was set so that 10 percent of the counts were not recorded, and the counting period of two half-lives was such that only 75 percent of the nuclei decayed during the period. Therefore, the correction to the cross section should be increased by a factor 1.48, giving a final value of 0.24. Because of the necessary crudeness of this calculation, it is considered that it may be in error by as much as 50 percent.

In Figure 16, the cross section for the formation of the metastable state in the vicinity of the threshold is plotted with this factor applied to the minimal cross section. A plot of the cross section for the formation of the compound nucleus by an  $\ell = 3$  neutron is



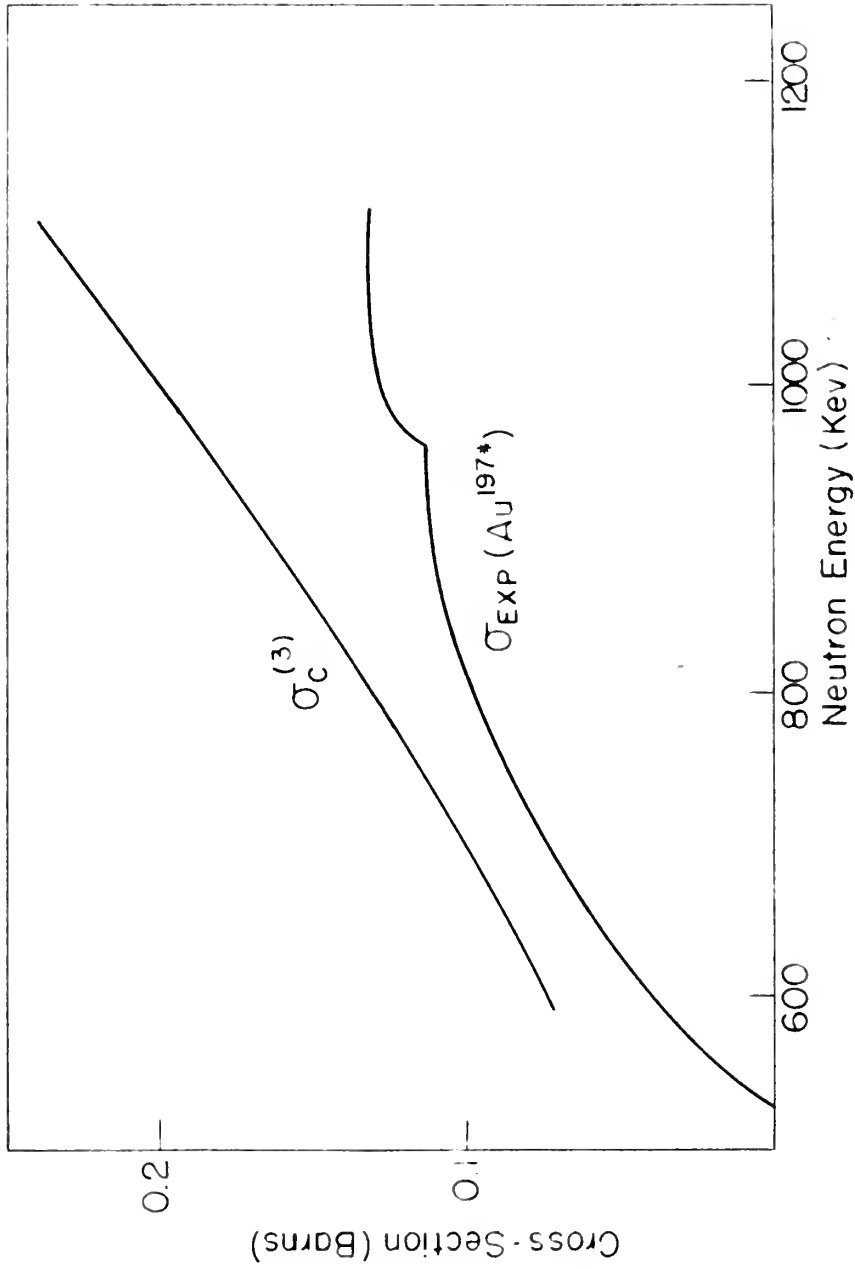


Figure 16

COMPARISON of EXPERIMENTAL CROSS-SECTION for PRODUCTION of  $\text{Au}^{197*}$  with  $\sigma_c^{(3)}$  SHOWING THAT  $\ell=3$  for the INCIDENT NEUTRONS IS POSSIBLE.



also shown on the same graph.

It is expected that the cross section for production of the isomeric state could be smaller compared to  $\sigma_c^{(3)}$ . However, the transition to the metastable state can compete very successfully with the transition to the ground state or other excited levels because it involves the emission of an  $\ell = 0$  neutron. Decay of the compound nucleus to the ground state requires that an  $\ell = 3$  neutron be emitted. Assuming that only the ground state and the metastable state compete, a calculation, such as described in Chapter II, reveals that 75 percent of the compound nuclei will go to the metastable level. Recalling that the experimental cross section may be in error by 50 percent in absolute magnitude, it is seen that the results are in agreement with the assumption that the activation takes place with an  $\ell = 3$  neutron.

Figure 17 shows a plot of the neutron excitation curve from threshold to the first excited state above it, corrected for the cross section for the production of the compound nucleus. The resulting curve is the probability of emitting a neutron from the compound nucleus with  $\ell = 0$  and the spin opposite to that of the incident neutron. This curve has the typical shape for the emission curve of an  $\ell = 0$  neutron starting out as an  $(E - E_{th})^{1/2}$  curve (also shown) and then falling below due to competition with decay to other levels.

also a very small amount of the

of the reaction is due to the reaction of the

reaction rate will be smaller compared to  $k_1$ . However, the

transition to the metastable state can compete very successfully with

the transition to the ground state or other excited levels because the

involves the emission of an  $\ell = 0$  neutron. Energy of the compound

medium to the ground state requires that an  $\ell = 3$  neutron be emitted.

Assuming that only the ground state and the metastable state compete,

a calculation, such as described in Chapter II, reveals that 75 percent

of the compound nuclei will go to the metastable level. Recalling that

the experimental cross section may be in error by 50 percent in absolute

magnitude, it is seen that the results are in agreement with the

assumption that the activation takes place with an  $\ell = 3$  neutron.

Figure 19 shows a plot of the neutron excitation curve from

threshold to the first excited state above it, corrected for the cross

section for the production of the compound nucleus. The resulting

curve is the probability of emitting a neutron from the compound

nucleus with  $\ell = 0$  and the spin opposite to that of the incident neutron.

This curve has the typical shape for the excitation curve of an

$\ell = 0$  neutron starting out as an  $\ell = 3$  wave (also shown) and

then falling below due to competition with decay to other levels.

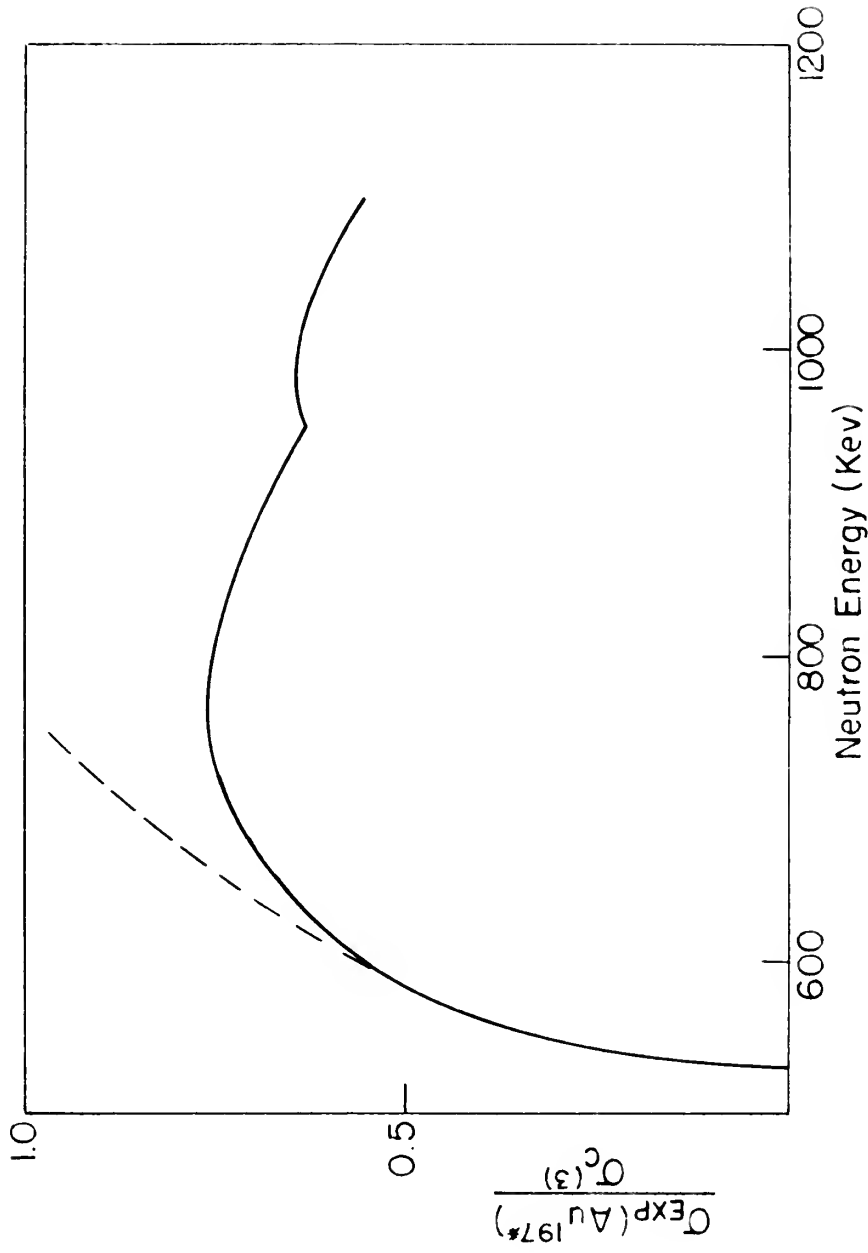


Figure 17

PROBABILITY OF COMPOUND NUCLEUS DECAYING TO METASTABLE STATE. THE BROKEN CURVE IS  $Y = \text{const.} (E - E_{\text{TH}})^{1/2}$ .





## V. INVESTIGATION OF INDIUM

HISTORY OF  $\text{In}^{115*}$  EXCITATION

The metastable state in  $\text{In}^{115}$  has been studied by numerous investigators, not only to determine the properties of the state itself, but also as a convenient threshold detector. The relatively large cross section for production of the isomer and its convenient half-life make it ideal for many problems.

In 1939, Goldhaber, Hill, and Seillard<sup>42</sup> reported the excitation of  $\text{In}^{115*}$  by inelastic scattering of neutrons from a radon-alpha-beryllium source giving neutrons of a maximum energy of about 13.5 Mev. The results were checked by exciting the state with 2.5-Mev d-d neutrons. It was shown that the activity belonged to the mass 115 indium isotope and not to the mass 113 by producing  $\text{Cd}^{115}$  from  $\text{Cd}^{116}$  by an (n,2n) reaction. The  $\text{Cd}^{115}$  they decayed to  $\text{In}^{115*}$ . On the other hand,  $\text{Cd}^{113}$  is stable and, hence, could not lead to  $\text{In}^{113*}$ .

The metastable state has since been produced by Barnes and Aradine<sup>43</sup> with 6.7-Mev protons and by Lark-Morovitz, Kisser, and Smith<sup>44</sup> with 16-Mev alpha-particles.

The first extensive excitation curve for this level was obtained by Waldman and Wiedenbeck<sup>45</sup>. Using x-rays to produce the isomer, they reported levels at 1.12, 1.55, 2.13, and 2.64 Mev which decay to the metastable level. Subsequent measurements by Miller and Waldman<sup>46</sup> have confirmed the existence of the first two levels but corrected their energy to 1.04 and 1.42 Mev. The work by Waldman and Wiedenbeck re-

The metastable state in  $^{113}\text{In}$  has been studied by numerous investigators, not only to determine the properties of the state itself, but also as a convenient threshold detector. The relatively large cross section for production of the isomer and its convenient half-life make it ideal for many problems.

In 1932, Goldhaber, Hill, and Seifried<sup>1</sup> reported the excitation of  $^{113}\text{In}$  by the elastic scattering of neutrons from a radon-alpha-polyonium source giving neutrons of a maximum energy of about 13.5 mev. The results were checked by exciting the state with 2.5-4.4 mev. It was shown that the activity belonged to the mass 113 isotope and not to the mass 115 by producing  $^{113}\text{In}$  from  $^{116}\text{In}$  by an  $(n, 2n)$  reaction. The  $^{113}\text{In}$  they decayed to  $^{113}\text{Sn}$ . On the other hand,  $^{115}\text{In}$  is stable and, hence, could not lead to  $^{113}\text{Sn}$ .

The metastable state has since been produced by Harries and Arvidson<sup>2</sup> with 0.7-mev protons and by Lark-Hovivitz, Harries, and Seifried<sup>3</sup> with 1-mev alpha-particles.

The first extensive excitation curve for this level was obtained by Waldman and Staderback<sup>4</sup>. Using x-rays to excite the isomer, they reported levels at 1.12, 1.42, 2.13, and 3.44 mev which decay to the metastable level. Subsequent measurements by Miller and Waldman<sup>5</sup> have confirmed the existence of the first two levels but corrected their energy to 1.04 and 1.43 mev. The work by Waldman and Staderback re-

quired the use of a thick x-ray target and therefore suffered from the same difficulty in interpretation as did Niedenbeck's work on gold. However, Miller and Waldman found it possible to use a thin target that gave much more pronounced breaks in the excitation curve corresponding to the levels. In addition, they found a weak activity (twice the background) with 880-kev x-rays which was considered to be possibly the excitation of an 873-kev level, reported by Lawson and Cork<sup>47</sup>.

A neutron excitation curve has been obtained by Cohen<sup>48</sup> using  $C^{13}(d,n)$  and d-d neutrons from a 1-Mev Cavendish generator. Because of the reaction that was necessary to produce the neutrons, the curve could not be carried to the threshold of the excitation but had to be stopped at about 2 Mev. Figure 18 shows the results that were obtained. It is to be noted that the presence of individual levels was not detected. This is probably because so many levels contribute to the excitation at the high energy involved that the breaks due to the individual levels could not be seen.

In connection with an investigation of threshold detectors, Taschek<sup>49</sup> obtained four points on the neutron excitation curve in the energy region from 600 to 1500 kev. Of course, these data are too sketchy to show more than the general trend of the curve.

#### DESCRIPTION OF ENERGY LEVELS IN $Ln^{115}$

The energy of the isomeric state has been measured by Bell, Kettle, and Cassidy<sup>50</sup> using both a scintillation counter and a magnetic lens spectrometer. It is found that the K-conversion electrons have an energy of 312 kev, corresponding to an energy of 340 kev for the level.

the energy of the incident wave is not sufficient to excite the atom to the next level. In addition, they found a weak activity (near the peak) with 200-keV x-rays which was considered to be possibly due to the excitation of an 873-keV level, reported by Jansen and Corb.<sup>14</sup>

A reaction excitation curve has been obtained by Jansen and Corb.<sup>14</sup> using  $^{60}\text{Co}$  and  $^{60}\text{Fe}$  sources from a 1-lit. gas-filled detector. Because of the reaction that was necessary to produce the positrons, the curve could not be carried to the threshold of the excitation and had to be stopped at about 2 Mev. Figure 11 shows the results that were obtained. It is to be noted that the presence of individual levels was not detected. This is probably because no very low energy levels are the excitation of the high energy levels that the peaks due to the individual levels could not be seen.

In connection with an investigation of threshold detectors, Jansen<sup>15</sup> obtained four points on the reaction excitation curve in the energy region from 600 to 1200 keV. Of course, these data are too sketchy to show more than the general trend of the curve.

# DESCRIPTION OF ENERGY MEASUREMENT IN LITHIUM

The energy of the incident wave was measured by Jell, Jellison, and Jellison<sup>16</sup> using a lithium crystal and a magnetic field. It is found that the 7-conversion electrons have an energy of 12 keV, corresponding to an energy of 350 keV for the level.

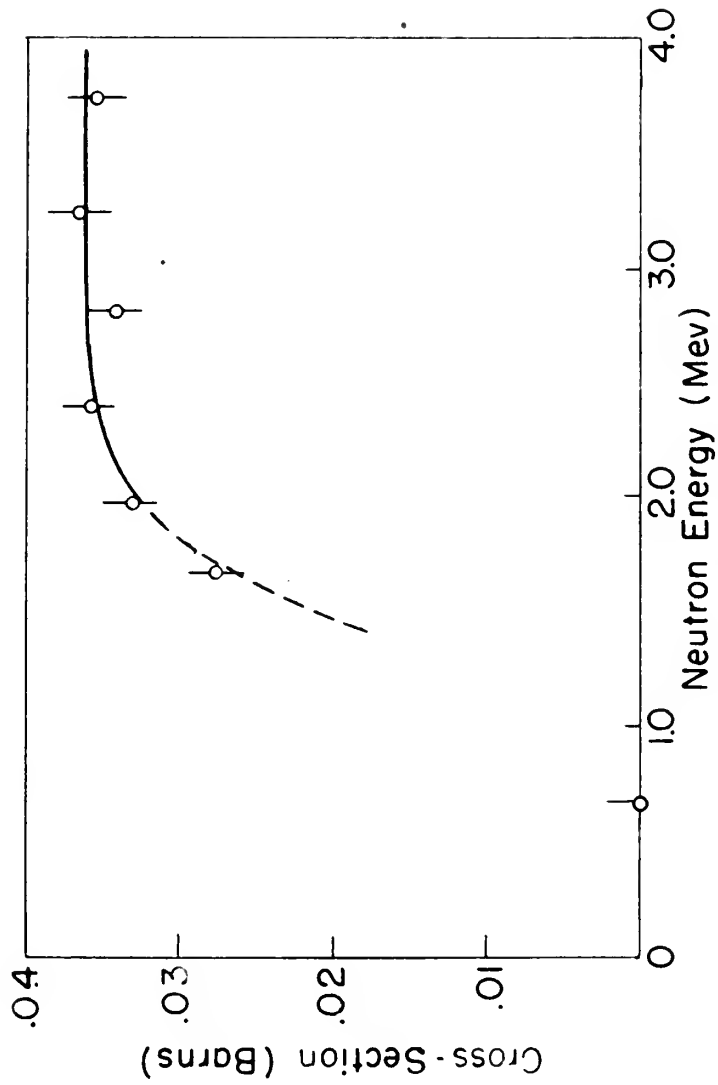


Figure 18

CROSS SECTION MEASURED BY COHEN for NEUTRON  
EXCITATION of  $\text{In}^{115*}$ . (From Nature 161, 475 (1948))



The half-life of the state, according to the determination of Lawson and Cork<sup>51</sup>, is 4.5 hours.

Assuming the transition to be of the  $\Delta = 4$  type,  $\Delta$  defined in Chapter IV, the Weissacker hypothesis predicts a half-life of 4 seconds; while, if it is assumed to be  $\Delta = 5$ , the result is 800 hours. Although the agreement is not too good, it seems highly probable that the transition is of the latter type involving an electric  $2^5$  pole or a magnetic  $2^4$  pole radiation.

The K- to L-conversion ratio in this case does not give a conclusive decision between these two possibilities. Axel and Dancoff<sup>52</sup> report a theoretical value of 6.8 for the magnetic case and 2.64 for the electric multipole transition. The experimental value given is 5.0. Thus, it would seem to favor choosing the magnetic transition.

Consideration of the spins involved, however, removes the ambiguity. The ground state has a spin of  $9/2$ . The electric  $2^5$  pole transition requires a spin change of 5 between the ground and metastable states. If the possibility of a spin of  $19/2$  is ruled out because it is too large, there is no possibility for an  $\ell = 5$  transition. On the other hand, assuming the metastable level to have a spin of  $1/2$  agrees with a magnetic  $2^4$  pole transition having a spin change of 4 and a parity change.

Figure 19 shows the metastable levels, together with those found at 600, 960, and 1370 kev from the neutron excitation curve determined in this investigation. Also shown is the competitive decay of the metastable level in about 5 percent of the cases by emission of a





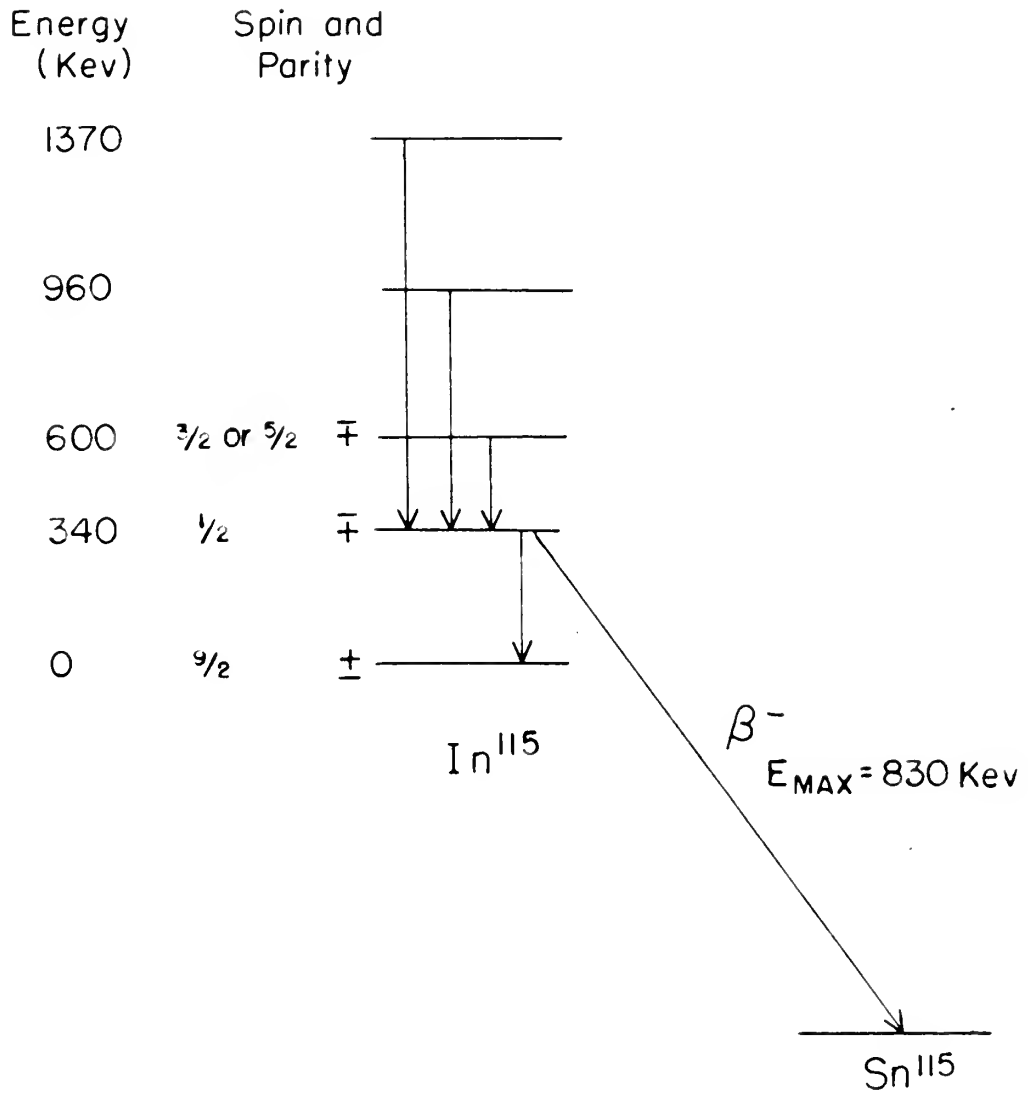


Figure 19

ENERGY LEVELS MEASURED in In<sup>115</sup> by NEUTRON  
EXCITATION of the METASTABLE LEVEL.



beta-particle having a maximum energy of 830 kev, as found by Bell, Ketelle, and Cassidy<sup>53</sup>.

The existence of this beta-decay has been confirmed in connection with this study of indium. Figure 20 shows a pulse-height distribution obtained from an 8-mil indium foil bombarded with neutrons from the M. I. T. cyclotron. The shape of the curve is distorted because the foil was thick compared with the range of the electrons, but the existence of the 312-kev conversion electron and 830-kev beta-decay is clearly shown.

It seems likely that the quantum-induced activity below 900 kev reported by Miller and Waldman and by Lawson and Cork was actually exciting of the 600-kev level. If this is assumed, it follows that the spin and parity of that level must be such that this process can take place often enough to be observed but that the process is somewhat forbidden.

$\Delta \Lambda = 2$  or lower transition (electric quadrupole or magnetic dipole) may be ruled out because this makes the transition to the ground state so much more probable than that to the metastable state that excitation would not be observed. On the other hand,  $\Delta \Lambda = 4$  or higher can be eliminated for the transition from the ground state to the 600-kev level because such a transition is too improbable for quantum excitation.

The remaining possibility  $\Delta \Lambda = 3$  involves a parity change and a spin change of 3 for electric  $2^3$  pole or of 2 for magnetic  $2^2$  pole

detected having a maximum energy of 200 eV, as found by Bell, Kato, and Gossard.

The existence of this beta-ray has been confirmed in connection with this study of indium. Figure 20 shows a pulse-height distribution obtained from an 8-ml indium foil sandwiched with neutron from the N. I. T. cyclotron. The shape of the curve is distorted because the foil was thick compared with the range of the electrons, but the existence of the 115-keV conversion electron and 530-keV beta-ray is clearly shown.

It seems likely that the gamma-rayed activity below 200 keV reported by Miller and Waldman and by Lawson and Gossard was actually existing of the 600-keV level. If this is assumed, it follows that the spin and parity of that level must be such that this process can take place often enough to be observed but that the process is somewhat forbidden.

A  $\Delta = 2$  or inner transition (electric quadrupole or magnetic dipole) may be ruled out because this makes the transition to the ground state so much more probable than that to the metastable state that excitation would not be observed. On the other hand,  $\Delta = 1$  or higher can be eliminated for the transition from the ground state to the 600-keV level because such a transition is too improbable for gamma-ray excitation.

The remaining possibility  $\Delta = 3$  involves a parity change and a spin change of 3 for electric 3<sub>2</sub> pole or of 2 for magnetic 3<sub>2</sub> pole.

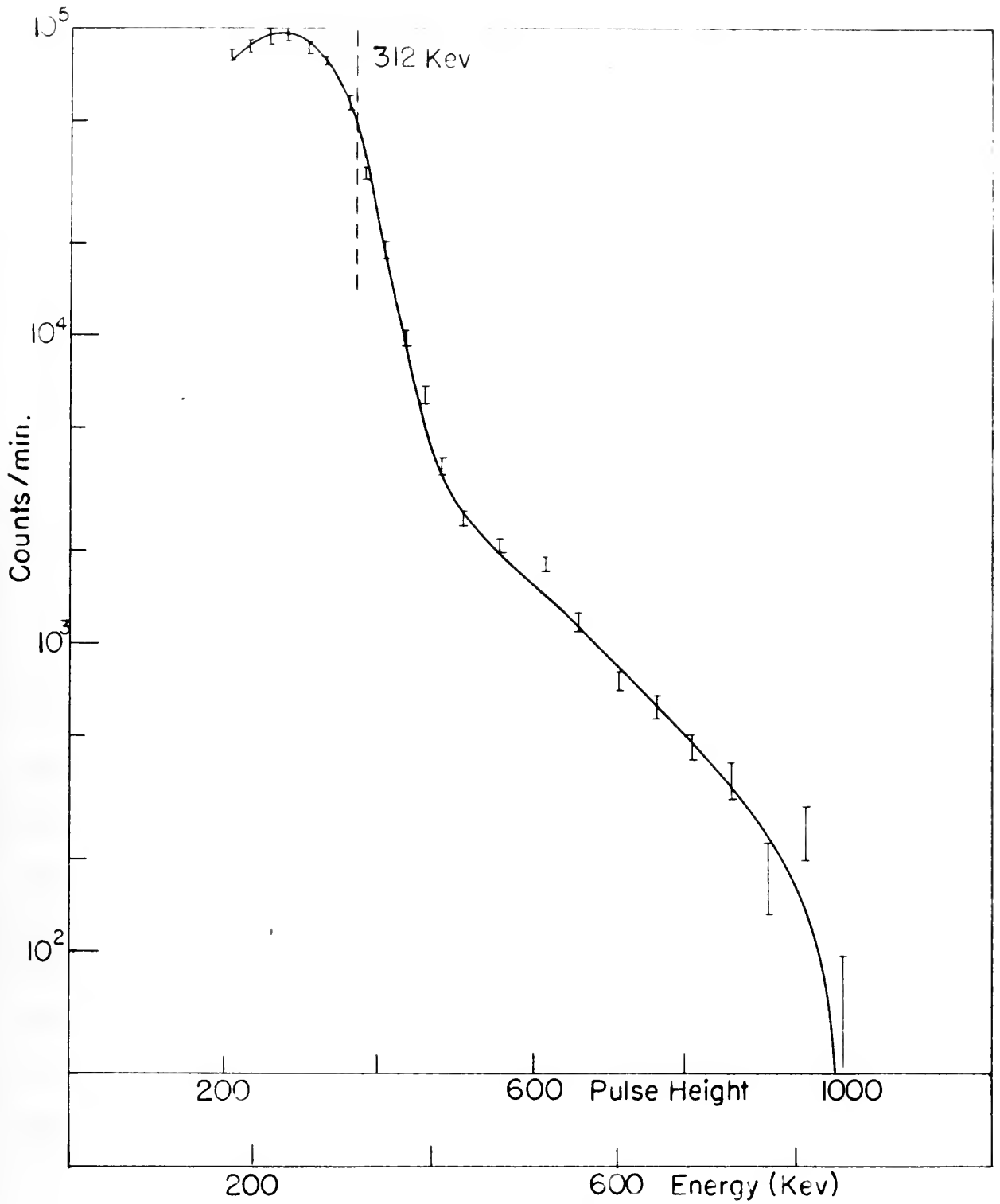


Figure 20

DIFFERENTIAL PULSE HEIGHT DISTRIBUTION for  $\text{In}^{115}$  from THICK FOIL SHOWING 312 Kev CONV. ELECTRON LINE and 830 Kev BETA DECAY (Energy calib. from Fig. 6)



excitation. A spin change of 2 with parity change could be provided by an  $\ell = 1$  or an  $\ell = 3$  neutron; if this is the case, neutrons will excite this level strongly. On the other hand, a spin change of 3 with parity change requires an  $\ell = 3$  neutron, giving a small probability.

Unfortunately, it was not possible to determine the cross section for neutron excitation in this region. Therefore, no choice can be made between these two, and both spins are given on Figure 19.

For the case of the higher levels, many spin and parity choices will give results consistent with the observed excitation curves.

#### EXPERIMENTAL SETUP

The indium samples were in the form of foils 6 mils thick and 3 cm. diameter. These foils were irradiated for 4 hours with monoenergetic neutrons from the  $\text{Li}^7(p,n)$  reaction using a 20-kev thick target on the Rockefeller generator. After irradiation, the foils were counted in the scintillation counter, described in Chapter III.

Such a long exposure, necessitated by the long lifetime of the isomer, introduces several problems into the determination of the excitation curve. It is impossible to keep the neutron flux constant over the exposure without sacrificing a portion of it to provide a range of adjustment. If the flux changes during this period, a simple integration of the neutron flux is not sufficient for the determination of the cross section. At the time these measurements were made, a continuously recording neutron-flux indicator was not available. It was therefore nec-





essary to obtain several points on the excitation curve during the same irradiation, thus determining a section of the curve. These sections could then be joined by overlapping.

Another factor to be considered is the availability of generator time. If each point on the excitation curve is determined separately, the exposure time required becomes prohibitive.

For these reasons, advantage was taken of the dependence of the neutron energy on angle, and seven foils were exposed simultaneously at angles ranging from 0 to 75 degrees. Figure 21 shows the foil arrangement for exposure.

In order to obtain sufficient activity in the foils, it was necessary to place the foils so that the nearest edge was only 1 cm. from the neutron source. At this distance, the energy resolution was preserved by rolling the foils into small cylinders about 3 mm. in diameter and mounting them radially about the source.

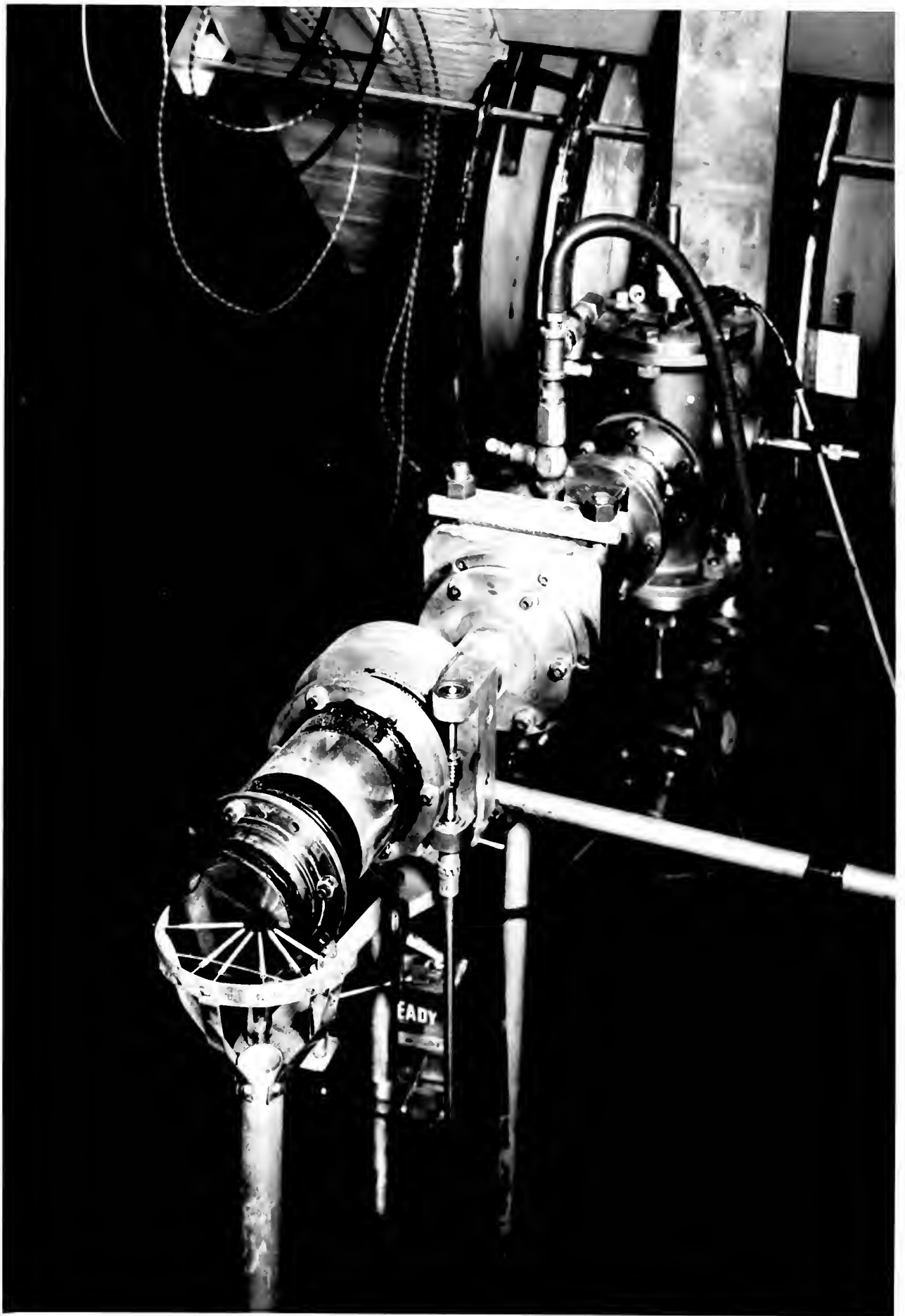
The effect of capture of thermal neutrons was minimized by counting the side of the foil rolled inside. All of this capture activity is located in the very thin layer which was outside; so that most of the foil is shielded from thermal neutrons.

After irradiation the foils were counted in rotation six to eight times over a period of about 8 hours, starting with the lowest activity to separate the 54-minute capture activity from the 4.5-hour activity of  $\text{In}^{115*}$ . To increase the ratio of  $\text{In}^{115*}$  to  $\text{In}^{116}$  counts, advantage was taken of the energy sensitivity of the scintillation counter. The



Figure 21. Foil arrangement for the indium activation showing the foils rolled on the wire of the spider.







levels of the differential discriminator were set to record counts corresponding to an energy between 150 and 450 kev. This includes most of the counts from  $\text{In}^{115*}$  (see Figure 20) but includes only part of the counts from  $\text{In}^{116}$  ( $E_{\text{max}} = 850$  kev for the beta-particle emitted).

An attempt to separate the two activities was made by comparing the number of counts above and below the pulse height corresponding to 450 kev, thus using the difference in shape of their pulse-height distributions. However, it was found that the statistical uncertainty in this method made it impracticable.

#### TREATMENT OF THE DATA

In order to take proper account of all points making up the decay curve of a given foil, it was considered desirable to compare the experimental curve with a theoretical decay curve. Since the construction of such a theoretical curve presupposes a knowledge of the relative amounts of the two activities present, a curve to include all cases had to be found.

All the experimental curves were plotted with the same scale on the same type of semilogarithm graph paper. A master decay curve was then constructed, also using the same scale, on a large sheet of paper starting with an assumption of the shorter-lived activity being 100 times that of the longer-lived and continued until the shorter-lived activity had decayed to 1/100 of the longer-lived. It is evident that, if the experimental curve is made up of a combination of the two activities within these limits, it must fit the master curve over some

level of the 111 spectral distribution was set to record counts corresponding to an energy between 150 and 155 keV. This includes most of the counts from  $^{111}\text{In}$  (see Figure 30) but includes only part of the counts from  $^{111}\text{In}$  ( $E_{\text{max}} = 850$  keV for the beta-particle emitted). An attempt to separate the two activities was made by comparing the number of counts above and below the pulse height corresponding to 150 keV, thus using the difference in shape of their pulse-height distributions. However, it was found that the statistical uncertainty in this method made it impracticable.

#### TREATMENT OF THE DATA

In order to take proper account of all points making up the decay curve of a given foil, it was considered desirable to compare the experimental curve with a theoretical decay curve. Since the construction of such a theoretical curve presupposes a knowledge of the relative amounts of the two activities present, a curve to include all cases had to be found.

All the experimental curves were plotted with the same scale on the same type of semi-logarithmic graph paper. A master decay curve was then constructed, also using the same scale, on a large sheet of paper starting with an assumption of the shorter-lived activity being 100 times that of the longer-lived and continued until the shorter-lived activity had decayed to  $1/100$  of the longer-lived. It is evident that if the experimental curve is made up of a combination of the two activities within those limits, it must fit the master curve over some



interval. By superposing the experimental curve on the master and by sliding the former to find the best fit, each point could be given its proper weight. To permit determination of the amount of each activity, two lines were drawn on the master corresponding to the contribution of each activity to the total curve. It was then a simple matter to read off the amount of each activity at any time and in particular at the time corresponding to  $t = 0$  on the experimental plot.

In this investigation, the 105-minute isomeric activity in  $\text{In}^{113}$  was neglected. That this would be possible was predicted from the relative abundance (4.2 percent for  $\text{In}^{113}$ , compared with 95.8 percent for  $\text{In}^{115}$ ). The decay curves obtained justify this assumption, inasmuch as the combination of the 54-minute and the 4.5-hour activities were sufficient in all cases to explain their shape.

The accuracy of the method described above was high enough so that the uncertainty in the determination of the  $\text{In}^{115*}$  activity was estimated to be less than 10 percent.

Since the neutron flux is anisotropic, the various activities must be corrected as a function of the exposure angle. Taschek and Homendinger<sup>54</sup> have shown that the flux is not even isotropic in the center-of-mass coordinates for the  $\text{Li}^7(p,n)$  reaction because of the resonance in the compound nucleus. The flux as a function of angle must therefore be measured. Taschek and Homendinger's measurements do not extend into the region of interest in this work. In conjunction with Willard, the neutron flux as a function of angle from 0 to 90

to show. The experimental conditions were such that the number and the  
 activity of the cells could be determined. The results of the activity  
 of the cells were shown on the number corresponding to the concentration of  
 each activity to the total curve. It was then a simple matter to read  
 off the amount of each activity at any time and to determine the  
 time corresponding to  $t = 0$  as the experimental phase.

In this investigation, the 100-minute inactive activity in the  
 was neglected. That this would be possible was predicted from the re-  
 active substance (0.2 percent for 100), compared with 99.8 percent for  
 the 100-minute inactive activity. The decay curves obtained justify this assumption, inasmuch as  
 the completion of the 50-minute and the 100-minute activities were not  
 different in all cases to explain their shape.

The accuracy of the method described above was high enough so  
 that the uncertainty in the determination of the  $100^{th}$  activity was  
 estimated to be less than 10 percent.

Since the reaction time is anisotropic, the various activities  
 must be corrected as a function of the exposure angle. Tardieu and  
 Hammett<sup>1</sup> have shown that the time is not even isotropic in the  
 center-of-mass coordinates for the  $100^{th}$  reaction because of the  
 resonance in the exposed material. The time as a function of angle  
 must therefore be measured. Tardieu and Hammett's measurements do  
 not extend into the region of interest in this work. In comparison  
 with Figure 1, the reaction time as a function of angle from 0 to 90

degrees was measured for proton energies from the  $\text{Li}^7(p,n)$  threshold to 3.75 Mev using the long counter described in Chapter III. The scattered neutron background was determined by use of a paraffin cone to shadow the counter. The results of these measurements are reported by Willard<sup>55</sup>, and are plotted here in Figure 21a.

Each irradiation of foils covered an energy interval of from 300 to 500 keV. The intervals were chosen so that they overlapped approximately half of their extent. Each segment of the  $\text{In}^{115*}$  excitation curve determined in the interval was corrected for the anisotropy of the flux and energy resolution and was then normalised to the preceding segment. This technique involves a propagation of errors but does not affect the location of energy levels found by means of the curve. Figure 22 shows the complete curve.

#### DISCUSSION OF THE RESULTS

In spite of the scattering of the points on the excitation curve (Figure 22), the presence of three levels is shown at 600 keV, 960 keV, and 1.37 MeV with possibly a fourth level at 1.75 MeV. The uncertainty in these energy assignments is estimated to be of the order of 40 keV. This uncertainty, however, is considered hardly sufficient to bring the 960 keV and the 1.37 MeV level into agreement with Miller and Waldman's values of 1.02 and 1.42 MeV for quantum-excited levels. The correspondence is close enough to leave little doubt that the same levels are being excited and suggests that the energy calibration for one of the experiments is in error. Unfortunately, there is not a third accurate



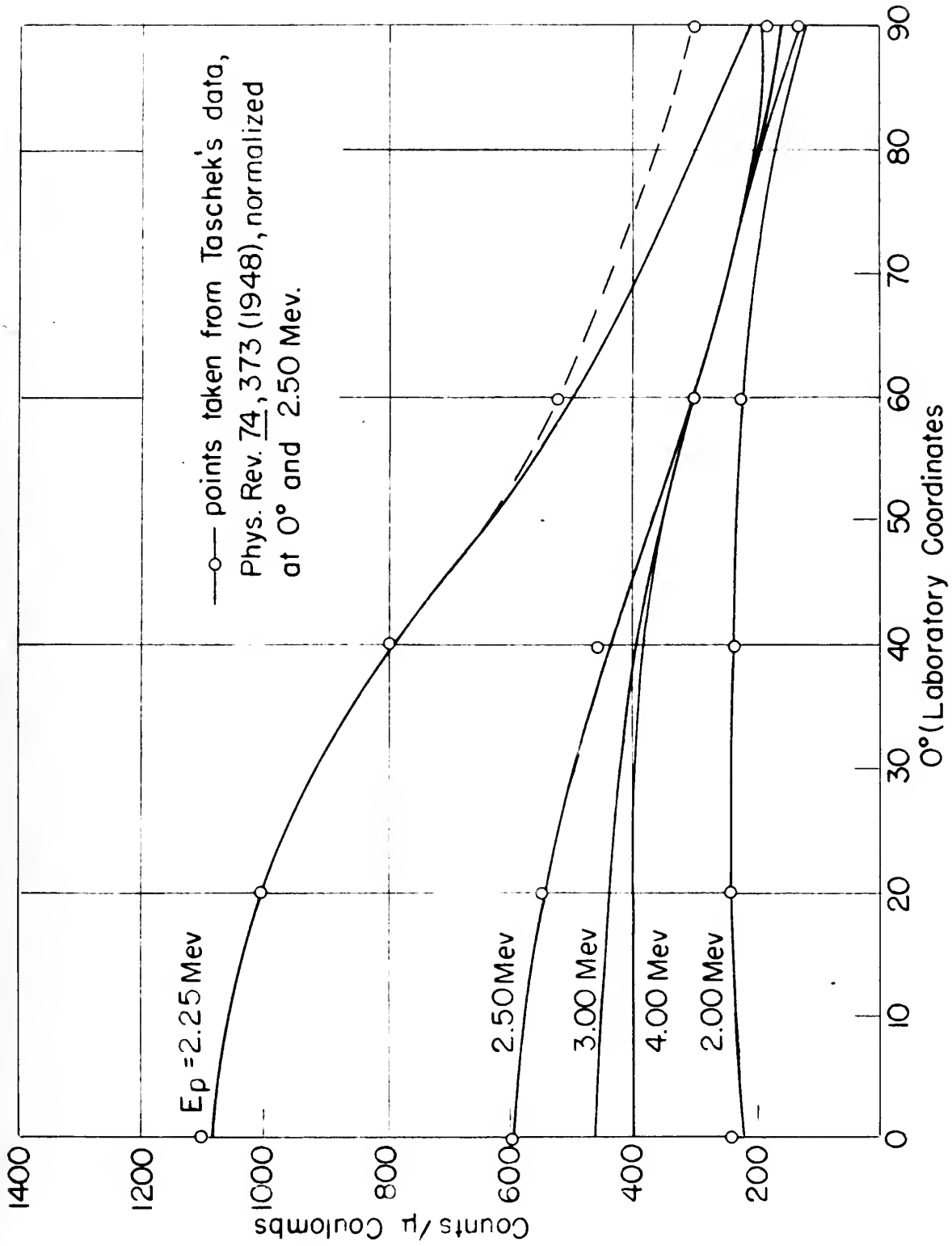


Figure 21a

RELATIVE DIFFERENTIAL CROSS SECTION for the  $\text{Li}^7(p,n)\text{Be}^7$  REACTION



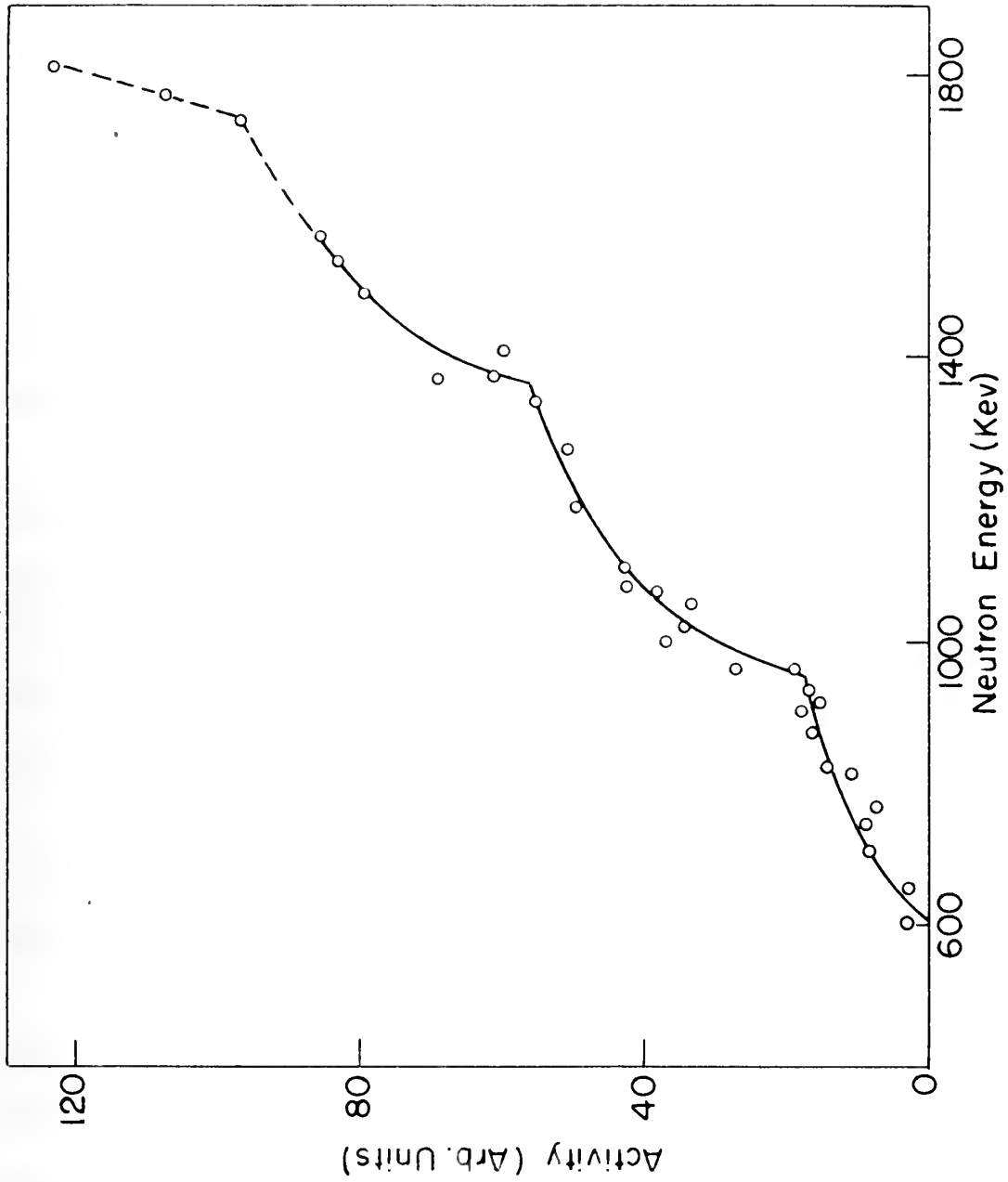


Figure 22  
NEUTRON EXCITATION CURVE for  $\text{In}^{115}$ \*





determination of either of these levels for comparison. From the reproducibility of the calibration of the Rockefeller generator, it is difficult to see how it could be in error by the amount suggested above.

Probably the greatest source of error in the individual points on the excitation curve is due to the stringent requirements on positioning the foils. Since the point at which the foil may be considered concentrated for the irradiation is only 2.1 cm. from the target (found by integrating an inverse square activity over a circular foil), a 2-mm. error in the mounting of the foils or in determining the point at which the proton beam strikes the target results in a 20 percent error in the induced activity.

The location of the beam cannot be observed after the target has been installed so that it is impossible to know whether the beam has wandered slightly during the irradiation. This error can be corrected for, however, because foils were exposed at angles on both sides of 0 degrees. It was then assumed that the beam actually hit the target at such a point that the activities were symmetrical about 0 degrees.

The placement of the individual foils on the circumference of a circle with its center at the target could not be checked in such a simple fashion and is no doubt the reason for the spread in the points.

In further investigation of this problem, it is suggested that a thicker target (of the order of 50 kev) be used and the foils be mounted farther from the target, even at the expense of reducing the activity below that obtained in this investigation.

From the response of the target to the irradiation, it is difficult to see how it could be in error by the amount suggested above. Probably the greatest source of error in the individual points on the excitation curve is due to the stringent requirements on position- ing the foils. Since the point at which the foil was so considered con- sidered for the irradiation is only 2.1 cm. from the target (toward the center of the target) it is not surprising that the error in the mounting of the foils in determining the point at which the proton beam strikes the target results in a 50 percent error in the induced activity.

The location of the beam cannot be observed after the target has been irradiated so that it is impossible to know whether the beam has wandered slightly during the irradiation. This error can be corrected for, however, because foils were exposed at angles on both sides of 0 degrees. It was then assumed that the beam actually hit the target at such a point that the activities were symmetrical about 0 degrees.

The placement of the individual foils on the circumference of a circle with the center at the target could not be checked in such a simple fashion and is no doubt the reason for the spread in the points. In further investigation of this problem, it is suggested that a thinner target (of the order of 50  $\mu$ ) be used and the foils be mounted further from the target, even at the expense of reducing the activity below that obtained in this investigation.

## VI. CONCLUSIONS AND SUGGESTIONS FOR FURTHER INVESTIGATION

## SUMMARY OF RESULTS

Neutron excitation reveals the existence of energy levels in  $\text{Au}^{197}$  at 1.14 Mev and 1.24 Mev. It is found that the metastable state at 540 kev can be excited directly by  $\ell = 3$  neutrons. The spin of this level is shown to be  $11/2$  with parity opposite that of the ground state. This fixes the spin of the 270-keV level to which the metastable level decays at  $5/2$  with parity also opposite that of the ground state.

Since the 1.14-Mev level is also excited by photons, its spin is shown to be  $7/2$  or  $9/2$  with parity opposite to that of the ground state.

An analysis of the data for direct production of the metastable state shows the cross section to be reasonably in agreement with that predicted by the continuum theory for the production of the compound nucleus by an  $\ell = 3$  neutron.

The levels found in  $\text{In}^{115}$  by neutron excitation are at 600 kev, 960 kev, and 1370 kev. The latter two are also found by quantum excitation, but the quantum values are slightly higher (8 percent). An analysis shows that the metastable level has a spin equal to  $1/2$ , and the 600-keV level, a spin of  $5/2$  or  $3/2$ . Both of these levels have a parity different from the ground state.

FURTHER INVESTIGATION OF  $\text{Au}^{197m}$ 

Because of the disagreement between energy levels obtained in the investigation and those obtained by Wiedenbeck using thick-target x-rays,

It is shown to be  $\frac{1}{2}$  with parity opposite to that of the ground state. Since the  $1.1\text{-}\mu$  level is also excited by neutrons, this is decayed as  $\frac{1}{2}$  with parity also opposite that of the ground state. This shows the spin of the  $1.1\text{-}\mu$  level to which the metastable level is shown to be  $\frac{1}{2}$  with parity opposite that of the ground state. At this point can be excited directly by  $\beta^-$  neutrons. The spin of this level is shown to be  $\frac{1}{2}$  with parity opposite that of the ground state. At  $1.1\text{-}\mu$  level and  $1.1\text{-}\mu$  level. It is shown that the metastable state is identical with the ground state.

an analysis of the data for direct production of the sustainable state shows the error section to be reasonably in agreement with that predicted by the continuous theory for the production of the exponential function in an S reaction.

The levels found in the by section correlation are as follows:

1000 feet, and 1270 feet. The latter two are also found by comparison with the section of the latter two are slightly higher (5 feet) than the former level, a sign of a slight rise in the level of the latter two. Both of these levels have a small amount of water in them.

and of his life's work. The book is a masterpiece of scholarship and of literary style. It is a book that every student of the history of the United States should read. It is a book that every student of the history of the world should read. It is a book that every student of the history of the human race should read.

it would seem of great value to redetermine the quantum excitation curve using x-rays from a thin target. Determination of the relative probability for exciting the various levels in this fashion would indicate possible spin and parity values for some of the higher excited levels.

An extension of the neutron excitation curve to higher energies would probably reveal the presence of other levels. A logical choice for the neutron source in such a study is the d-d reaction which will yield from 2.5-Mev to 7-Mev neutrons with the Reckefeller generator. The use of deuterons as the particle accelerated has the disadvantage of giving very high backgrounds of neutrons even though the beam is not striking the target. This is partly because so many of the deuteron reactions have low thresholds. In addition, deuterons in the beam are imbedded in the metal a distance corresponding to their range. When the accelerating voltage is raised slightly, this forms an effective target for the d-d reaction.

However, if a counter for the gold activity can be found that is insensitive to this background or if it is possible to cut off the beam farther from the counter, it will be possible to extend the results of this investigation.

#### FURTHER INVESTIGATION OF $\text{In}^{115*}$

Better results could be obtained for the excitation of  $\text{In}^{115*}$  if the positioning error could be reduced by exposing the foils at a greater distance from the target. In Chapter V, it was suggested that



this be accomplished by use of a thicker lithium target. In addition, the beam current available from the Rockefeller generator has been increased by a factor of 3 or 4 since the exposure were made. It is felt that, with a 50-kev lithium target and the present beam current on the order of 5 microamperes, sufficient activity could be obtained in the foils when they are mounted with the nearest edge on the order of 6 cm. from the target.

By connecting the output of the long counter to a counting-rate meter that operates a continuously recording meter, such as an Esterline-Angus pen recorder, the neutron flux on the foils would be determined as a function of time. This, plus a measurement of the efficiency of the  $\text{In}^{115*}$  activity counter, would enable a determination to be made of the cross section for neutron excitation of the state as a function of energy. A comparison of this cross section with the theoretical value will remove the ambiguity in the spin of the 600-kev level.

#### INVESTIGATION OF OTHER ISOTOPES

Several other isotopes (see Table I) lend themselves to an investigation similar to that made on gold and indium. All may either be treated according to the technique used for gold or that used for indium.

Rhodium has the advantage of being composed of 99.9 percent of the isotope containing the metastable state,  $\text{Rh}^{103}$ . The excitation by x-rays has been accomplished by Wiedenbeck, as reported in Chapter I. The metastable state is only of the order of 60 kev above the ground state, but radiation of this energy can be detected easily by a scintil-

in addition, the following results were obtained: (1) the rate of reaction was independent of the concentration of the reactants; (2) the rate of reaction was independent of the concentration of the products; (3) the rate of reaction was independent of the concentration of the catalyst; (4) the rate of reaction was independent of the concentration of the solvent; (5) the rate of reaction was independent of the concentration of the other components of the reaction mixture. These results are consistent with the proposed mechanism of the reaction.

The following table shows the effect of the concentration of the reactants on the rate of reaction. The rate of reaction was measured by the volume of gas evolved per unit time. The results show that the rate of reaction is proportional to the concentration of the reactants. This is consistent with the proposed mechanism of the reaction.

#### DISCUSSION OF RESULTS

The results of the experiments show that the rate of reaction is proportional to the concentration of the reactants. This is consistent with the proposed mechanism of the reaction. The rate of reaction is also independent of the concentration of the products, the catalyst, the solvent, and the other components of the reaction mixture. These results are consistent with the proposed mechanism of the reaction.



lation counter. Its half-life of 15 minutes requires that any extensive investigation be carried on in a fashion similar to that used for indium.

The excitation of  $\text{Cd}^{111}$  by Wiedenbeck has also been reported in Chapter I. This state has an energy of 11.9 kev with a half-life of 48.7 minutes. In addition, a metastable state in  $\text{Cd}^{113}$  has been found by Helmholtz and McGinnis<sup>56</sup> with a half-life of 2.3 minutes. The cross sections for both of these activities are expected to be small because they occur in isotopes with only about 12 percent relative abundance. However, there is no activity expected that would confuse the results, and their lifetimes are such that counting may be made at some distance from the generator, resulting in low background.

Another possible choice for investigation is  $\text{Ba}^{137}$  with a 158-second half-life. Unfortunately, this isotope is also low in relative abundance, being 11 percent. There have been no investigations of the excitation curve reported for this state.

Hafnium has a 19-second, 200-kev activity assigned to either  $\text{Hf}^{177}$  or  $\text{Hf}^{179}$ . The former is 13 percent abundant and the latter, 14 percent. Although it may prove possible to lower the background during the counting period by removing the accelerator voltage, it is more likely that the beam will have to be cut off by a flap valve as in the case of gold. If this is true, the discussion for wolfram given below also applies to hafnium.

...the ... of ... to ... of ...  
...the ... of ... to ... of ...  
...

The ... of ... by ... has also been reported in  
... This state has an energy of ... with a ... of ...  
... In addition, a ... state in ... has been found  
... with a ... of ... The cross  
... for both of these activities are expected to be ... because  
... only about 10 percent relative abundance.  
... there is no activity expected that would ... the ...  
... and ... are such that ... may be ... of ... distance  
... resulting in ...

Another possible choice for investigation is ... with a ...  
... In ... this ... is also low in relative  
... being ... There have been no investigations of the  
... for this state.

... has a ... of ... assigned to either  
... The former is ... percent abundant and the latter, ...  
... Although it may prove possible to lower the background during  
... by removing the ... voltage, it is more  
... that the ... will have to be cut off by a ... valve as in the  
... of ... If this is true, the discussion for ... given below  
... also applies to ...

Last among the logical choices is  $W^{183}$ . This isotope of wolfram could be investigated with the technique used for gold, since its half-life is 5.5 seconds. The isotopic abundance of 14 percent will result in a low cross section in all probability. Unlike barium and cadmium, however, the lifetime is so short that the voltage cannot be removed from the accelerator, and backgrounds on the order of those obtained for gold will be encountered. If the same cross section per nucleus is assumed for  $W^{183}$  as was found for  $Au^{197}$ , the activity expected is so low that the determination of the wolfram curve is a marginal case.

In summary, if several rhodium foils could be obtained,  $Rh^{103}$  would seem the best choice for future investigation, followed by the two cadmium isotopes and  $Ba^{137}$ . Hafnium and wolfram appear to pose a very difficult problem with the present neutron source strength.



## VII. ACKNOWLEDGMENTS

I wish to thank Dr. Clark Goodman for his advice, interest, and constructive criticism during the progress of this research and the preparation of this thesis. Drs. Victor F. Weisskopf and Marvin L. Goldberger contributed many valuable suggestions on the theoretical aspects of the problem. I am also indebted to Dr. William W. Buschner for helpful discussions about this research.

These experiments could not have been performed without the generous support of the Nuclear Shielding Project at M. I. T. under the sponsorship of the U. S. Navy, Bureau of Ships, and Office of Naval Research.

My thanks are due Dr. Truman S. Gray and the group working with him for their assistance in assembling the equipment. Mr. H. B. Frey provided invaluable aid in the building of the scintillation spectrometer and in the electronic problems with the associated apparatus.

Mr. Harvey B. Willard assisted in many of these measurements and contributed many worthwhile suggestions.

I am grateful to Drs. M. Stanley Livingston and Robley D. Evans and to Messrs. Joel B. Bulkley and Marle F. White and the M. I. T. cyclotron group for irradiating the indium foils used to determine the pulse-height distribution.

I thank Dr. William M. Preston and the men who work with him, Messrs. Donald C. Thompson, Ira E. Slawson, Vincent Yaras, and Edgar Jansen, for their assistance in operation of the Rockefeller generator. I also thank Dr. David H. Frisch for the rotating target that made possible the neutron intensity that was needed.

I wish to thank Mr. J. H. D'Arbigny for his interest and  
 constructive criticism during the progress of this research and the  
 preparation of this thesis. Mr. J. H. D'Arbigny and Mr. J. H.  
 Goldberger contributed many valuable suggestions on the theoretical  
 aspects of the problem. I am also indebted to Mr. William W. Weaver  
 for helpful discussions about this research.

These experiments could not have been performed without the  
 generous support of the Naval Research Council at N. S. S. under  
 the sponsorship of the U. S. Navy, Bureau of Ships, and Division of  
 Naval Research.

My thanks are due Mr. Thomas H. Gray and the group working with  
 him for their assistance in assembling the apparatus. Mr. H. B. Fry  
 provided invaluable aid in the building of the rectification spectro-  
 meter and in the electronic problems with the associated apparatus.

Mr. Harvey W. Willard assisted in many of these measurements and  
 contributed many worthwhile suggestions.

I am grateful to Mr. M. Stanley Livingston and Robert D. Evans  
 and to Messrs. Jack H. Phillips and Marie F. White and the N. S. S.  
 cyclotron group for furnishing the Lanthan Tella used to determine  
 the pulse-height distribution.

I thank Mr. William K. Treloar and the men who work with him,  
 Messrs. Donald C. Thompson, Mr. E. K. Klemm, Vincent Taven, and others,  
 for their assistance in operation of the Cyclotron Generator.

I also thank Mr. David H. Bryan for the rotating target and also for  
 able the neutron intensity that was needed.

My appreciation is due Mrs. Mary E. White and Mrs. Charles Rowe, Jr. for their excellent work in the preparation of the manuscript.

Drs. Edoardo Arnoldi and Samuel A. Goudsmit very kindly contributed their time for valuable discussions of this work.

I should also like to express my indebtedness to Dr. Nathaniel H. Frank and Dr. George G. Harvey for their guidance and suggestions throughout my graduate work at M. I. T.

[illegible]



## REFERENCES

1. O. Hahn, Chem. Berichte 54, 1131 (1921)
2. E. Segre and A. C. Holmholz, Rev. Mod. Phys. 21, 271 (1949)
3. G. T. Seaborg and I. Perlman, Rev. Mod. Phys. 20, 535 (1948)
4. C. F. von Weizsacker, Naturwiss. 24, 913 (1936)
5. S. Flugge, Physik. Zeit. 42, 221 (1941)
6. M. G. Mayer, Phys. Rev. 78, 16 (1950)
7. S. Flugge, op. cit.
8. M. L. Wiedenbeck, Phys. Rev. 67, 92 (1945) for the case of Cd and Ag
9. M. L. Wiedenbeck, Phys. Rev. 67, 267 (1945)
10. S. G. Cohen, Nature 161, 475 (1948)
11. R. F. Taschek, L. A. D. C. No. 135
12. M. L. Wiedenbeck, Phys. Rev. 68, 1 (1945)
13. E. Segre and A. C. Holmholz, op. cit.
14. H. Bethe, Rev. Mod. Phys. 9, 220 (1937)
15. M. H. Hebb and G. E. Uhlenbeck, Physica 5, 605 (1938)
16. S. Flugge, op. cit.
17. W. Heitler, Proc. Camb. Phil. Soc. 32, 112 (1936)
18. H. M. Taylor and H. F. Mott, Proc. Roy. Soc. A142, 215 (1933)
19. S. M. Dancoff and P. Morrison, Phys. Rev. 55, 122 (1939)
20. M. E. Rose, G. H. Goertzel, B. I. Spinrad, J. Harr, and P. Strong,  
Phys. Rev. 76, 1883 (1949)
21. P. Axel and S. M. Dancoff, Phys. Rev. 76, 892 (1949)
22. J. M. Blatt and V. F. Weisskopf, Lab. for Nuclear Sci. and Eng.,  
M. I. T. Technical Report No. 42, p. 47 ff (1950)

1. J. H. ... (1901)
2. J. H. ... (1902)
3. J. H. ... (1903)
4. J. H. ... (1904)
5. J. H. ... (1905)
6. J. H. ... (1906)
7. J. H. ... (1907)
8. J. H. ... (1908)
9. J. H. ... (1909)
10. J. H. ... (1910)
11. J. H. ... (1911)
12. J. H. ... (1912)
13. J. H. ... (1913)
14. J. H. ... (1914)
15. J. H. ... (1915)
16. J. H. ... (1916)
17. J. H. ... (1917)
18. J. H. ... (1918)
19. J. H. ... (1919)
20. J. H. ... (1920)
21. J. H. ... (1921)
22. J. H. ... (1922)

23. V. F. Johnson, L. J. Allen, E. A. Laubenstein, and F. T. Richards,  
Phys. Rev. 77, 413 (1950)
24. R. Taschek and A. Homzendinger, Phys. Rev. 74, 373 (1948)
25. H. Willard, private communication
26. A. O. Hanson and J. L. McKibben, Phys. Rev. 72, 673 (1947)
27. A. O. Hanson, R. Taschek, and J. H. Williams, Rev. Mod. Phys.  
21, 635 (1949)
28. J. Mattauch, Zeits. f. Phys. 117, 249 (1941)
29. M. L. Wiedenbeck, Phys. Rev. 67, 53 (1945)
30. M. L. Wiedenbeck, Phys. Rev. 68, 1 (1945)
31. O. Huber, R. Steffen, and F. Husbhel, Helv. Phys. Acta 21, 192 (1948)
32. F. K. McGowan, Phys. Rev. 77, 138 (1950)
33. M. Deutsch and W. E. Wright, Phys. Rev. 77, 139 (1950)
34. M. E. Rose, O. H. Goertzel, B. I. Spinrad, J. Harr, and P. Strong,  
op. cit.
35. O. Huber, R. Steffen, and F. Husbhel, op. cit.
36. H. Frauenfelder, P. C. Gugelot, O. Huber, H. Medicus, P. Freiswerk,  
P. Sherrer, and R. Steffen, Helv. Phys. Acta 20, 233 (1947)
37. P. Axel and S. M. Dancoff, op. cit.
38. H. Frauenfelder, P. C. Gugelot, O. Huber, H. Medicus, P. Freiswerk,  
P. Sherrer, and R. Steffen, op. cit.
39. E. Segre and A. C. Helmholtz, op. cit.
40. H. Willard, private communication
41. A. O. Hanson, R. Taschek, and J. H. Williams, op. cit.
42. M. Goldhaber, E. D. Hill, and L. Szillard, Phys. Rev. 55, 47 (1939)

1. ... (1911)
2. ... (1912)
3. ... (1913)
4. ... (1914)
5. ... (1915)
6. ... (1916)
7. ... (1917)
8. ... (1918)
9. ... (1919)
10. ... (1920)
11. ... (1921)
12. ... (1922)
13. ... (1923)
14. ... (1924)
15. ... (1925)
16. ... (1926)
17. ... (1927)
18. ... (1928)
19. ... (1929)
20. ... (1930)
21. ... (1931)
22. ... (1932)
23. ... (1933)
24. ... (1934)
25. ... (1935)
26. ... (1936)
27. ... (1937)
28. ... (1938)
29. ... (1939)
30. ... (1940)
31. ... (1941)
32. ... (1942)
33. ... (1943)
34. ... (1944)
35. ... (1945)
36. ... (1946)
37. ... (1947)
38. ... (1948)
39. ... (1949)
40. ... (1950)
41. ... (1951)
42. ... (1952)
43. ... (1953)
44. ... (1954)
45. ... (1955)
46. ... (1956)
47. ... (1957)
48. ... (1958)
49. ... (1959)
50. ... (1960)
51. ... (1961)
52. ... (1962)
53. ... (1963)
54. ... (1964)
55. ... (1965)
56. ... (1966)
57. ... (1967)
58. ... (1968)
59. ... (1969)
60. ... (1970)
61. ... (1971)
62. ... (1972)
63. ... (1973)
64. ... (1974)
65. ... (1975)
66. ... (1976)
67. ... (1977)
68. ... (1978)
69. ... (1979)
70. ... (1980)
71. ... (1981)
72. ... (1982)
73. ... (1983)
74. ... (1984)
75. ... (1985)
76. ... (1986)
77. ... (1987)
78. ... (1988)
79. ... (1989)
80. ... (1990)
81. ... (1991)
82. ... (1992)
83. ... (1993)
84. ... (1994)
85. ... (1995)
86. ... (1996)
87. ... (1997)
88. ... (1998)
89. ... (1999)
90. ... (2000)

43. S. W. Barnes and P. M. Aradine, Phys. Rev. 55, 50 (1939)
44. K. Lark-Horovitz, J. R. Risser, and E. M. Smith, Phys. Rev. 55,  
878 (1939)
45. B. Waldman and M. L. Wiedenbeck, Phys. Rev. 63, 60 (1943)
46. W. C. Miller and B. Waldman, Phys. Rev. 75, 425 (1949)
47. J. L. Lawson and J. M. Cork, Phys. Rev. 57, 982 (1940)
48. S. G. Cohen, op. cit.
49. R. F. Taschek, op. cit.
50. P. R. Bell, B. H. Ketelle, and J. M. Cassidy, Phys. Rev. 76,  
574 (1949)
51. J. L. Lawson and J. M. Cork, op. cit.
52. P. Axel and S. M. Dancoff, op. cit.
53. P. R. Bell, B. H. Ketelle, and J. M. Cassidy, op. cit.
54. R. Taschek and A. Hemmendinger, op. cit.
55. H. Willard, "The Interaction of Neutrons with Nuclei," Ph. D.  
Thesis, M. I. T., September 1950.
56. A. C. Helmholtz and C. L. McGinnis, Phys. Rev. 74, 1559 (1948)



## BIOGRAPHICAL SKETCH

Born: Waterloo, Iowa, June 14, 1920

Education:

West High School, Waterloo, Iowa, graduated 1938

Iowa State Teachers College, Cedar Falls, Iowa, B. A., 1942

Naval Post-Graduate School, Annapolis, Maryland, 1946-1947

Honors:

Tuition Scholarship, Iowa State Teachers College, 1941-1942

Professional Experience:

United States Navy 1942 -

Present Rank of Lieutenant

Associations:

Associate Member, The Society of the Sigma Xi

Member, The American Physical Society

THE UNIVERSITY OF CHICAGO

Chicago, Ill., June 11, 1950

Dear Sir:

Enclosed

are two copies of the report of the  
Committee on the Status of the  
University of Chicago, dated June 11, 1950.

Sincerely,

Very truly yours,  
The University of Chicago

Enclosure

Very truly yours,

The University of Chicago

Enclosure

Very truly yours,

The University of Chicago





11-17-77  
89







**DATE DUE**[illegible]

Thesis

13233

E15

Ebel

Metastable states  
in medium- and heavy-  
weight nuclei.

Thesis  
E15

h

thesE 15

Metastable states in medium- and heavy-w



3 2768 001 90290 1

DUDLEY KNOX LIBRARY